



universität
wien

MASTERARBEIT

Titel der Masterarbeit

„Impact of Vitrification on Ovarian Tissue and Cells“

verfasst von

Chrysanthi-Maria Kokotsaki

angestrebter akademischer Grad

Master of Science (MSc)

Wien, 2014

Studienkennzahl lt. Studienblatt: A 066 877

Studienrichtung lt. Studienblatt: Masterstudium Genetik und Entwicklungsbiologie

Betreut von: Prof. Dr. Christian Schneeberger

*“To succeed in science, one must doubt;
To succeed in life, one must be sure.”*
Le’o Errera

ZUSAMMENFASSUNG

Das Ovarian Tissue Banking (OTB) ist für Patientinnen mit dem Risiko eines frühzeitigen Verlustes der Eierstockfunktion eine Möglichkeit des Fertilitätserhalts. Diese seit ca. 15 Jahren angebotene Möglichkeit der Kryokonservierung von Ovargewebe betrifft vor allen Dingen jüngere Frauen mit onkologischen Erkrankungen, bei denen die notwendigen Therapien zu einer deutlichen Beeinträchtigung der Fertilität und der endokrinen Funktion führten.

OTB kann durch zwei Verfahren erreicht werden: Langsames Einfrieren (Slow Freezing) und ultraschnelles Einfrieren (Vitrifikation). Heutzutage wird die Vitrifikation als Verfahren am häufigsten angewendet, da es vor allen Dingen mehr praktische Vorteile als das langsame Einfrieren bietet. Allerdings sind die bisherigen Daten zu diesen beiden Verfahren begrenzt und die Ergebnisse sind oft widersprüchlich und umstritten.

In der vorliegenden Studie wurde anhand von Mausovarien (C57BL/6J Mäuse) und einer Granulosazelllinie (KGN) die Auswirkungen von zwei Vitrifikationslösungen und den dazugehörigen Protokollen auf die Vitalität und Proliferationsfähigkeit von Zellen und Ovarien untersucht, und die Genexpression ausgewählter Gene in der Granulosazelllinie analysiert.

Die Vitalität und Proliferation der Zellen wurde mit Hilfe einer FACS Analyse bestimmt, für Mäuseovarien wurde zusätzlich die Progesteronproduktion mit Hilfe eines ELISA-Verfahren bestimmt. Es wurden folgende Gene mit Hilfe einer Real Time PCR analysiert: Fas, FasL, Bax, Bcl2, Bcl-xL, PLSCR4, TNF- α , HIF1A, LGALS, CIRBP1, RBM3, HSP47, HSPH1, HSP70, HSP27, FABP3, CRIPT. Die untersuchten Vitrifikationslösungen enthielten im ersten Fall Dimethylsulfoxid (DMSO) (Protokoll 1; P1) und im zweiten Fall Propandiol (PROH), Ethylenglykol (EG) und Saccharose als Gefrierschutzmittel (Protokoll 2; P2). Bei dieser Lösung handelte es sich um eine industriell hergestellte Lösung zur Vitrifikation von Oozyten im Rahmen einer in Vitro Fertilisations Behandlung.

Die Experimente mit den Mäuseovarien ergaben, dass vitrifizierte Mäuseovarien deutlich weniger Progesteron produzieren als frische Ovarien, was als ein Hinweis auf mögliche Zellschädigungen des vitalen Gewebes durch den Einfrierprozess gewertet werden kann.

Der Vergleich der Vitalität der KGN Zelllinie nach Behandlung mit den unterschiedlichen Vitrifikationslösungen ergab dass die Überlebensrate der Zellen nach Behandlung mit P1, der DMSO-haltigen Lösung deutlich höher war als bei Behandlung mit P2. Beide Protokolle zeigten allerdings einen deutlichen Unterschied der Überlebensraten, gegenüber nicht behandelten Zellen auf, so dass auch hier ein negativer Effekt des Einfrierprozess als solcher angenommen werden muss. Ähnliches ergab auch eine Zellzyklusanalyse für vitrifizierte Zellen im Vergleich zu unbehandelten Zellen. Hier zeigte sich eine geringere Anzahl von Zellen, in der G1 und G2 Phase, sowie eine Steigerung des Anteils von Zellen in der S-Phase in den vitrifizierten Proben.

Auch der Vergleich der beiden Protokolle bezüglich der Expression der untersuchten Gene, zeigte, dass die Vitrifikation an sich im Vergleich zu nicht vitrifizierten Zellen, zu deutlichen Expressionsunterschieden führt. Auffallend ist jedoch, dass die Expression von TNF-alpha in beiden Protokollen gegenüber der Kontrolle deutlich gesteigert ist. Dies gilt insbesondere für das Protokoll 2, die industriell hergestellte Vitrifikationslösung. Da in den vorigen Experimenten gezeigt worden ist, dass die Vitalität der Zellen nach Behandlung mit P2 im Vergleich zu P1 deutlich vermindert ist, und eine hohe Expression von TNF-alpha in vielen Zellen Apoptose-induziert, lässt dies den Schluss zu, dass die Vitrifikation über einen TNF-alpha gesteuerten Mechanismus zu einer Abnahme der Zellvitalität führt. Da in den hier durchgeführten Experimenten dieser Prozess abhängig zu sein scheint, von dem jeweils benutzten Protokoll, kommt der Herstellung und Überprüfung kommerzieller Vitrifikationslösungen, die im klinischen Bereich angewandt werden, eine besondere Bedeutung zu.

ABSTRACT

Ovarian Tissue Banking (OTB) is an option of fertility preservation for patients at the risk of premature ovarian failure (POF). This type of ovarian tissue cryopreservation is offered since 15 years, and concerns especially young women suffering from cancer and due to the necessary treatments a significant fertility and endocrine function impairment can occur.

OTB can be accomplished by two methods: slow freezing and vitrification. Nowadays, the vitrification method is applied most often, as it seems to provide more benefits than slow freezing. However, data on both methods are still limited, and the results are often conflicting and controversial.

The present study was based on mouse ovaries (from C57BL/6J mice) and on KGN cells, a human granulosa-like tumor cell line, to investigate two vitrification solutions and the related protocols on mouse ovaries viability, KGN viability and proliferation ability, and on KGN selected – gene expression analysis.

The viability and proliferation of KGN cells was tested by FACs analysis. For the mouse ovaries was additionally measured the progesterone production by ELISA. Following genes were analyzed by Real Time PCR: Fas, FasL, Bax, Bcl2, Bcl-xL, PLSCR4, TNF- α , HIF1A, LGALS, CIRBP1, RBM3, HSP47, HSPH1, HSP70, HSP27, FABP3, CRIPT. The two vitrification solutions tested, contained in the first case (Protocol 1; P1) dimethyl sulphoxide (DMSO), and in the second case (Protocol 2; P2) propanediol (PROH), ethylene glycol (EG), and Sucrose as cryoprotectants. The last solution is a commercial produced solution used for oocyte vitrification in in vitro fertilization treatment.

Mouse ovaries experiments resulted that vitrified mouse ovaries produce less progesterone than fresh ovaries, which can be interpreted as an indication of possible cell damage of vital tissue by the freezing process.

Comparing KGN cell line viability after treatment with the different vitrification solution showed that the survival rate after treatment with P1, the DMSO-containing solution, was much higher than the treatment with P2. However, both protocols showed a significant difference in survival rates, compared to untreated cells, leading to the adoption of the negative freezing process affect. Similar results were shown from cell cycle analysis, when vitrified cells were compared to untreated cells. A smaller number of cells were in G1 and G2 phase, as well an increase in the proportion of cells in S-phase was shown for the vitrified samples.

In addition, the two protocols comparison regard to the selected-gene expression showed that vitrification, in contrast to the non-vitrified cells, changed the expression of the genes studied. Remarkable is the significant increase of TNF- α expression in both protocols, compared to the control, this occurs especially for P2, the industrially produced vitrification solution. As has been shown in previous experiments, cell viability is reduced after treatment with P2 compared

to P1, and additionally TNF-alpha high expression can induce apoptosis in many cells, it can be concluded that through a TNF-alpha driven mechanism, vitrification process decreases cell viability. The experiments carried out in this study showed that vitrification process depends on the particular protocol used, therefore the preparation and verification of commercial vitrification solutions applied in the clinical field is particular important.

Table of Contents

Zusammenfassung	2
Abstract.....	4
Abbreviations and Acronyms	9
1 Introduction	11
1.1 The Ovary	11
1.1.1 The ovarian follicle: - the basic functional unit of the ovary	12
1.1.2 Development of oocytes and ovarian follicles.....	13
1.2 Reproductive Endocrinology.....	15
1.3 Effects of Chemotherapy and Radiotherapy on the Human Reproductive System	16
1.3.1 Chemotherapy	17
1.3.2 Radiotherapy.....	17
1.4 Premature Ovarian Failure (POF).....	17
1.5 Fertility Preservation.....	18
1.5.1 Embryo cryopreservation.....	18
1.5.2 Oocytes cryopreservation	19
1.5.3 Ovarian tissue banking (OTB) (Ovarian cortical tissue cryopreservation (OTC))	20
1.6 Cryobiology	21
1.6.1 Freezing injury and cryoprotection.....	22
1.6.2 Slow freezing - Vitrification.....	23
1.6.3 Vitrification of human ovarian tissue.....	23
1.7 Genes	24
1.7.1 Apoptosis-related genes	24
1.7.2 Stress-responded genes.....	30
1.7.3 Genes related to cell development.....	34
1.8 Human Granulosa-Like Tumor Cell Line, KGN.....	36
2 Aim of the study.....	37
3 Materials and Methods.....	38
3.1 Materials	38
3.1.1 Equipment.....	38
3.1.2 Chemicals and Kits	39
3.1.3 Chemicals prepared in the laboratory	40

3.1.4	Oligonucleotide primers	40
3.2	Methods.....	43
3.2.1	Human Granulosa-Like Tumor Cell Line, KGN.....	43
3.2.2	Vitrification of Mouse Ovaries and KGN cells	44
3.2.3	Thawing Procedure of Vitrified Mouse Ovaries or Cells	45
3.2.4	Ovarian Tissue Vitality Test (Collagenase)	45
3.2.5	Hematoxylin Staining Of Mouse Ovaries Sections	46
3.2.6	Progesterone ELISA	47
3.2.7	Trypsin/EDTA Cell Detachment Process.....	48
3.2.8	Purification of Total RNA from KGN Cells using RNeasy Technology.....	48
3.2.9	cDNA Synthesis From Total RNA Samples.....	49
3.2.10	PCR using JumpStart RedTaq Ready Mix	50
3.2.11	Agarose Gel Electrophoresis (1,5%).....	51
3.2.12	Quantitative PCR using Power SYBR Green PCR Master Mix.....	51
3.2.13	Double Staining of KGN cells in slides with -Cell stain- Double Staining Kit	54
3.2.14	Flow Cytometry and Fluorescence-Activated Cell Sorting (FACS):	54
3.2.15	Statistics	56
4	Results.....	57
4.1	Influence of vitrification on mouse ovaries	57
4.1.1	Hematoxylin Staining Of Mouse Ovaries Sections	57
4.1.2	Ovarian Tissue Vitality Test (Collagenase)	59
4.1.3	Progesterone production ability of mouse ovaries	59
4.2	Influence of vitrification on KGN cells.....	62
4.2.1	KGN characterization experiments.....	62
4.3	Viability test of KGN cells	65
4.3.1	Viability test of KGN cells by double staining.....	65
4.3.2	Viability test of KGN cells by Propidium Iodide staining.....	67
4.4	Vitrified KGN cell cycle analysis	68
4.5	Selected-gene expression analysis of vitrified KGN cells	69
5	Discussion.....	80
6	Table of figures	84
7	Acknowledgements.....	85
8	References	86

9	Appendix	101
10	Curriculum Vitae	115

ABBREVIATIONS AND ACRONYMS

18sRNA	18s ribosomal RNA
Bak	Bcl-2 homologous antagonist/killer
Bax	Bcl-2-associated X protein
Bcl-2	B-cell lymphoma 2
Bcl-xl	B-cell lymphoma-extra-large
BSA	Bovine Serum Albumin
CIRBPT	Cold-inducible RNA-binding protein
CPAs	Cryoprotective agents
CRIPT	Cysteine-Rich PDZ-Binding Protein
ctr	control (not vitrified KGN cells)
CYP19	Cytochrome P450, Family 19, Subfamily A, Polypeptide 1
DMEM	Dulbecco's Modified Eagle's Medium
DPBS	Dulbecco's Phosphate-Buffered Saline
DMSO	Dimethyl Sulphoxide
EG	Ethylene Glycol
FABP3	Fatty acid-binding protein 3
FADD	Fas-Associated Death Domain
Fas	Fas cell surface death receptor
FBS	Fetal Bovine Serum
FCS	Fetal Calf Serum
FSC	Forward Scatter Channel
FSH	Follicle Stimulating Hormone
GAPDH	Glyceraldehyde - 3 – Phosphate Dehydrogenase
GM	growth medium
GnRH	gonadotropin-releasing hormone
HAS	Human Albumin Solution
HIF-1A	Hypoxia-inducible factor 1-alpha
Hsp27	Heat shock protein 27 kDa
Hsp47	Heat shock protein 47 kDa
Hsp70	Heat shock protein 70 kDa
HspH1 or Hsp105	Heat shock protein H1/105 kDa
HSPs	Heat shock proteins
IGF-1	Insulin-like growth factor system
KGN	Human Granulosa-Like Tumor Cell Line
LBP	Lipid-binding proteins
LGALS	lectin, galactoside-binding, soluble
LH	lutensising hormone
LH/hCG	luteinizing hormone/choriogonadotropin receptor
MADD	MAPK Activating Death Domain

Mcl-1	Induced myeloid leukemia cell differentiation protein
MOMP	mitochondrial outer membrane permeabilization
mPRa	membrane progesterone receptor alpha
mPRb	membrane progesterone receptor beta
mPRγ	membrane progesterone receptor gamma
mPRδ	membrane progesterone receptor delta
ODPFs	Oocyte-Derived Paracrine Factors
OM	Mitochondrial outer membrane
OTB	Ovarian tissue banking
OTC	Ovarian tissue cryopreservation
p1h	vitrified KGN cells by protocol 1/treated 1 hour after thawing
p1i	vitrified KGN cells by protocol 1/ immediately treated after thawing
p2h	vitrified KGN by protocol 2/ treated 1 hour after thawing
p2i	vitrified KGN cells by protocol 2/ immediately treated after thawing
PCR	Polymerase Chain Reaction
PGC	Primordial germ cells
PGMC1	progesterone receptor membrane component-1
PI	Propidium Iodide
PLSCR4	Phospholipid scramblase 4
POF	Premature Ovarian Failure
POI	Primary Ovarian Insufficiency
PR-A/B	progesterone receptor isoform A/B
PR-B	progesterone receptor isoform B
PROH	1,2-propanediol
PTPC	Permeability transition pore complex
PUMA	p53-upregulated modulator of apoptosis
RAIDD	RIP-Associated ICH-1/CED-3-homologous protein with a Death Domain
RBM3	RNA-binding motif protein 3
RIP	Receptor-Interacting Protein
RRM	RNA-recognition motif
RT	Room Temperature
RT-qPCR	Reverse Transcription-quantitative Polymerase Chain Reaction
SSC	Side Scatter Channel
TAE Buffer	Tris Acetic Acid EDTA Buffer
TNF-a	Tumour necrosis factor-alpha
TNFR	TNF Receptor
TRADD	TNFR-Associated Death Domain
VDAC	Voltage-dependent anion channel
VS	Vitrification Solution

1 INTRODUCTION

Infertility is a significant public health problem that affects about 10% of couples of fertile age worldwide (McDonald Evens 2004). A large number of factors can cause infertility. One cause is cancer treatment. Cancer is an ever more rapidly spreading disease that is responsible for a real crisis in public health (www.who.int). In women, approximately 10% of cancers occur in those under the age of 45 years old. Chemotherapy, radiotherapy, and bone marrow transplantation can cure up to 90% of girls and young women with diseases that require such treatments (Donnez & Dolmans 2013). Unfortunately, ovarian damage is a common side effect of chemotherapy and radiotherapy for women and girls who after such a treatment are at a risk of losing their germ cells, as ovaries are sensitive to cytotoxic drugs (Donnez et al. 2013). Loss of ovarian function can also be the consequence of genetic disorders (Rodriguez-Wallberg et al. 2010).

Nowadays, infertility as a consequence of these causes can be faced by oocyte, embryo, or ovarian tissue cryopreservation - the last one being the most suitable technique for pre-pubertal and young women who do not yet have mature oocytes for in vitro fertilization (IVF) and cannot delay the start of chemotherapy, as well for women who don't have a partner (Hovatta 2004).

OTB (Ovarian Tissue Banking) is the process whereby ovarian tissue is removed from the patient's body, frozen, and maintained in liquid nitrogen. It is a feasible method since 1996 with functioning tissue after thawing. It has been used for young women, including girls with Turner's syndrome (Hreinsson et al. 2002). The first healthy child has been born after autologous re-transplantation of frozen/-thawed tissue in 2004, and since then 24 children have been born (Donnez et al. 2004; Donnez et al. 2013).

Cryopreservation of ovarian tissue can be accomplished by two methods: slow freezing, and vitrification (Hovatta 2005). Cells are exposed to different stresses caused by ice formation during cooling and warming. These stresses vary due to the cryopreservation techniques used. The vitrification method provides the benefits of cryopreservation without danger of tissue damage due to ice crystal formation, but it can influence the expression of genes (Larman et al. 2011).

1.1 THE OVARY

The ovaries are the female's gonads. The ovaries have two functions: the generation of mature oocytes, and the production of steroid and peptide hormones that create an environment in which fertilization and subsequent implantation in the endometrium can occur (Rogers 2011; Hoffman et al. 2012, p. 424).

The ovary develops from three major cellular sources: (1) primordial germ cells, which arise from the endoderm of the yolk sac and differentiate into the primary oogonia; (2) coelomic epithelial cells, which develop into granulosa cells; (3) mesenchymal cells from the gonadal ridge, which become the ovarian stroma (Hoffman et al. 2012 p. 424). Histologically, the ovary has 2 main sections, the outer cortex and the inner medulla. The cortex is where the follicles and oocytes are found at various stages of development and degeneration, and is made of tightly packed connective tissue. The medulla is where the ovarian vasculature is found, and consists primarily of loose stromal tissue. The immature ovary is in a continuous process of growth and development, accompanied by a concurrent continuous degeneration of oocytes and follicles (Peters 1969).

1.1.1 The ovarian follicle: - the basic functional unit of the ovary

The ovarian follicle, consisting of an oocyte surrounded by granulosa and theca cells, represents the basic functional unit of the ovary (Fig. 1).

Women are born with approximately two million eggs in their ovaries, but about eleven thousand of them die every month prior to puberty. As a teenager, a woman has only three hundred thousand to four hundred thousand remaining eggs, and from that point on, approximately one thousand eggs are destined to die every month, thirty to thirty-five eggs every day (Silber 2007).

Follicular atresia is not a passive, necrotic process, but rather a precisely controlled active process, namely apoptosis, which is under hormonal control (Hoffman et al. 2012, p. 424). The ovary at birth consists mainly of two types of cells: the highly specialized oocytes and the multipotential stroma cells, from which granulosa cells, theca cells, and others will arise (Peters 1969).

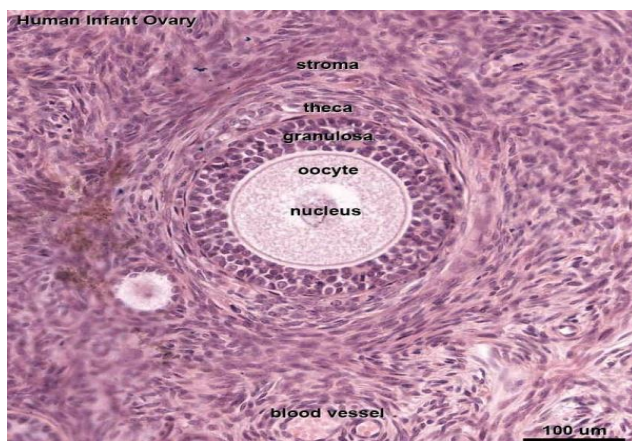


Figure 1. Representative picture of a primary follicle. The oocyte, surrounded by granulosa and theca cells, is displayed (Hill (2014) Embryology.)

Before reproductive senescence, mammalian ovaries have a pool of primordial follicles, each consisting of an oocyte arrested in prophase I of meiosis and a single layer of granulosa cells. Each month, a cohort of follicles grows under the influence of gonadotrophins. Normally, only one of them ovulates under a hormonally regulated process (Adhikari and Liu 2009). As a result, throughout the entire reproductive period of a woman only 400-500 follicles become ovulated, whereas the others degenerate by a procedure called atresia. The number of primordial follicles continually decreases by atresia at an exponential rate during reproductive life (Gougeon 1996; Faddy 2000).

1.1.2 Development of oocytes and ovarian follicles

Oogenesis is a complex process of female gamete formation, regulated by a vast number of intra- and extra-ovarian factors (Sánchez & Smitz 2012).

Primordial germ cells (PGC) multiply during fetal development. At birth, the ovary contains around 400.000 primordial follicles that contain primary oocytes. There are two types of follicles, preantral (primordial, primary, secondary, tertiary) and antral (graafian, small, medium, large, preovulatory). Follicular growth can be classified into three phases according to their developmental stage and gonadotropin dependence: (1) follicular growth through primordial, primary, and secondary stages (gonadotropin-independent phase); (2) transition from the preantral to the early antral stage (gonadotropin-responsive phase); and (3) continuous growth beyond the early antral stage (gonadotropin-dependent phase), which includes follicle recruitment, selection, and ovulation (Erickson 2008; Richards et al. 2010; Orisaka et al. 2009).

The development of the follicles requires coordinated communication between the oocyte and the granulosa and theca cells. Granulosa cells provide nutrients and molecular signals to the developing oocyte, whereas the oocyte is needed for granulosa cells to proliferate and differentiate, in addition to promoting the organization of the follicle (Gilchrist et al. 2004; Reddy et al. 2010; Sánchez & Smitz 2012). Intercellular gap junctions develop between adjacent granulosa cells and between granulosa cells and the developing oocyte. These connections allow the passage of nutrients, ions, and regulatory factors between cells (Hoffman et al. 2012, p. 429).

Follicles have the potential to either ovulate their egg into the oviduct at mid-cycle to be fertilized or to die by atresia. Only a few follicles in the human ovary survive to complete the cytodifferentiation process; the others contribute to the endocrine function of the ovary, with 99.9% dying by apoptosis (Sciarra 2004).

In the fetal period in the gonad, the primordial germ cells differentiate into oogonia, which mitotically divide to increase their population. Many oogonia differentiate further into primary oocytes, which begin meiosis. A primary oocyte with its surrounding epithelial cells is called a primordial follicle. Primary oocytes remain suspended in prophase I until the beginning of

puberty. From puberty on and through the reproductive years, several primordial follicles mature each month into primary follicles. A few of these continue development to secondary follicles. One or two secondary follicles progress to a tertiary or Graafian follicle stage. At this stage, the first meiotic division completes to produce a haploid secondary oocyte and a polar body. The secondary oocyte halts meiosis at its second metaphase. One of the secondary oocytes is then released at ovulation. If the oocyte is fertilized, completion of the second meiotic division follows. If fertilization doesn't occur, the oocyte degenerates prior to completion of the second meiotic division. In women the process is long, requiring almost 1 year for a primordial follicle to grow and develop to the ovulatory stage (Erickson 2008; Lauralee 2010).

In Figure 2 are shown the developmental stages of follicular growth and the gonadotropin dependence at different stages, which will be analyzed in paragraph 1.2, and the coordinated communication between the oocyte and granulosa and theca cells.

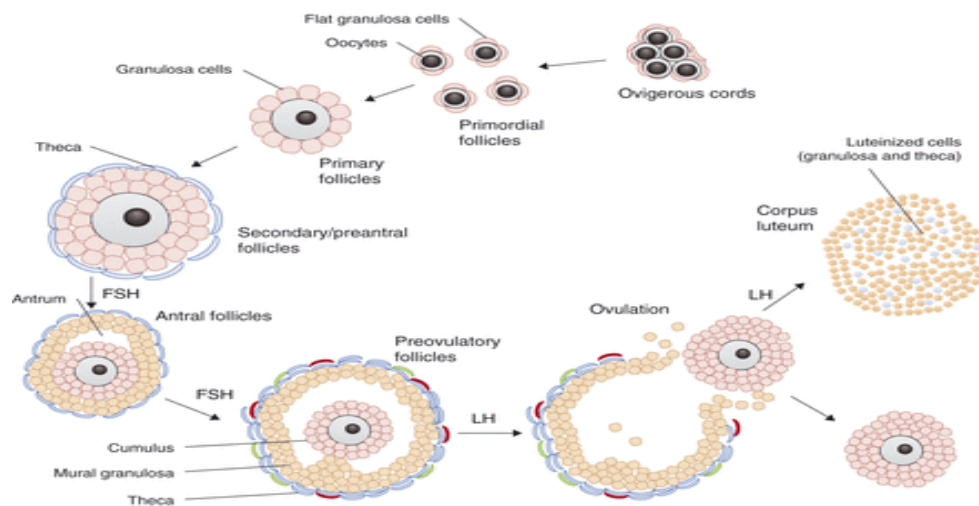


Figure 2. The main steps of folliculogenesis. Folliculogenesis starts with primordial follicles that are subsequently recruited to become primary follicles. Proliferating GCs progressively form several layers around the oocyte. From the stage of secondary to late preantral follicles, a layer of theca cells surrounds the follicle, and the follicles start to produce oestrogens. Follicular growth to the secondary/preantral stage is independent of gonadotrophins, progression beyond this stage strictly depends on FSH stimulation. At the stage of antrum, selection occurs between growing follicles, and only one or a limited number of follicles continue growing to the preovulatory stage while others undergo atresia. After a peak of FSH and LH ovulation occurs. (Georges et al. 2013)

1.2 REPRODUCTIVE ENDOCRINOLOGY

Cyclic ovarian function is regulated by the hypothalamic-pituitary-ovarian axis. Within the hypothalamus, specific nuclei release gonadotropin-releasing hormone (GnRH) in pulses every 90 minutes (Silber 2007). This decapeptide binds to surface receptors on the gonadotrope subpopulation of the anterior pituitary gland. In response, gonadotropes secrete glycoprotein gonadotropins, that is, luteinizing hormone (LH) and follicle-stimulating hormone (FSH), into the peripheral circulation. Within the ovary, LH and FSH bind to theca and granulosa cells to stimulate folliculogenesis as well as ovarian production of an array of steroid hormones (estrogens, progesterone, and androgens), gonadal peptides (activin, inhibin, and follistatin), and growth factors (Schorge et al. 2008, p. 681).

Theca cells (and to a lesser extent, the stroma) produce androgens, granulosa cells are responsible for conversion of androgens to estrogens, as well as progesterone synthesis. Estrogen levels increase with increased follicular size, enhance the effects of FSH on granulosa cells, and create a feed-forward action on follicles that produce estrogens. In response to LH stimulation, theca cells synthesize androgens, which are secreted into the extracellular fluid and diffuse across the basement membrane to the granulosa cells to provide precursors for estrogen production. In contrast to theca cells, granulosa cells express high levels of aromatase activity in response to FSH stimulation. Thus, these cells efficiently convert androgens to estrogens, primarily the potent estrogen estradiol (Havelock et al. 2004; Hoffman et al. 2012, p. 425).

Estrogen is responsible for the appearance of secondary sex characteristics in females at puberty and for the maturation and maintenance of the reproductive organs in their mature functional state (Wallace and Kruger 2014).

During the luteal-follicular transition, a small increase in FSH levels is responsible for the selection of the single dominant follicle that will ultimately ovulate (Schipper et al. 1998). The intrafollicular levels of members of the insulin-like growth factor family (IGFs) may synergize with FSH to help select the dominant follicle (Hoffman et al. 2012, p. 429).

After ovulation, progesterone is produced by the corpus luteum. Progesterone prepares the uterus for the implantation of a fertilized ovum, the mammary glands for lactation and to maintain pregnancy. Additionally, progesterone functions with estrogen by promoting menstrual cycle changes in the endometrium (Wallace and Kruger 2014).

If fertilization and implantation occur, the embryo produces Human Chorionic Gonadotropin (HCG), which maintains the corpus luteum and causes it to continue producing progesterone until the placenta can take over the production of progesterone. If fertilization and implantation do not occur, the corpus luteum degenerates into a corpus albicans, and progesterone levels fall (Silber 2007, p. 25).

Fig. 3 shows the sequence of events that take place in a female body to make ovulation occur.

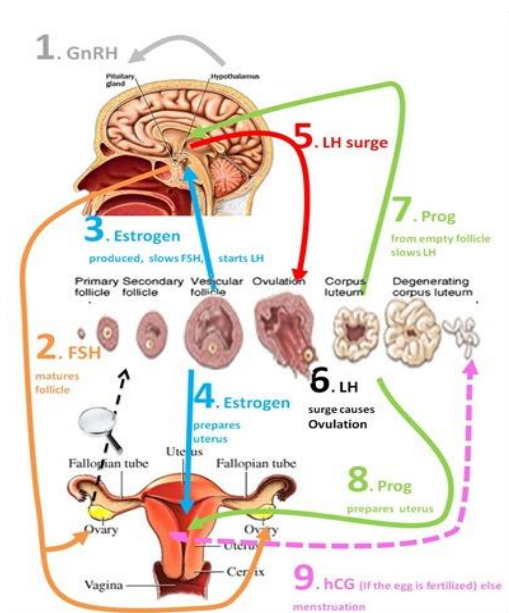


Figure 3. The sequence of events that make ovulation occur. Development of the follicles is stimulated by production of follicle stimulating hormone (FSH) by the pituitary gland. Maturing of the follicles then results in an increase in estrogen levels. This increase in estrogen levels feeds back to the pituitary, and suppresses further release of FSH. The follicles also release a second hormone called inhibin, which suppresses further production of FSH. As the estrogen levels rise, a second pituitary hormone called Lutenising hormone (LH) is surged, which causes the follicle to ovulate. LH also causes ruptured follicles to lutenise, forming a transitory endocrine organ called the corpus luteum. The corpus luteum secretes progesterone and estrogen. The progesterone levels feed back to the pituitary and suppress further release of LH. When fertilization does not occur, the corpus luteum degenerates and is called the corpus

albicans. The decline in estrogen levels, feeds back to the pituitary and there is a corresponding increase in FSH to being the cycle all over again. (Sherwood 2010)

1.3 EFFECTS OF CHEMOTHERAPY AND RADIOTHERAPY ON THE HUMAN REPRODUCTIVE SYSTEM

Exposure to certain substances such as drugs may lead to temporary or permanent damage to the ovaries or testes (gonadotoxicity). Chemotherapy and radiotherapy treatment of cancer and other pathologies has resulted in improved survival rates but is also the most common cause of gonadotoxicity and subsequent infertility.

Ovaries are extremely sensitive to cytotoxic drugs that induce an irreversible gonadal damage. It has been also suggested that anticancer drugs cause follicular depletion by inducing apoptosis. The end result of the chemotherapy is premature ovarian failure (POF), leading to premature menopause and permanent infertility (Sonmezer and Oktay 2004).

Gonadotoxicity depends on several factors, including the age of the patient, as the cumulative dose needed to cause POF decreases as age increases. However, many younger patients will naturally recover their ovarian function and fertility, especially if the applied chemotherapy doses are low (Meirow et al. 2001). Gonadotoxicity depends also on the initial status of the ovaries, the treatment applied and cumulative doses, and the type of agent used (Wallace et al. 2011; Brougham & Wallace 2005).

1.3.1 Chemotherapy

The mechanism of chemotherapy causing POF is not well known, but most chemotherapeutic agents work by affecting cell cycle division. Therefore it can be expected that oocytes that enter a phase of maturation and the growth and proliferation of granulosa cells would be the most chemotherapy-sensitive cell types in the ovary (Levine 2011; Morgan et al. 2012).

Chemotherapeutic agents can cause mutations, DNA adducts and structural breaks, as well as oxidative damage in somatic and germ cells. Chemotherapy's alkylating agents join with DNA, avoiding its replication and transcription (Sonmezer and Oktay 2004). They are extremely gonadotoxic by acting at any phase of the cellular cycle, as after chemotherapy antral follicle count and ovarian volume decrease (Domingo et al. 2011, p. 24). Histological studies of human ovaries have shown chemotherapy to cause ovarian atrophy and global loss of primordial follicles. Injury to blood vessels and focal fibrosis of the ovarian cortex are further patterns of ovarian damage caused by chemotherapy (Meirow et al. 2007).

1.3.2 Radiotherapy

Likewise, the effect of radiotherapy on the gonads depends on age, cumulative doses, fractioned doses and irradiation area. The average doses needed to destroy oocytes in humans is 2 Gy (Wallace 2003). Irradiation at an ovarian dose above 6 Gy usually results in permanent ovarian failure (Howell and Shalet 1998). Cranial irradiation can damage the hypothalamus–pituitary–gonadal axis, but as gonads are not affected, they recover their function with gonadotropin replacement (Gleeson and Shalet 2004).

1.4 PREMATURE OVARIAN FAILURE (POF)

Surviving a malignant disease can leave the patient with late side effects like endocrine disorders and premature ovarian failure (POF), resulting in infertility and psychological distress.

The average age for menopause in western populations of women is approximately 51 years. Premature Ovarian Failure (POF), also known as Primary Ovarian Insufficiency (POI), is a loss of ovarian function before the age of 40. These subjects can be identified with primary ovarian defect, characterized by absent menarche (primary amenorrhea) or premature depletion of ovarian follicle/arrested folliculogenesis before the age of 40 (secondary amenorrhea) (Santoro 2003; Timmreck et al. 2003).

About one out of every six survivors of a malignant disease experience POF. The risk of fertility impairment increases with patients' age and is associated with the type, dose, and duration of the chemotherapy and/or radiotherapy that is administered. Approximately 1 in 10.000 women

by age 20, 1 in 1000 women by age 30, and 1 in 100 women by the age of 40 are affected by POF (Beck-Peccoz et al. 2006). Women with POF suffer from anovulation and hypoestrogenism and primary or secondary amenorrhea, infertility, sex steroid deficiency, and elevated gonadotrophins: All of these factors greatly reduce the probability of pregnancy (Dolmans et al. 2013; Kalantaridou et al. 1998). A reduced follicular reserve may result in POF and menopause, and many years of post-treatment, even in patients undergoing chemotherapy at a very young age (Sklar et al. 2006).

The causes of POF are of iatrogenic origin (e.g. chemotherapy, radiation, surgery), autoimmune, infections, chromosome X defects, monogenic defects (e.g., FSH receptor mutations or LH receptor mutations), idiopathic (Beck-Peccoz et al. 2006; Goswami et al. 2005). As the causes of POF are extremely heterogeneous, in the majority of cases the cause(s) remains undetermined.

1.5 FERTILITY PRESERVATION

Several methods exist to preserve fertility for those facing premature ovarian failure, including embryo, oocyte, or ovarian tissue cryopreservation. Cryopreserved ovarian tissue can be used after thawing in two ways: grafting (transplantation) and in vitro culture. The graft can be transplanted to human (autografting) or non-human species (xenografting). In the case of autografting, tissue can be transplanted to the original ovary site (orthotopic grafting) or to a non-ovary site (heterotopic grafting). Natural fertility is possible only after orthotopic grafting; otherwise, in vitro fertilization and embryo transfer is necessary (Donnez et al. 2006). The choice of fertility preservation depends on various parameters: the type and timing of chemotherapy, the type of cancer, the patient's age, and the partner status. The future of fertility preservation is promising, however; continuous efforts to improve current strategies and to develop new strategies will benefit many women.

1.5.1 Embryo cryopreservation

Since 1949, experiments have been performed to manage embryo cryopreservation. By the 1980s, the freezing of human embryos had emerged as a common procedure (Michelmann and Nayudu 2006). In 1983, Trounson and Mohr reported a pregnancy following cryopreservation, thawing and transfer of an 8-cell embryo, the pregnancy terminated at 24 weeks' gestation (Trounson and Mohr 1983). The first child was born after a pregnancy resulting from a frozen embryo transfer in 1984 (Zeilmaker et al. 1984).

Nowadays, human embryo cryopreservation is a safe procedure that is used in all fertility clinics. In the past, oocytes needed fertilization to be preserved, as thawed embryos were considered to achieve higher survival rates than oocytes. The female patient required a partner or sperm donor to fertilize the retrieved oocytes, creating embryos that may not have been used in the future, a circumstance that implied various ethical considerations (Donnez & Kim 2011).

Children born after frozen embryo transfers have not shown any increased risk of birth defects compared to children born after fresh blastocysts transfer (Wikland et al. 2010). Additionally, data shows that women who had transfers of fresh and frozen embryos obtained 8% additional births by using their cryopreserved embryos (Konc et al. 2014).

Embryo cryopreservation must occur before cancer treatment as the efficacy of IVF is dramatically reduced after chemotherapy. However, this procedure needs conventional ovarian stimulation, which may require up to two-three weeks (Dolmans et al. 2005). Moreover, many cancer patients respond poorly to conventional ovarian stimulation, which may result in poor quality of the oocytes collected during the cycle. Ovarian stimulation procedure may not be an optimal option for women with hormone-sensitive tumors because of increased estrogen concentrations in serum during the stimulation (Pena et al. 2002; Chen et al. 2003).

Cryopreservation of embryos is not a workable option for pre-pubertal or adolescent girls or single women. Moreover, the cryopreservation of human embryos poses severe ethical problems as the surplus frozen embryos must either be destroyed or used for research. In such cases, embryo adoption may be a solution.

1.5.2 Oocytes cryopreservation

Oocyte cryopreservation is an alternative option for patients with the same characteristics as for embryo cryopreservation but who do not have a partner and do not wish to use donated sperm.

The first successful attempt that led to a twin pregnancy was in 1986 (Chen 1986). Vitrification of oocytes has resulted in much higher survival rates after warming in contrast to those by slow freezing. Survival rates of 97% have been reported, with no differences in fecundation and implantation rates, embryo quality, or pregnancy rates compared to fresh oocytes. However, this approach is also limited by the number of oocytes that can be obtained (Cobo et al. 2008; Anderson and Wallace 2011; Donnez & Kim 2011).

Compared to embryo cryopreservation, oocyte cryopreservation offers more advantages, such as fertility preservation in women at risk of losing fertility due to oncological treatment or chronic disease, egg donation, and postponing child birth. Additionally, it eliminates the religious, ethical, and legal concerns of embryo freezing. However, oocyte cryopreservation is technically

challenging and requires ovarian stimulation, thus potentially resulting in a delay in cancer treatment (Anderson and Wallace 2011).

The metaphase II oocyte has a very special structure that leads to complex difficulties associated with its cryopreservation (Konc et al. 2014). But oocytes at the diplotene stage of prophase I, or germinal vesicle (GV) stage, survive the cryopreservation procedure better than those frozen at the M-II stage (Boiso et al. 2002). These cells have reached full size and complete meiotic competence but have not yet resumed their maturation process and initiated their second metaphase (Donnez et al. 2006).

Oocyte cryopreservation can be performed for single women, couples without sperm available on the day of oocyte uptake, and also for already menstruating adolescent girls. Cryopreservation of immature oocytes after in vitro maturation (IVM) is also another possible option for fertility preservation, although better results can be achieved by vitrifying mature oocytes rather than immature oocytes (Cao et al. 2009).

The number of pregnancies resulting from oocyte cryopreservation is constantly increasing, without an accompanying apparent increase in adverse postnatal outcome such as low birth weight or congenital abnormalities (Donnez & Kim 2011).

1.5.3 Ovarian tissue banking (OTB) (Ovarian cortical tissue cryopreservation (OTC))

Ovarian tissue cryopreservation (OTC) is proposed to prepubertal girls, patients without a partner, or patients unable to undergo ovarian stimulation due to lack of time (Dolmans et al. 2005). Storing of frozen ovarian tissue for later transplantation may also benefit patients with non-malignant diseases such as recurrent ovarian endometriosis. Orthotopic transplantation of the frozen/-thawed ovarian cortex would allow natural fertility and, in the case of failure, in vitro fertilization would still remain an option (Oktay et al. 1998; Donnez et al. 2000; Gosden 2002; Hovatta 2003; Marhhom and Cohen 2007).

Cryopreservation of ovarian cortex is the only option for restoring both endocrine function and fertility. To date, re-transplantation of frozen/-thawed ovarian tissue has resulted in 24 births of healthy infants (Roux et al. 2010; Amorim et al. 2012; Greve et al. 2012; Dolmans et al. 2013). Ovarian biopsy can be performed via laparoscopy or laparotomy immediately before or after initiation of cancer therapy. Usually, about 25- 50% of the cortical tissue from one ovary is removed as the vast majority of the follicles are located there. The cortical tissue removed varies depending on the expected ovarian follicle injury after exposure to cancer treatment, but should be large enough and representative as follicle density in the ovary is unequally distributed (von Wolff et al. 2009; Qu et al. 2000; Schmidt et al. 2003).

Primordial follicles constitute a majority of 70-90% of all follicles in the ovary, and a small piece of ovarian tissue may contain hundreds of these small follicles (Gougeon 1986; Lass et al. 1997). Using cryopreservation, most primordial follicles are preserved as they resist cryoinjury due to their small size, low metabolic rate, and lack of zona pellucida and cortical granules (Hovatta et al. 1996; Shaw et al. 2000). In addition, primordial follicles have more time for repairing sub-lethal injury to organelles and other structure during their prolonged growth phase (Picton et al. 2000).

Cryopreservation of ovarian tissue is an attractive method for fertility preservation. The main disadvantage of this technique is that it requires laparoscopy to obtain the ovarian tissue and a further re-implant. Currently, ovarian tissue cryopreservation is only recommended as an experimental treatment in selected patients. Research is needed to investigate the revascularization process with the aim of reducing the follicular loss that occurs after tissue grafting. Ovarian tissue cryopreservation can serve as a source of follicle for IVM. Thus, though still experimental, future fertility preservation techniques will tend towards combining ovarian cryopreservation and immature egg retrieval for further in-vitro oocyte maturation and vitrification (Donnez & Kim 2011).

1.6 CRYOBIOLOGY

Cryobiology studies the effect of low temperatures on living cells, tissues, or organs. Cryopreservation is the use of very low temperatures to preserve structurally intact living cells and tissues for a variety of research and clinical purposes.

Freezing is lethal to most living systems, yet it can preserve cells and their constituents, and permit the long-term storage of tissues or whole organs (Mazur 1970).

For cryopreservation of ovarian cortical tissue there are two main methods, slow freezing and vitrification. Both methods permit cells to be stored indefinitely by using extremely cold temperatures to stop metabolic activities, and both are based on the ability of certain small molecules, called cryoprotectants, to enter cells and prevent dehydration and formation of intracellular or extracellular ice crystals, that can cause cell death and destruction of cell organelles during the freezing process. Once cells are frozen or vitrified, they can be stored by plunging them into liquid nitrogen.

In the present thesis we focused on the vitrification method, which is a promising novel technique in reproductive technology, but comparative success rates are yet to be established. Due to these methods, ice crystal formation is avoided completely as the temperature drops so rapidly that the water inside the cell never becomes ice (from 15000 to 30000°C per minute) (Kuwayama 2007; Donnez & Kim 2011).

1.6.1 Freezing injury and cryoprotection

Water movement across the cell membranes during freezing and thawing is controlled by both intracellular and extracellular phase changes, and by other factors such as the nature of any cryoprotective agent present, and the rates of cooling and thawing (Farrant 1977).

In 1963, Mazur discovered the importance of the rate of temperature change that controls the movement of water across the cell membrane and hence, indirectly, the possible intracellular freezing.

Crystallization starts when cooling temperature falls below the freezing point (0°C) and builds crystals. The growth of ice crystals is maximal just below the freezing point; by further cooling it is arrested. At lower temperature (approximately at -50°C) the concentration of the solution surrounding the cells is changed, which results in increased viscosity of the fluid by osmotic gradient. The cells will dehydrate and shrink at a rate depending on the rate of ice formation. The rate of temperature changes influences the rate at which water moves out of cells (during cooling) or into the cells (during warming). Increased viscosity prevents ice crystal formation. Water leaves the cells quickly across the cell membranes, and the cytoplasm will not cool below its freezing point. On the other side, if the cooling is too fast, sufficient transport of water out of the cells will not be possible, and the cytoplasm of the cells will freeze. Each cell type has a maximal survival at a characteristic cooling rate due to the effects of solution and intracellular freezing (Mazur 1963).

Ice crystals can also be rebuilt during warming. The rate of warming has an important effect because very small amounts of intracellular ice crystals are capable to grow. Based on the rate of warming, the behavior of these small ice crystals is different. During slow warming, the ice crystals are recrystallized and grow together, but during rapid warming there is no time to recrystallize and the ice simply will melt (Pegg 2007).

Cryoprotective agents (CPAs) protect cellular damage during freezing and thawing. When they are added in cryopreservation solution, they create an osmotic gradient that causes water moving out of the cells that become shrunken. In addition, CPAs function by lowering the freezing points of the extracellular solution. In this manner, cells have enough time to become dehydrated before the temperature reaches the freezing point of the cytoplasm. Hence, the main function of CPAs is to avoid intracellular ice crystal formation, which is the main cause of damage during freezing and thawing processes. Additionally, CPAs penetrate the cell membrane and stabilize intracellular proteins during freezing (Hovatta et al. 1996; Picton et al. 2000).

In order to lower the freezing temperature CPAs must be highly water-soluble, even at low temperatures. To be biologically acceptable, cryoprotectants must be able to penetrate into the cells and have low toxicity (Pegg 2007). Glycerol, dimethyl sulphoxide (DMSO), 1,2 propanediol (PrOH) and ethylene glycol (EG) are some of the cryoprotectants with these properties.

Dimethylsulfoxide (DMSO) was proposed in 1960 by Lovelock and Bishop as a cryoprotectant. It rapidly proved to have far more widespread applicability than glycerol, particularly for the preservation of cells in tissue culture (Mazur 1970). In the procedure that led to the live birth after orthotopic transplantation of cryopreserved ovarian tissue, DMSO was used as a cryoprotectant (Donnez et al. 2004).

1.6.2 Slow freezing - Vitrification

Slow freezing is a method where ovarian tissue is cooled very slowly in 2-3 hours from room temperature or 4°C to -196°C using a programmable freezer, followed by storage in liquid nitrogen (-196°C), and thawed rapidly in 1 minute from -196°C to room temperature. Before freezing, the tissue is first equilibrated in cryoprotectant solution, allowing its penetration into the cells (Newton et al. 1998).

Vitrification is another process of cryopreservation using high concentrations of cryoprotectant to solidify the cell in a glass state without formation of intracellular ice. Cells are cooled rapidly by direct immersion in liquid nitrogen. To avoid the toxicity of each individual CPA, a combination of cryoprotectants including other permeating cryoprotectants is used (Vicente & García-Ximénez 1994; Isachenko et al. 2003).

Although slow freezing method has been applied in human ovarian tissue cryopreservation for more than 10 years (Donnez et al. 2004), vitrification is more technologically promising. It is simpler, quicker, and cheaper, but the protocols are still in the experimental phase (Isachenko et al. 2009).

1.6.3 Vitrification of human ovarian tissue

Cryopreservation of human ovarian cortical tissue is a complex procedure that requires preservation of multiple cell types varying in volume and membrane permeability. These cells have different requirements for optimal survival during the cryopreserving and thawing processes.

Cryopreservation of ovarian tissue by slow freezing is limited by relatively poor survival of the stroma. The stroma and blood vessels play a critical role in the development of follicles and restoration of gonadal function after transplantation. Hence, a proper preservation of stroma and blood vessels is basically important (Woodruff & Shea 2007). Therefore, vitrification protocols were developed for human ovarian tissue to improve the viability of the stroma in addition to the follicles and oocytes.

Vitrification of human ovarian tissue has been investigated in the last decade. Researchers have studied various vitrification solutions and carrier systems and evaluated the effect of different vitrification protocols on ovarian tissue. Many of the conclusions from these diverse early studies have been contradictory. However, most studies support vitrification as the cryopreservation method of choice for human ovarian tissue (Amorim et al. 2011).

1.7 GENES

Larman et al. have shown that vitrification can influence gene expression (Larman et al. 2011). In this study, genes that have a role in apoptosis, or in controlling the cellular response upon confronting a variety of cellular stresses (like temperature changes), and genes associated with cell development were selected to determine their influence by the vitrification and thawing processes.

1.7.1 Apoptosis-related genes

Apoptosis and related forms of cell death have central importance in development, homeostasis, tumor surveillance, and the function of the immune system. Apoptotic stimuli can be propagated via two distinct molecular cascades: (1) extrinsic apoptosis, triggered by the binding of an extracellular ligand to a receptor on the plasma membrane (e.g., FAS, TNFR1), or by so-called dependence receptors when the concentration of their ligands falls below a specific threshold; and (2) intrinsic (or mitochondria-mediated pathway) apoptosis, responding to perturbations of intracellular homeostasis. Intrinsic apoptosis is usually activated in response to intracellular stress signals, which include DNA damage and high levels of reactive oxygen species (ROS), as well as by viral infection and activation of oncogenes (Michels et al. 2013; Ricci & Zong 2006).

Death receptors are members of the tumor necrosis factor receptor (TNFR) superfamily characterized by a cytoplasmic region known as the “death domain” that enables the receptors to initiate cytotoxic signals when engaged by cognate ligands. Binding to the ligand results to a receptor aggregation and recruitment of adaptor proteins, which in turn initiates a proteolytic cascade by recruiting and activating initiator caspases 8 and 10. Caspases, a family of cysteine proteases, are the central regulators of apoptosis (Guicciardi and Gores 2009).

Intrinsic apoptosis can be triggered by a plethora of perturbations in intracellular homeostasis, including DNA damage, oxidative stress, and cytosolic Ca²⁺ overload. Independently of the initiating stimulus, the signaling cascades that mediate intrinsic apoptosis are opposed to each other at the level of mitochondria. If lethal signals prevail, the majority of mitochondria become

permeabilized. Upon mitochondrial outer membrane permeabilization (MOMP), the mitochondrial transmembrane potential is rapidly dissipated, and cytotoxic proteins that are normally seclused within the mitochondrial intermembrane space are released into the cytosol, where they promote the activation of caspases as well as of caspase-independent cell death executioner mechanisms (Michels et al. 2013).

1.7.1.1 Tumor necrosis factor (TNF) family and tumor necrosis factor receptors (TNFR)

TNF family and the receptors of these ligands activate the extrinsic pathway. Most TNF family members bind receptors that activate signals involved in pro-inflammatory responses and do not signal cell death. TNF ligands that can induce apoptosis are TNF- α , FasL, and TRAIL (TNF receptor apoptosis-inducing ligand). The ligand-bound Fas or TRAIL death receptors recruit the adapter protein Fas-associating death domain-containing protein (FADD), and bound FADD recruits initiator caspase-8 and -10 (Ricci and Zong 2006).

1.7.1.1.1 Tumor necrosis factor-alpha (TNF- α)

Tumor necrosis factor alpha (TNF- α) is a potent proinflammatory cytokine that plays an important role in immunity, inflammation, and the control of cell proliferation, differentiation, and apoptosis. (Baud and Karin 2001). This cytokine is mainly secreted by activated macrophages (M1), although it can be produced by many other cell types as well. Members of the TNFR (TNF Receptor) superfamily can send both survival and death signals to cells, as TNF- α may activate both pro-apoptotic and anti-apoptotic pathways (Onuki et al. 2006).

TNF- α induces a heterogeneous array of biological effects according to cell type. TNF- α acts by binding to its receptors, TNFR1 and TNFR2, on the cell surface. Binding of TNF- α to its two receptors results in recruitment of signal transducers (Baud and Karin, 2001). Initially, TRADD (TNFR-Associated Death Domain) protein, binds to TNFR1. Then, TRADD recruits FADD (Fas-Associated Death Domain), RAIDD (RIP-Associated ICH-1/CED-3-homologous protein with a Death Domain), MADD (MAPK Activating Death Domain) and RIP (Receptor-Interacting Protein). Binding of TRADD and FADD to TNFR1 leads to the recruitment, oligomerization, and activation of Caspase8. Activated Caspase8 subsequently initiates a proteolytic cascade that includes other Caspases (Caspases3, 6, 7) and ultimately induces apoptosis (Wajant et al. 2003).

At the level of the ovary, TNF- α has been proposed as an intraovarian modulator of granulosa cell function; granulosa cells are a source of ovarian TNF- α . Additionally, TNF has been shown to alter ovarian steroidogenesis, by effecting dose-dependent alterations in the elaboration of progesterone and androstenedione, but not estrogen. TNF may play a role in the processes of

atresia or luteolysis. It is also possible that locally produced TNF- α plays an important role as an autocrine and/or paracrine mediator in the corpus luteum during pregnancy. Luteal TNF- α may contribute to maintaining the pregnancy by stimulating the production of PGF2 α and PGE2 by the corpus luteum, indirectly resulting in an increase in progesterone output. TNF- α also stimulates thecal progestin production in adult rat preovulatory follicles (Terranova et al. 1991; Kol et al. 2008; Lanuza et al. 2002).

1.7.1.1.2 Fas–Fas ligand (FasL)

Fas (also called Apo-1 or CD95) is a death domain–containing member of the tumor necrosis factor receptor (TNFR) superfamily. It has a central role in the physiological regulation of programmed cell death and has been implicated in the pathogenesis of various malignancies and diseases of the immune system (Wajant 2002).

The Fas Receptor induces an apoptotic signal by binding to Fas ligand (FasL or CD95L) expressed on the surface of other cells. Fas is a Type-I transmembrane protein, and FasL a Type-II Transmembrane protein of TNF family (Lopez-Hernandez et al. 2006).

The interaction of this receptor with its ligand (FasL) allows the formation of a death-inducing signaling complex that includes Fas-associated death domain protein (FADD), caspase 8, and caspase 10. The auto-proteolytic processing of the caspases in the complex triggers a downstream caspase cascade leading to apoptosis. Several alternatively spliced transcript variants have been described, some of which are candidates for nonsense-mediated mRNA decay (NMD). The isoforms lacking the transmembrane domain may negatively regulate the apoptosis mediated by the full-length isoform (Lüschen et al. 2005).

1.7.1.2 *B-cell lymphoma-2 (BCL-2) family members*

Bcl-2-family proteins play central roles in cell death regulation and are capable of regulating diverse cell death mechanisms that encompass apoptosis, necrosis and autophagy. Members of the Bcl-2 family share one or more of the four characteristic domains of homology named Bcl-2 homology (BH) domains (BH1, BH2, BH3 and BH4), and can form hetero- or homodimers, which are further categorized into three subgroups, namely, prosurvival, multidomain proapoptotic, and BH3-only Bcl-2 proteins (Gross et al. 1999; Yip and Reed 2008; Yi et al. 2011).

The BCL-2 family members are the main regulators of mitochondrial outer membrane permeabilization (MOMP) as they regulate the efflux of apoptogenic proteins from mitochondria. Their proteins includes both pro- and anti-apoptotic molecules, anti-apoptotic members contain all four BH domains and include Bcl-2, Bcl-xL, Mcl-1, Bcl-w, and Bf1/A1. Pro-apoptotic members

lack the BH4 domain and are divided into two groups, the BH3-only members and the multidomain BH1-3 pro-apoptotic members Bax and Bak (Yi et al. 2011; Ricci and Zong 2006). A considerable portion of the pro- versus anti-apoptotic BCL-2 members localize to separate subcellular compartments in the absence of a death signal. Both antiapoptotic and proapoptotic members, have C-terminal transmembrane domains that insert in the outer membrane of mitochondria (Yip and Reed 2008).

Bax and Bak induce mitochondrial outer membrane permeabilization (MOMP), causing the release of caspase-activating proteins and other cell death mediators, whereas antiapoptotic proteins such as Bcl-2 serve as guardians of the outer membrane and preserve its integrity by opposing Bax and Bak. Induction of MOMP correlates with oligomerization of Bax and/or Bak in the outer mitochondrial membrane, which is opposed by antiapoptotic proteins such as Bcl-2 and Bcl-XL (Yip and Reed 2008).

Anti-apoptotic members are initially integral membrane proteins found in the mitochondria, endoplasmic reticulum (ER), or nuclear membrane. In contrast, a substantial fraction of the pro-apoptotic members localize to cytosol or cytoskeleton prior to a death signal. Following a death signal, the pro-apoptotic members that have been examined to date undergo a conformational change that enables them to target and integrate into membranes, especially the mitochondrial outer membrane (Gross et al. 1999).

1.7.1.2.1 Bcl-2-associated X protein (Bax)

Bax forms a heterodimer with BCL-2, and functions as an apoptotic activator. Bax protein interacts with, and increases the opening of, the mitochondrial voltage-dependent anion channel (VDAC), which leads to the loss in membrane potential and release of cytochrome c (www.ncbi.nlm.nih.gov/gene/581).

Bax and Bak function by interacting and antagonizing the antiapoptotic members of the family such as Bcl-2 and Bcl-xL. Overexpression of either Bax or Bak is sufficient to accelerate apoptotic cell death, suggesting that increased protein levels of these proteins could overcome the inhibitory effect of Bcl-2/Bcl-xL (Yi et al. 2011).

Bax and Bak normally exist as inactive monomers in cells, and are activated by BH3-only proteins. Following a death stimulus, cytosolic and monomeric BAX translocate to the mitochondria, where they become an integral membrane protein, and cross-linkable as a homodimer. Once at the mitochondria, Bax form clusters in the outer mitochondrial membrane and facilitates pore formation through which cytochrome c is released, and cells are killed despite the presence of survival factors (Yi et al. 2011; Gross et al. 1999).

Tumor suppressor P53 activates the expression of Bax and it has also been shown that Bax involves in P53-mediated apoptosis (Xiang et al. 1998). The presence of an anti-apoptotic molecule such as BCL-2 or BCL-XL can inhibit the activation of BAX following a death signal. It is conceivable that the signal for BAX activation emanates from the mitochondria, although other sources are not excluded (Gross et al. 1999).

1.7.1.2.2 B-cell lymphoma 2 (Bcl-2), B-cell lymphoma-extra-large (Bcl-xl)

Bcl-2 was initially identified as a proto-oncogene implicated in human follicular lymphomas carrying a chromosomal translocation, and has been associated with suppression in cytochrome c release from mitochondria (Yi et al. 2011).

Bcl-xL can form a pore-forming complex in liposomes, which can function as a pH-sensitive cation-selective channel. Thus, it is possible that Bcl-xL may alter mitochondrial permeability and volume homeostasis by influencing the open/closed configuration of VDAC. Additionally, the Bcl-2 gene encodes an integral outer mitochondrial membrane protein that blocks the apoptotic death of some cells such as lymphocytes (Yi et al. 2011; Huang et al. 1999).

Except for the antiapoptotic function of Bcl-2/Bcl-xL, there is evidence that Bcl-2/Bcl-xL may display additional antiapoptosis activity independently of Bax/Bak. They intercept upstream proapoptotic signals such as those mediated by BH3 only proteins (Yi et al. 2011; Michels et al. 2013).

Depending on which proteins Bcl-2 and Bcl-XL interact with, their phenotypes can be converted from anti- to proapoptotic, revealing an additional level of complexity to these proteins that has clear therapeutic implications for malignancies over-expressing these Bcl-2-family proteins (Yip and Reed 2008).

Damage to the Bcl-2 gene has been identified as a cause of a number of cancers, but also as a cause of resistance to cancer treatments. Bcl-2 as well as Bcl-xL expression also protects thymocytes against multiple pathological insults such as radiation, growth factor withdrawal, and heat stress (Ricci & Zong 2006; Yi et al. 2011).

Bcl-2 and Fas-signaling pathways can coexist within the same cell, as the signaling pathway to cell death induced by Fas is distinct from those regulated by Bcl-2 (Huang et al. 1999).

1.7.1.3 Phospholipid scramblases (PLSCR) family

Phospholipid scramblases are a group of homologous proteins that are conserved in all eukaryotic organisms. They are believed to be involved in destroying plasma membrane

phospholipid asymmetry at critical cellular events like cell activation, injury, and apoptosis (Sahu et al. 2007).

In humans, PL scramblases constitute a family of four homologous proteins named hPLSCR1-HPLSCR4. The biological functions of all identified members of the scramblase family are not yet completely understood, but they are supposed to play an important role in both intrinsic and extrinsic apoptotic responses that are linked to each other via the activation of caspase 8. Activated caspase 8 causes the cleavage of the amino terminal portion of the cytosolic protein Bid to generate t-Bid that is translocated into mitochondria during apoptosis. The activated t-Bid induces activation of Bax and Bak proteins to form cytochrome c channels that facilitate the release of cytochrome c during apoptosis (Sahu et al. 2007).

PLSCR4 may mediate accelerated ATP-independent bidirectional trans-bilayer migration of phospholipids upon binding calcium ions that results in a loss of phospholipid asymmetry in the plasma membrane. They may play a central role in the initiation of fibrin clot formation, the activation of mast cells, and the recognition of apoptotic and injured cells by the reticuloendothelial system (www.genecards.org/cgi-bin/carddisp.pl?gene=PLSCR4).

1.7.1.4 Galectin family (Lectin, galactoside-binding, soluble (LGALS), genes encoding galectins)

Galectins form a family of structurally related carbohydrate binding proteins (lectins). They are involved in many biological processes such as morphogenesis, control of cell death, immunological response, and cancer (Houzelstein et al. 2004). Members of the galectin family are defined by two properties: shared characteristic amino acid sequences, and affinity for β -galactoside sugars. They function both extracellularly by interacting with cell-surface and extracellular matrix glycoproteins and glycolipids, and intracellularly by interacting with cytoplasmic and nuclear proteins to modulate signaling pathways (Barondes et al. 1994; Liu & Rabinovich 2005; Cooper & Barondes 1999).

Galectins have been presumed to function in important biological processes. The most extensively-studied function of galectins is the regulation of apoptosis. Some galectins can induce apoptosis when added exogenously to cells, whereas others regulate apoptosis through intracellular mechanisms. Galectin-1 and galectin-3 can interact with oncogenic Ras and mediate cell transformation induced by this oncogene. Galectins can modulate cell adhesion and cell migration, thereby affecting the process of tumor metastasis. Galectin-3 has angiogenic activity. Galectins have pro- and anti-inflammatory functions and modulate the immune response. Furthermore, galectin-1 functions as a soluble mediator employed by tumor cells to evade the immune response. Secretion levels of many galectins increase also in response to stress, such as inflammation or heat shock (Liu & Rabinovich 2005; Barondes et al. 1994).

Galectin-3, -7, and -12 have been shown to regulate cell growth, and apoptosis, being either anti-apoptotic or pro-apoptotic. Galectin-3 and -12 have been shown to regulate the cell cycle, by arresting G₁ or G₂/M phase. Additionally, some galectins protect cells from a variety of death signals, including Fas receptor cross-linking and loss of cell anchorage (Liu et al. 2002; Hsu et al. 2015)

Galectins have important roles in cancer; they contribute to neoplastic transformation, tumor cell survival, angiogenesis, and tumor metastasis. They can modulate the immune and inflammatory responses and might have a key role helping tumors to escape immune surveillance (Liu & Rabinovich 2005).

1.7.2 Stress-responded genes

1.7.2.1 Hypoxia-inducible factor 1- α (HIF-1A)

Hypoxia-inducible factor 1 (HIF-1) is a basic helix–loop–helix transcription factor that mediates homeostatic responses to hypoxia. HIF-1 is a heterodimer consisting of the hypoxic response factor HIF-1 α and a HIF-1 β subunit. In the absence of oxygen, HIF-1 α / HIF-1 β heterodimers bind to hypoxia-response elements, thereby activating the expression of numerous hypoxia-response genes (Semenza et al. 1996; Wellmann et al. 2004).

Hypoxia is a reduction in the normal level of tissue oxygen tension that occurs in humans living in high altitudes; it is common in a variety of acute and chronic vascular, pulmonary, and neoplastic diseases. Under hypoxic conditions, the transcription of a variety of genes involved in glucose metabolism, cell proliferation, angiogenesis, erythropoiesis, and other adaptive responses increases. Gene regulation by hypoxia is widely dependent on activation of the transcriptional complex HIF-1. Thus HIF-1 plays an essential role in embryonic vascularization, tumor angiogenesis, and the pathophysiology of ischemic disease (Wang et al. 1995).

1.7.2.2 Heat shock proteins (HSPs)

The most conserved cellular response to stress is the expression of heat shock proteins (hsp). These proteins participate in the repair of cellular damage after stress, which is necessary for a positive recovery, and confers further protection from subsequent insults (De Maio 2014).

However, some of these hsps are present in unstressed cells and play an important role in the folding and translocation of polypeptides across membranes. They have thus been termed molecular chaperones. Hsps are expressed in response to hyperthermia, oxygen radicals, heavy

metals, ethanol, and amino acid analogues. In addition, the heat shock response is induced during clinically relevant situations such as ischemia/reperfusion and circulatory and hemorrhagic shock. All of the above stresses have in common that they disturb the tertiary structure of proteins and have adverse effects on cellular metabolism (De Maio 1999).

In the current study, four Hsps were studied: Hsp27, Hsp47, Hsp70 and HspH1 (Hsp105). Heat-shock proteins are mainly named according to their molecular weight. This means that the hsp studied are referred to families of heat shock proteins in the order of 27, 47, 70, and 105 kilodaltons in size, respectively.

1.7.2.2.1 Heat shock protein 27 (Hsp27)

Hsp27 has important roles in many cellular processes, including cytoskeleton dynamics, cell differentiation, and apoptosis. Heat shock protein 27 (HSP27) belongs to the small molecular weight heat shock protein (HSP) family (12–43 kDa). HSP27 was initially characterized in response to heat shock as a protein chaperone that facilitates the proper refolding of damaged proteins. Furthermore, HSP27 protein responds to cellular stress conditions other than heat shock, for example oxidative stress and chemical stress. During oxidative stress, HSP27 functions as an antioxidant, lowering the levels of reactive oxygen species (ROS) by raising levels of intracellular glutathione, and lowering the levels of intracellular iron. The Hsp27 protein functions as an anti-apoptotic agent under conditions of chemical stress by interacting with both mitochondrial-dependent and -independent pathways of apoptosis. HSP27 is particularly involved in protection from programmed cell death by inhibition of caspase-dependent apoptosis. Lastly, HSP27 has been characterized with the ability to regulate actin cytoskeletal dynamics during heat shock and other stress conditions, functioning both to promote actin polymerization and as an actin capping protein (Robitaille et al. 2010; Vidyasagar et al. 2012).

1.7.2.2.2 Heat shock protein 47 (Hsp47)

Heat shock protein 47 (Hsp47) is a procollagen/collagen-specific molecular chaperone protein derived from the serpin family of proteins, and essential for the early stages of collagen biosynthesis (Dafforn et al. 2001).

It is a stress protein that resides in the endoplasmic reticulum, and is thought to participate in intracellular processing, folding, assembly, and secretion of procollagens. Irrespective of the tissue site and organ, induction of colligin/HSP47 expression is always noted during the process of fibrosis, particularly in and around the fibrotic lesions in both humans and experimental

models. Its expression is highly tissue- and cell-specific, and restricted to mostly phenotypically altered collagen-producing cells (Razzaque and Taguchi 1999).

Autoantibodies to the encoded protein have been found in patients with rheumatoid arthritis. Expression of this gene may be a marker for cancer, and nucleotide polymorphisms in this gene may be associated with preterm birth caused by preterm premature rupture of membranes. Alternatively spliced transcript variants have been observed for this gene, and a pseudogene of this gene is located on the short arm of chromosome 9 (www.ncbi.nlm.nih.gov/gene/871).

1.7.2.2.3 Heat shock protein 70 (Hsp70)

The HSP70 family of proteins is the most temperature-sensitive and highly conserved among the HSPs. Hsp70 is a dimeric, ubiquitous protein that binds its substrates in an extended conformation through hydrophobic interactions (Kregel 2002; Burston and Clarke 1995). HSP70 contains three domains: the ATPase N-domain that hydrolyzes ATP; the substrate domain that binds proteins; and the C-domain that provides a “lid” for the substrate domain. Because of its three-domain structure, HSP70 forms a single ATPase cycle that involves the association and disassociation of the client protein (Malyshev 2013).

Hsp70s assist a wide range of folding processes, including the folding and assembly of newly synthesized proteins, refolding of misfolded and aggregated proteins, membrane translocation of organellar and secretory proteins, and control of the activity of regulatory proteins. Hsp70s thus have housekeeping functions in the cell in which they are built-in components of folding and signal transduction pathways, and quality control functions in which they proofread the structure of proteins and repair misfolded conformers. All of these activities appear to be based on the property of Hsp70 to interact with hydrophobic peptide segments of proteins in an ATP-controlled fashion. The substrate binding and release cycle is driven by the switching of Hsp70 between the low-affinity ATP bound state and the high-affinity ADP bound state. Hsp70 proteins with their co-chaperones and cooperating chaperones thus constitute a complex network of folding machines (Burston and Clarke 1995; Mayer and Bukau 2005).

Hsp70 is also associated with the development of tolerance to a variety of stresses, including hypoxia, ischemia, acidosis, energy depletion, cytokines such as tumor necrosis factor- α (TNF- α), and ultraviolet radiation (Kregel 2002).

1.7.2.2.4 Heat shock protein H1/105 (HspH1 or Hsp105)

HspH1 is a protein that in humans is encoded by the HSPH1 gene (www.ncbi.nlm.nih.gov/gene/10808). It prevents the aggregation of denatured proteins in cells under severe stress, on which the ATP levels decrease (Yamagishi et al. 2003).

Hsp105 is a member of the Hsp70 super family of molecular chaperones. It serves as a nucleotide exchange factor for Hsc70, independently prevents the aggregation of misfolded proteins, and functionally relates to Hsp90. Like Hsp70, it consists of an amino-terminal ATPase domain and a carboxyl terminal substrate binding domain (SBD). It refolds denatured proteins in vitro in the absence of Hsc70, and in the cytosol forms high molecular weight complexes with Hsc70. Furthermore, Hsp105 stabilizes apolipoprotein B in the ER and promotes its secretion. There are two mammalian Hsp105 isoforms: Hsp105 α and Hsp105 β . Hsp105 α is constitutively expressed, and is further inducible by heat shock or stress. Hsp105 β is an alternatively spliced form of Hsp105 α , and strictly heat-induced (Saxena et al. 2012).

1.7.2.3 CIRBPT (*Cold-inducible RNA-binding protein*)

In response to low temperature, mammalian cells change various physiological functions. Cold stress changes the lipid composition of cellular membranes, and suppresses the rate of protein synthesis and cell growth. Cold stress induces the synthesis of several cold-shock proteins, which are involved in various cellular processes such as transcription, translation, and DNA recombination (Nishiyama et al. 1997).

Cold-inducible RNA-binding protein (CIRP), a cold-shock 18-kD protein, consists of an N-terminal RNA-binding domain and a C-terminal Gly-rich domain, and is a member of the glycine-rich RNA-binding protein (GRP) family. The human CIRP gene has been mapped to the chromosomal locus 19p13 (Nishiyama et al. 1997; Danno et al. 1997; Hamid et al. 2003).

In response to mild hypothermia CIRP is up-regulated. The exact function of this protein is unknown, but it is thought to function as an RNA chaperone, facilitating mRNA translation upon the perception of cold stress. Additionally, CIRP plays an essential role in cold-induced suppression of cell proliferation, as its overexpression results in prolongation of G1 phase in vitro. CIRP is also involved in temperature-dependent regulation of cell growth (Al-Fageeh & Smales 2009; Nishiyama et al. 1997 Dec; Nishiyama et al. 1997, May).

CIRP is also localized in the nuclei of glandular, stromal, and endothelial cells. It has been suggested that it may participate in the cell-cycle regulation of normal endometrium, and the loss of its expression may be involved in endometrial carcinogenesis (Hamid et al. 2003).

1.7.2.4 *RBM3 (RNA-binding motif protein 3)*

The human RNA binding motif protein 3 (RBM3) is structurally highly similar to the cold-inducible RNA-binding protein (CIRP). Like CIRP, RBM3 is a member of the GRP family. It is induced in human cells in response to cold stress (32 °C), and low oxygen tension where it plays distinct roles (Danno et al. 2000; Danno et al. 1997).

RBM3 is one of three X-chromosome related RBM-genes (RBMX, RBM3, RBM10) mapped to Xp11.23. It is expressed in various human fetal tissues, and is one of the earliest proteins induced by hypothermia (Ehlén et al. 2010). It contains a RNA-recognition motif (RRM) through which it binds to both DNA and RNA. Proteins containing specific RRM motifs play an important role in the stabilization of mRNA by reversibly binding to conserved sequence elements (Ehlén et al. 2011). Splicing, transport of mRNA, and ultimately mRNA translation into proteins are also tightly regulated by RNA-binding proteins. The RBM3 is an evolutionary highly conserved RNA binding protein of 157 amino acids with a predicted mass of 17 kD (Wellmann et al. 2010).

RBM3 mRNA and protein are up-regulated in human tumors. RBM3 is a novel proto-oncogene that induces transformation when overexpressed and is essential for cells to progress through mitosis. It also induces non-transformed cells to grow in an anchorage-independent manner (Sureban et al. 2008).

Under conditions of RBM3 down-regulation, cells undergo mitotic catastrophe, because RBM3 increases mRNA stability and translation of otherwise rapidly degraded transcripts. In addition, as RBM3 is a global translation inducer, it is tempting to speculate that it not only transports the mRNAs, but also loads them onto ribosomes to induce translation. The observation that the increase in RBM3 expression is dependent on the tumor stage suggests that it may play a role in tumorigenesis. Therefore, it may represent a potential target for chemotherapeutic and chemopreventive strategies (Sureban et al. 2008).

1.7.3 Genes related to cell development

1.7.3.1 *FABP3 (Fatty acid-binding protein 3)*

Fatty acid-binding proteins (FABPs) are members of the superfamily of lipid-binding proteins (LBP). According to the tissue-specific distribution, 9 different FABPs have been identified: L (liver), I (intestinal), H (muscle and heart), A (adipocyte), E (epidermal), IL (ileal), B (brain), M (myelin) and T (testis). They are divided into at least three distinct types, namely the hepatic, intestinal, and cardiac -type (Chmurzyńska 2006; Spener et al. 1990).

All FABPs are involved in lipid metabolism by intracellular transport of long-chain fatty acids. Their genes consist of 4 exons and 3 introns; a few of them are located in the same chromosomal region, and they form 14-15 kDa proteins (Hashimoto et al. 2004; Chmurzyńska 2006). FABPs may be responsible in the modulation of cell growth and proliferation (Yang et al. 1994).

Human FABP3, one of the FABPs, is present in a wide variety of tissues with highest concentration in cardiac and skeletal muscle. It may play an important role in fatty acid transport, cell growth, cellular signaling, and gene transcription. Zhu et al. and Shen et al. have shown that overexpression of FABP3 can inhibit proliferation and promote apoptosis in embryonic carcinoma cells (P19 cells). Moreover FABP3 may be involved in the differentiation of cardiac myocytes (Shin et al. 2003; Zhu et al. 2011; Shen et al. 2013).

Differences occur in the level of the FABP3 gene product in different tissue types and variations in response to environmental stimuli. The highest relative expression occurs in the heart, with lower levels of expression in “slow” skeletal muscle. Lower but detectable levels of expression occur in “fast” skeletal muscle, the aorta, placenta, adrenal, ovary, and testis. The same gene is expressed in a highly regulated manner in the mammary gland, where it arrests the growth of mammary epithelial cells, and is termed mammary-derived growth inhibitor (MDGI) (Qian et al. 1999). FABP3 may also play an important role during embryonic heart development; either overexpression or silencing of FABP3 will lead to an imbalance between proliferation and apoptosis, which may result in embryonic cardiac malformations (Shen et al. 2013).

1.7.3.2 *CRIPT (Cysteine-Rich PDZ-Binding Protein)*

Cysteine-rich PDZ-binding protein is a protein that in humans is encoded by the CRIPT gene. The CRIPT protein is a cytoskeletal protein involved in microtubule production. The C-terminal domain is essential for binding to the PDZ3 domain of the PSD-95/SAP90 protein, one of a superfamily of PDZ-containing proteins. PDZs are small globular domains composed of approximately 90 amino acids exhibiting high sequential homology, and functioning as protein-protein interaction modules (Piserchio et al. 2006).

Synaptic associated proteins (SAPs), a family of multidomain proteins, act as molecular scaffolds, playing an important role in the signaling and maintenance of several receptors and channels. The SAPs consist of 3 PDZ (PSD95, Disc Large, Zo1) domains. The 3 PDZ domains bind the C-termini of specific receptors and channels, leading to the transient association with cytoskeletal and signaling proteins. Molecules targeting specific domains of the SAPs may provide a novel route for the regulation of channel and receptor function (Piserchio et al. 2006).

CRIPT is a postsynaptic protein, highly conserved from mammals to plants, that binds selectively to the third PDZ domain (PDZ3) of PSD-95/SAP90, and is suggested to regulate PSD-95 interaction with a tubulin-based cytoskeleton in excitatory synapses. CRIPT also binds directly to

microtubules, thereby linking PSD-95/SAP90 to the microtubule cytoskeleton (Niethammer et al. 1998; Passafaro et al. 1999).

1.8 HUMAN GRANULOSA-LIKE TUMOR CELL LINE, KGN

The KGN cell line is considered to be a very useful model for studying human granulosa cells. It originated from a Stage III granulosa cell carcinoma removed from a 63-years old Japanese woman in 1984. The tumor recurred and was surgically removed in January 1994. A portion of the tumor recurrence was removed from establishment of the cell line. The cells grew as a monolayer, with a doubling time of 46, 4 hours (Havelock 2004).

KGN cell line is extensively used in studies as was shown to maintain many of the physiological features of normal human granulosa cells, including steroidogenesis and secretion of estrogens (Nishi et al. 2001; Deura et al. 2005; Horling et al. 2011). Furthermore, several studies have demonstrated that KGN cells respond similarly to primary human granulosa cells upon stimulation with hormones (Reverchon et al. 2012; Reverchon et al. 2013). Therefore, this cell line is an excellent and applicable in vitro model to study effects on human granulosa cell functioning.

2 AIM OF THE STUDY

The aim of this study is the investigation of two vitrification methods.

In Protocol 1, a self-manufactured protocol, solutions with increasing concentrations of dimethyl sulphoxide (DMSO) are used. In protocol 2, a commercial protocol used for IVF treatment of women, 12mg/ml human albumin solution (HAS), and the cryoprotectants, 1,2-propanediol (PROH), ethylene glycol (EG), and Sucrose are used.

The protocols are compared in terms of cell survival rates, mouse ovary survival, changes in selected-gene expression, and changes in the cell cycle.

For this analysis a Human Granulosa-Like Tumor Cell Line, KGN and mouse ovaries, were used as models for the in vitro vitrification processes.

This study is expected to yield the following results:

- To determine whether certain genes are influenced by the vitrification/thawing process.
- If the expression of those genes is different also between the different vitrification protocols.
- To find the protocol with the best viability rate in KGN cells and mouse ovaries.

3 MATERIALS AND METHODS

3.1 MATERIALS

3.1.1 Equipment

Equipment	Company	Equipment	Company
0.2ml thin-walled microcentrifuge tubes	AB Applied Biosystems	FACs tubes	FALCON
1.5 ml Eppendorfs Sterile	eppendorf	Flasks 150 cm ²	
10µl Pipette Tips	Biozym	Fluorescence microscope	OLYMPUS BX50
1000 µl Pipette Tips	Biozym	Gilson Pipettes	Gilson
10ml Pipettes	SARSTEDT	Heating Block	Eppendorf
15ml Tubes Sterile	SARSTEDT	Incubator 37°C + 5%CO ₂ + 90% Relative Humidity	HERA cell
-20°C Refrigerator	LIEBHERR	Laboratory scale	
200µl Pipette Tips	Biozym	Light Microscope	ZEISS Axiovert 200
25ml Pipettes	SARSTEDT	Liquid Nitrogen Tank	Biosystem
2ml Eppendorfs Sterile	Biozym	MicroAmp Optical 96-Well Reaction Plates	
2ml Pipettes	Nalge Nunc International	MicroAmp Optical Adhesive Film	
4°C Refrigerator	LIEBHERR	Microscope Slides	Thermo Scientific
50 ml Tubes Sterile	SARSTEDT	Microtiter Plate Reader	FLUOstar OPTIMA
5ml Pipettes	costar	NanoDrop 2000	
BD FACS (Flow Cytometer)	BECTON DICKINSON	Thermal Cyclor (PCR machine)	MJ Research Peltier Thermal Cycle
Centrifuge	Eppendorf (5415R)	Thermal Cyclor (qPCR machine)	AB Biosystems
Centrifuge	Hettich (Rotanta 460 PC)	Ultraviolet (UV) Transilluminator	UVP Laboratory Products
Cryotome		Vortex	LABINCO
Electrophoresis Tank		Water Bath	GFL

3.1.2 Chemicals and Kits

Chemical/Buffer	Company	Chemical/Buffer	Chemical/Buffer
0,5 kbp DNA Ladder		Gentamicin (50 mg/ml)	PAA
0.25% Trypsin-EDTA solution		JumpStart REDTaq ReadyMix PCR Reaction Mix	SIGMA
1kbp DNA Ladder	Fermentas	Liquid nitrogen	
Agarose	Biozym LE	MediCult Vitrification Cooling	origio
BSA		Penicillin/ Streptomycin 100	
Calcein-AM	SIGMA - ALDRICH	PI/RNase Staining Buffer	BD Pharmigen
Cellstain Double Staining Kit	Fluka Analytical	Power SYBR Green PCR Master Mix (5ml)	Applied Biosystems
Collagenase	SIGMA	Primers	SIGMA
Dimethyl sulfoxide (DMSO)	CryoSure	Progesterone Enzyme Immunoassay Kit (ELISA)	IBL International
DNA Loading 6x Dye	Thermo Scientific	Ready-to-use Propidium Iodide (PI)	BD Pharmigen
Dulbecco's Modified Eagle's Medium (DMEM)	GIBCO	REDTaq® ReadyMix™ PCR Reaction Mix	SIGMA
DPBS – Dulbecco's Phosphate-Buffered Saline	GIBCO	RNase-free water	
FACs tubes		Scott's tap water	
Fetal Bovine Serum		Sucrose	USB
First Strand cDNA Synthesis Kit	Fermentas	Total RNA Purification Kit	QIAGEN
GelRed 10 000X stock reagent	Bioticum		

3.1.3 Chemicals prepared in the laboratory

Solution	Content
70% ethanol	70ml+30ml H ₂ O
Culture Media	DMEM+10% FBS+1% Progesterone-Streptomycin
DNA Electrophoresis Agarose Gel	1,5% Agarose (1,5g agarose in 100ml TAE buffer)
Elisa Wash Solution	15 ml 40x concentrated Wash Solution+585 ml deionized water
Sucrose Solutions (0,75M)	2,65gr Sucrose+9ml DPBS+9µl Gentamicin+0,9ml BSA
Vitrification Solution with DMSO	23% DMSO+10% BSA+67% DMEM

3.1.4 Oligonucleotide primers

Oligo Name	Sequence 5' to 3'	Gene Name	Size (bp)
18SRNA-fw	GTAACCCGTTGAACCCATT	18s ribosomal RNA- forward	150
18SRNA-rev	CCATCCAATCGGTAGTAGCG	18s ribosomal RNA- reverse	150
Bax-fw	TCTGACGGCAACTTCAACTG	Bcl-2-associated X protein-forward	185
Bax-rev	GAGGAGTCTCACCCAACCAC	Bcl-2-associated X protein-reverse	185
Bcl2-fw	TGCACCTGACGCCCTTCAC	B-cell lymphoma 2- forward	298
Bcl2-rev	AGACAGCCAGGAGAAATCAAACAG	B-cell lymphoma 2- reverse	298
BCL-2fw-02-2011	ATGTGTGTGGAGAGCGTCAACC	B-cell lymphoma 2- forward	196
BCL-2rev-02-2011	TGAGCAGAGTCTTCAGAGACAGCC	B-cell lymphoma 2- reverse	196
Bcl-xL-fw	GTAAACTGGGGTCGCATTGT	B-cell lymphoma-extra-large-forward	197
Bcl-xL-rev	TGCTGCATTGTTCCCATAGA	B-cell lymphoma-extra-large-reverse	197
CIRBP1-fw	TTAGGAGGCTCGGGTCGTTG	Cold-inducible RNA-binding protein- forward	137
CIRBP1-rev	GCGACTGCTCATTGGTGTCA	Cold-inducible RNA-binding protein- reverse	137

CRIPT-fw	GGAAGGATGGTGTGCGAAAA	Cysteine-Rich PDZ-Binding Protein- forward	102
CRIPT-rev	TCTTCCACCACTTTCTGTGGTA	Cysteine-Rich PDZ-Binding Protein- reverse	102
CYP19A1-fw	AGACGCAGGATTTCCACAGAAG AGA	Cytochrome P450, Family 19, Subfamily A, Polypeptide 1- forward	204
CYP19A1-rev	CCTCTTCAACATTAGGGTGCTTT GC	Cytochrome P450, Family 19, Subfamily A, Polypeptide 1- reverse	204
FABP3-fw	GGGGTGGAGTTCGATGAGAC	Fatty acid-binding protein 3- forward	105
FABP3-rev	CTCTTGCCCGTCCCATTCT	Fatty acid-binding protein 3- reverse	105
Fas-fw	ACACTGTGACCCTTGACCAA	Fas cell surface death receptor- forward	110
Fasrev	AGCCACCCCAAGTTAGATCTG	Fas cell surface death receptor- reverse	110
Fas-fw	TCACTTCGGAGGATTGCTCAA	Fas cell surface death receptor- forward	101
Fas-rev	GGGCATTAACACTTTTGGACG	Fas cell surface death receptor- reverse	101
FasL-fw	GGCCCATTTAACAGGCAAGTC	Fas Ligand- forward	104
FasL-rev	GGCCACCCTTCTTATACTTCAC	Fas Ligand- reverse	104
GAPDH-fw	CCACCCATGGCAAATTCC	Glyceraldehyde-3-Phosphate Dehydrogenase- forward	70
GAPDH-rev	GATGGGATTTCCATTGATGACA	Glyceraldehyde-3-Phosphate Dehydrogenase- reverse	70
GAPDH-fw	CCTGTTCGACAGTCAGCCG	Glyceraldehyde-3-Phosphate Dehydrogenase- forward	101
GAPDH-rev	CGACCAAATCCGTTGACTCC	Glyceraldehyde-3-Phosphate Dehydrogenase- reverse	101
HIF1A-fw	ATTCACCATGGAGGGCG	Hypoxia-inducible factor 1-alpha- forward	148
HIF1A-rev	GTGGAAGTGGCAACTGATGA	Hypoxia-inducible factor 1-alpha- reverse	148
HSP27-fw	GTCCCTGGATGTCAACCACT	Heat shock protein 27 kDa- forward	112
HSP27-rev	AGATGTAGCCATGCTCGTCC	Heat shock protein 27 kDa- reverse	112
HSP47-Ser-fw	AAGATGGTGGACAACCGTGG	Heat shock protein 47 kDa- forward	155

HSP47-Ser- rev	ATGAGGCTGGAGAGCTTGTG	Heat shock protein 47 kDa- reverse	155
HSP70-fw	ATGAGTATAGCGACCGCTGC	Heat shock protein 70 kDa- forward	115
HSP70-rev	TCCTTGGACTGTGTTCTTTGC	Heat shock protein 70 kDa- reverse	115
HSPH1-fw	TCGAGACCATCGCCAATGAG	Heat shock protein H1/105 kDa- forward	89
HSPH1-rev	GGCTGCAACTCCGATTGTTC	Heat shock protein H1/105 kDa- reverse	89
IGF1-fw	CCTCCTCGCATCTCTTCTACCTG	Insulin-like growth factor system- forward	166
IGF1-rev	CTGCTGGAGCCATACCCTGTG	Insulin-like growth factor system- reverse	166
LGALS- H159-fw	GGGGTGAAGAACAGTCAGCA	lectin, galactoside-binding, soluble- forward	86
LGALS- H159-rev	ACGTGGGTGCTCACAAAGAA	lectin, galactoside-binding, soluble- reverse	86
LH/hCGRec- fw	GAACTGAGTGGCTGGGACTA	Luteinizing hormone/choriogonadotropin receptor- forward	249
LH/hCGRec- rev	GCAAAAGTCTGCAAAGGAGA	Luteinizing hormone/choriogonadotropin receptor- reverse	249
mPRalpha- fw	GCTGTTCACATCCC	Membrane progestin receptor alpha - forward	289
mPRalpha- rev	TGGTGCAACCCCCAGA	Membrane progestin receptor alpha - reverse	289
mPRbeta- fw	GCGGCCCTGGTACTGCTGC	Membrane progesterone receptor beta- forward	200
mPRbeta- rev	CACGGCCACCCCCACA	Membrane progesterone receptor beta- reverse	200
mPRdelta- fw	CCCCAACTTCTCAAGTCCA	Membrane progesterone receptor delta- forward	114
mPRdelta- rev	CTGGAAGGAGCTGAGGACAC	Membrane progesterone receptor delta- reverse	114
mPRgamma -fw	CAGCTGTTTCACGTGTGTGTGAT CCTG	Membrane progesterone receptor gamma- forward	120
mPRgamma -rev	GCACAGAAGTATGGCTCCAGCT ATCTGAG	Membrane progesterone receptor gamma- reverse	120
PGRMC1-fw	TCTGGACTGCACTGTTGTCCTTG	Progesterone receptor membrane component 1- forward	250

PGRMC1-rev	GCAAACACCTGTTCTATTCTG	Progesterone receptor membrane component 1- reverse	250
PLSCR4-fw	CATGGGTCTCTGGCGTTTCT	Phospholipid scramblase 4- forward	93
PLSCR4-rev	AGTTTGTGTACGGTGCCCT	Phospholipid scramblase 4- reverse	93
PR-A/B-fw	TTTCGACCTCCAAGGACCAT	Progesterone receptor isoform A/B- forward	254
PR-A/B-rev	AGCCCACAATACAGCTTCGAG	Progesterone receptor isoform A/B- reverse	254
PR-B-fw	AGCAGTCCGCTGTCCTTTTCT	Progesterone receptor isoform B- forward	196
PR-B-rev	CCTGAAGTTTCGGCCATACCT	Progesterone receptor isoform B- reverse	196
RBM3-fw	CCATGAACGGAGAGTCTCTGGA	RNA-binding motif protein 3- forward	157
RBM3-rev	TAATACCTGCCACTCCCATAGC	RNA-binding motif protein 3- reverse	157
TNF-a-fw	ATCCTGGGGGACCCAATGTA	Tumor necrosis factor-alpha- forward	112
TNF-a-rev	AAAAGAAGGCACAGAGGCCA	Tumor necrosis factor-alpha- reverse	112

3.2 METHODS

3.2.1 Human Granulosa-Like Tumor Cell Line, KGN

The ovarian granulosa cell line (KGN) has been used for this study as human granulosa cell cultures have been difficult to use for research.

The KGN cell line is a useful model for understanding the regulation of steroidogenesis, cell growth, and apoptosis in human granulosa cells, as they show a pattern similar to that of steroidogenesis in human granulosa cells (Nishi 2001).

For this study KGN cells were kept in a DMEM/10% FBS/1% Progesterone-Streptomycin culture medium at 37°C and 5% CO₂.

3.2.2 Vitrification of Mouse Ovaries and KGN cells

For the vitrification of C57BL/6J mouse ovaries and KGN cells, two different protocols were tested: protocol 1, where solutions with increasing concentrations of dimethyl sulphoxide (DMSO) were used, and protocol 2, which has been designed for the vitrification, storage, and warming of oocytes and embryos, and is used for IVF treatment of women. Protocol 2 consists of an equilibration and a vitrification medium, which contain 12mg/ml human albumin solution (HAS), and the cryoprotectants, 1,2-propanediol (PROH), ethylene glycol (EG), and Sucrose. Until used, the ovaries were kept in D-PBS at 4°C.

3.2.2.1 *Protocol 1 Vitrification Procedure: Solution Containing Dimethyl Sulphoxide (DMSO), Bovine Serum Albumin (BSA), and Dulbecco's Modified Eagle Medium (DMEM)*

In the protocol 1 vitrification procedure, for mouse ovaries and KGN cells, solutions with increasing concentrations of dimethyl sulphoxide (DMSO) were used. A Vitrification Solution (VS) containing 23% DMSO, 10% BSA and 67% DMEM was prepared. Initially, the samples (mouse ovaries or KGN cells) were equilibrated in 25% VS for 5 minutes. Then 1 ml 50% VS was added for 5 minutes at room temperature (RT), and 1 ml 100% VS was added for 10 minutes. Every VS was removed by centrifugation at 300 rcf for 30 seconds at RT, and the supernatant aspirated. The tubes were plunged quickly into liquid nitrogen. The samples could be used immediately or stored in the storage tank, where the vitrified samples must be under liquid nitrogen at all times.

3.2.2.2 *Protocol 2 Vitrification Procedure: Media Containing HAS, PROH, EG and Sucrose.*

Protocol 2 consists of two vials, the first of which contains the Equilibration Medium, and the second the Vitrification Medium. Before this product was used, the two media were warmed at room temperature for at least 30 minutes, their content was mixed by a few gentle inversions; and a reservoir with liquid nitrogen was prepared. A 1000 µl pipette was used to transfer 1ml Equilibration Medium into each tube, which contained a mouse ovary or KGN cells. The cells initially shrink before re-expanding to their original size. Equilibration was completed once the ovary or the cells had re-expanded, a procedure that needed 5-15 minutes at room temperature. The equilibration medium was removed by centrifugation at 300 rcf for 30 seconds at room temperature. 1 ml Vitrification Medium was added in the sample, and the cells shrink again. The time from the Vitrification Medium addition until the sample is vitrified must not exceed 1 minute. The sample was centrifuged at 600 rcf for 30 seconds at room temperature and the Vitrification Medium removed. The tubes were immediately plunged into liquid nitrogen. The

samples could be used immediately or stored in the storage tank, where the vitrified samples must be under liquid nitrogen at all times.

3.2.2.3 *Vitrification procedure of KGN cells on slides*

KGN cells were also vitrified by the protocol 1 and 2 on slides. The procedures and the time of incubations were the same. The only difference were that the media were add and removed by using a 1000 µl pipette.

3.2.3 Thawing Procedure of Vitrified Mouse Ovaries or Cells

Six Sucrose Solutions (0,75M – 0,625M – 0,5M – 0,375M – 0,25M – 0,125M) were prepared for the gradual removal of the cryoprotectants. 2,65 g – 2,21 g – 1,77 g – 1,33 g – 0,89 g – 0,45 g sucrose respectively was weighted out using a laboratory scale, and put in 6 sterile Falcon Tubes. Additionally, a Stock Solution of, 60 ml DPBS, 60µl Gentamicin (50 mg/ml) and 6 ml BSA was prepared. 10 ml of the Stock Solution was added in each Falcon, the solutions were mixed until Sucrose was completely dissolved and stored at 4°C.

The vitrified samples, which were stored in liquid nitrogen in the storage tank, were taken out and incubated at RT for 30 seconds. They were then kept at 37°C in a water bath for around for 120 seconds; the frozen medium was observed, and when just a central ice crystal of the medium was left, the samples were taken out of the water bath.

For the removal of the cryoprotectant and the restoration of the cell volume, 1 ml of the highest concentration of the Sucrose Solutions (0,75M) was added to each vitrified sample for 15 minutes at room temperature. After 15 minutes the first sucrose solution was removed, and 1 ml of the second highest concentration of the Sucrose Solutions (0,625M) added; incubation lasted for 6 minutes. The incubation procedure was repeated sequentially for the rest of the Sucrose Solution (0,5M – 0,375M – 0,25M – 0,125M). For the removal of each Sucrose Solution a centrifugation at 300 rcf for 30 seconds at room temperature was performed. In all incubation steps, tubes were mixed by gentle inversions.

3.2.4 Ovarian Tissue Vitality Test (Collagenase)

Collagenase mediated tissue dissociation is an important step in cell isolation procedures. Collagenases are enzymes that are able to cleave the peptide bonds in the triple helical collagen

molecule. Through this enzyme, follicles can be isolated from mouse ovaries and stained with Calcein in order to test their viability.

In a Calcein aliquot (4mM), 600 µl DMEM medium was added, and the solution (8,5mM) was put in the first well of a 4-well dish. 7 mg Collagenase were dissolved in 20µl Calcein (4mM) and 973 µl Medium, and the solution was put in the second well of the 4-well dish.

The dissociation was achieved by perfusing whole mouse ovary with enzyme solution.

The mouse ovary was first incubated for 1 hour at 37°C in the first well of the 4-well dish, after which it was transferred to the second well, and the incubation lasted 2 hours. Using a 1000µl-Pipette, the first homogenization was done after the first hour of incubation, the second after the second hour of incubation. At the end, a 15 minutes incubation in light-protected conditions at room temperature was performed.

Using Fluorescence microscopy, the dissociated and stained mouse ovary was observed, for alive and dead follicles.

3.2.5 Hematoxylin Staining Of Mouse Ovaries Sections

Hematoxylin is a natural dye extracted by boiling the wood of the South American and West Indian logwood tree (*Haematoxylon campechianum*). The active dye is not hematoxylin itself, but its oxidized product, haematin.

Haematin exhibits indicator-like properties, being blue and less soluble in aqueous alkaline conditions, and red and more soluble in alcoholic acidic conditions. In acidic conditions, haematin binds to lysine residues of nuclear histones by linkage via aluminium metallic ion mordant (<http://stainsfile.info/StainsFile/stain/hematoxylin/hxintro.htm>).

Sections of mouse ovaries were made by a cryotome. Nuclei of the cells were stained with alum haematoxylin for 4 minutes. To ensure saturation of chemical binding sites, the stain was applied longer than necessary, resulting in the over-staining of the tissues with much non-specific background coloration. This undesirable coloration was selectively removed by two quick dips in 0.3% acid alcohol; the acid solution alters the color of the tissue to red.

The tissue color was changed to blue and gave a much better contrast with the usual red counterstains, by a process termed "differentiation". Differentiation is arrested by returning to an alkaline environment, whereupon the haematin takes on a blue hue, the process of "blueing-up". To manage this, the sections were rinsed in tap water, which tends to be slightly acid, with a pH in the range of 6.0 - 6.8. However, this is considerably more alkaline than the pH of most alum hematoxylin (2.6 - 2.9), so it leads to blueing results. Additionally, tap water has the added advantage that it washes out any excess alum, giving a crisper nuclear stain and preventing fading

during storage. Sections were rinsed also in Scott's tap water substitute, as blueing up is achieved in a much shorter time.

Finally, the sections were rinsed again in tap water, dehydrated, cleaned, and covered with a coverslip.

3.2.6 Progesterone ELISA

For the quantitative determination of Progesterone in mouse ovary serum the “Progesterone Enzyme Immunoassay Kit” was used as per manufacturer’s instructions. This is a solid phase enzyme-linked immunosorbent assay (ELISA) based on the principle of competitive binding.

Before proceeding with the assay, all reagents, serum references, and controls were brought to room temperature (20-27°C), and the Wash Solution was prepared: 15 ml of 40x concentrated Wash Solution were diluted in 585 ml deionized water to a final volume of 600 ml. Once the test has been started, all steps should be completed without interruption. As absorbance is a function of incubation time and temperature, this will ensure equal elapsed time for each pipetting step.

The microplates' wells were secured for each serum reference, control, and patient specimen to be assayed in duplicate. 25 µl of the appropriate serum reference, control or specimen were pipetted into the assigned well. The incubation lasted for 5 minutes at RT, so that Progesterone (antibody) could bind in Antigen of Progesterone.

Then 200 µl enzyme Conjugate was added to each well, the microplate was swirled gently for 10-20 seconds to mix, covered and the incubation lasted for 60 minutes at RT. In this step the enzyme Conjugate binds specific to Progesterone.

After incubation, the contents of the wells were briskly shaken out, and rinsed 4 times with diluted Wash Solution (200 µl per well). The plate was washed in order to remove unbound enzyme Conjugate and unbound antibodies or proteins of the serum.

After the final washing step, 200 µl of Substrate Solution were added to each well, and incubation lasted for 15 minutes at RT. The reaction of the substrate with the remaining enzymes produced a visible signal, which indicates the quantity of Progesterone in the sample. The enzymatic reaction was stopped to prevent eventual saturation of the signal, by adding 100 µl of Stop Solution to each well.

The absorbance was read within 30 minutes of adding the stop solution, at 450 nm with a microtiter plate reader.

3.2.7 Trypsin/EDTA Cell Detachment Process

For our experimental purposes, KGN cells were cultivated in 150 cm² plastic flasks and the cells were provided with growth medium (GM) (500 ml DMEM + 50 ml FCS + 5 ml Penicillin/Streptomycin).

This process of cell culture requires a method to dissociate the cells from the flask and each other. This method is called trypsinization, the enzyme used being trypsin. Trypsinization was done to permit passage of the cells to a new container, observation for experimentation, or reduction of the degree of confluence in the flask by removal of a percentage of the cells.

First the culture medium was removed from the flasks, and residual serum eliminated by gently rinsing the monolayers with 5 ml of sterile DPBS. The DPBS was removed, and 3 ml of a 0.25% Trypsin-EDTA solution slowly added to cover the cell monolayer. Incubation at RT lasted for 2-5 minutes.

When added to the cell culture, trypsin, which is a proteolytic enzyme, breaks down the proteins that enable the cells to adhere to the vessel.

Once cells have been detached from their container, they appear rounded. 7 ml of GM was added to deactivate the trypsin as cell surface proteins will also be cleaved over time, and this will affect cell functioning. The cells were suspended by gentle pipette action and put in-to a falcon.

To remove the GM and trypsin the sample was centrifuged for 4 minutes in 1200 rpm and supernatant was aspirated. To wash the cells and remove trypsin completely, the pellet was re-suspended in 5 ml DPBS and centrifuged again for 4 minutes in 1200 rpm. Supernatant was again aspirated and the cells were ready for further use.

3.2.8 Purification of Total RNA from KGN Cells using RNeasy Technology

The total RNA from KGN cells was extracted by using RNeasy technology as per manufacturer's instructions.

KGN cells must first be detached from the flask in which they are cultivated (see 1.2.7 Trypsin/EDTA cell detachment process). Afterwards, cells were disrupted by adding 350 µl Buffer RLT. Buffer RLT contains a high concentration of guanidine isothiocyanate that supports the binding of RNA to the silica membrane. 1x volume of 70% ethanol (350 µl) was added and mixed well by pipetting. Ethanol was added to provide appropriate binding conditions.

Up to 700 µl of the sample was transferred to an RNeasy spin column placed in a 2 ml collection tube. The tube was centrifuged for 15 seconds at ≥ 10.000 rpm, the total RNA bind to the membrane and the flow-through was discarded.

Then, 700 µl Buffer RW1 were added to the RNeasy spin column. Buffer RW1 contains a guanidine salt, as well as ethanol, and is used as a stringent washing buffer that efficiently removes biomolecules such as carbohydrates, proteins, fatty acids, etc. that are non-specifically bound to the silica membrane. At the same time, RNA molecules larger than 200 bases remain bound to the column. The tube was again centrifuged and the flow-through was discarded.

500 µl Buffer RPE were added to the RNeasy spin column. Buffer RPE is a mild washing buffer whose main function is to remove traces of salts that are still on the column due to buffers used earlier in the protocol. The tube was again centrifuged and the flow-through was discarded. The last step was repeated, but centrifugation now lasted 2 minutes. Then RNeasy spin column was placed in a new 2 ml collection tube and the sample centrifuged at full speed for 1 minute.

The RNeasy spin column was again placed in a new 1,5 ml collection tube, 30-50 µl RNase-free water was added directly to the spin column membrane and a centrifugation for 1 min at ≥ 10.000 rpm was done to elute the RNA in the collection tube.

Finally, the purified RNA was measured in Nanodrop. If the expected RNA yield was > 30 mg, the last step was repeated using another 30-50 µl RNase-free water.

3.2.9 cDNA Synthesis From Total RNA Samples

The First Strand cDNA Synthesis Kit (Fermentas) was used in order to synthesize the first strand cDNA from total RNA templates and be further used as a template in PCR or real-time PCR.

After thawing, the components of the First Strand cDNA Synthesis kit were mixed, briefly centrifuged, and stored on ice.

They were then added to a sterile, nuclease-free tube on ice in the following order: first were added 5 µg total RNA, 1µl random hexamer primer, as random hexamer primers bind non-specifically and are used to synthesize cDNA from all RNAs in total RNA population, and 5µl Nuclease-free Water, so that primer anneal to the RNA.

Then were added 4 µl 5x Reaction Buffer, 1µl RiboLock RNase Inhibitor (20 u/µl), which effectively protects RNA from degradation at temperatures up to 55°C, 2µl 10mM dNTP Mix and 2µl M-MuLV Reverse Transcriptase (20 u/µl), which maintains activity at 37°C and is suitable for synthesis of cDNA up to 9 kb.

After all the reagents were added, the tube was gently mixed, centrifuged, incubated for 5 minutes at 25°C and for 60 minutes at 37°C, to allow the transcription to occur. The reaction was terminated by heating at 70°C for 5 min to inactivate the enzyme.

The reverse transcription reaction product, cDNA, can be directly used or stored at -20°C for less than one week. For longer, -70°C is recommended.

3.2.10 PCR using JumpStart RedTaq Ready Mix

JumpStart REDTaq ReadyMix PCR Reaction Mix (Sigma) was used to perform all PCR experiments in this study. It is a prepared solution combining the performance benefits of hot start PCR with the dual convenience of Sigma's ReadyMix and REDTaq.

JumpStart Taq antibody is used in Hot Start PCR techniques and inactivates the Taq DNA polymerase during reaction preparation at RT. By limiting polymerase activity prior to PCR cycling, non-specific amplification is reduced, and target yield increased, while during the first denaturation step of PCR the complex dissociates and polymerase activity is fully restored.

Additionally, using REDTaq JumpStart ReadyMix reduces pipetting steps and risk of contamination, as inert red dye allows quick visual confirmation the enzyme has been added and properly mixed. After PCR, an aliquot may be loaded directly onto an agarose gel without the addition of loading buffers.

The reagents for the PCR reaction (total volume 25µl) were added to a 0.2 or 0.5 ml thin-walled microcentrifuge tube in the following order: 12,5 µl JumpStart REDTaq ReadyMix, 1 µl Forward primer (10 µM), 1 µl Reverse primer (10µM), 2µl Template cDNA (100 ng) and 9,5 µl Water

The tubes were mixed gently by vortexing and briefly centrifuged to collect all components at the bottom of the tube.

In the first cycle of PCR the DNA molecules are melted by raising the temperature to 94°C for 2 minutes. After the strands have separated, the temperature is lowered to 58°C for 30 seconds, so that each primer binds specifically to the 3' end of the target sequence on the appropriate strands of DNA. Taq polymerase synthesizes the complementary DNA strands from free nucleotides. In this step the temperature can be raised to the 72°C to speed up the reaction. This cycle was repeated 32 times, with a final extension for 5 minutes at 72°C. Finally, the samples were held at 4°C.

The final product consisted of thousands of copies of the target sequence.

3.2.11 Agarose Gel Electrophoresis (1,5%)

Agarose is a linear polymer extracted from seaweed and sold as a white powder that is melted in buffer and allowed to cool, whereby the agarose forms a gel by hydrogen bonding. The hardened matrix contains pores, the size of which depends on the concentration of agarose (Smith 1996).

To analyze the PCR and qPCR products of this study 1,5% agarose gels were made.

Agarose gel consisted of 1,5 g agarose powder, which was dissolved in 100 ml TAE buffer and melted by heating it to near-boiling point.

GelRed 10 000X stock reagent was diluted into the agarose gel solution (10 µL GelRed were added to 100 mL of the gel solution) and mixed thoroughly. GelRed can be added while the gel solution is still hot.

GelRed is a new generation of fluorescent nucleic acid gel stain designed to replace the highly toxic ethidium bromide (EtBr). GelRed is superior to EtBr and other EtBr alternatives by combining low toxicity, high sensitivity, and exceptional stability. When exposed to ultraviolet light it will fluoresce with an orange color that strongly intensifies after binding to DNA (Biotium Inc. 2012).

After GelRed addition, melted agarose was let to cool sufficiently before pouring the solution into a cast, where a comb was also placed to create wells. 20-30 minutes later, once the gel had been set, the comb was removed, leaving wells where DNA samples could be loaded.

Gel was removed to the electrophoresis tank, and the buffer used in the gel was the same as the running buffer. The samples were loaded, and a DNA marker for the estimation of the molecular weight of the DNA fragments and the gel was run at 90 V.

Around 60 minutes later, the gel was ready to be viewed with an ultraviolet (UV) transilluminator.

3.2.12 Quantitative PCR using Power SYBR Green PCR Master Mix

Quantitative PCR is a method used to detect relative or absolute gene expression level. All qPCR involves the use of fluorescence to detect the threshold cycle (Ct) during PCR when the level of fluorescence gives a signal over the background and is in the linear portion of the amplified curve. This Ct value is responsible for the accurate quantification of qPCR.

More specific, RT-qPCR (Reverse Transcription-quantitative Polymerase Chain Reaction) obeys the same principle as the normal PCR, but instead of looking at bands on a gel, the reaction is monitored in to a real-time PCR machine that measures the reaction occurring with a detector. Traditionally, RT-PCR involves two steps: RT reaction and PCR amplification. RNA is first reverse

transcribed into cDNA using a reverse transcriptase as described in protocol 1.9, and the resulting cDNA is used as templates for subsequent PCR amplification using primers specific for one or more genes.

SYBR dye is the fluorescence used to detect polymerase chain reaction (PCR) products by binding to double-stranded DNA formed during PCR. Specifically, when SYBR dye is added to a sample, it immediately binds to all double-stranded DNA present in the sample. During PCR, DNA polymerase amplifies the target sequence which creates the PCR products. SYBR dye then binds to each new copy of double-stranded DNA. As the PCR progresses, more PCR product is created, SYBR dye binds to all double-stranded DNA, so the result is an increase in fluorescence intensity proportioned to the amount of PCR product produced. The qPCR machine detects the fluorescence and software calculates Ct values from the intensity of the fluorescence.

For the preparation of qPCR, first, total RNA must be isolated from the samples (see protocol 1.8) and then cDNA synthesis must be performed (see protocol 1.9) so that the cDNA will be created in a 1:1 ratio to the RNA in the samples.

When the templates were ready, the RT Master Mix were prepared combining for each sample, 5 μ l SYBR Green PCR Master Mix, 2 μ l Template (cDNA 100ng/ml) and 3 μ l Water. The Master Mix was mixed and briefly centrifuged.

Additionally, all oligonucleotides used were re-suspended in nuclease-free water to a final concentration of 100 μ M, and the primers were diluted to a working concentration of 10 μ M with nuclease-free water, so that the final sample would have a final concentration of 10 pM.

For the qPCR, except the cDNA samples, the specific primers for the genes of interest, and the SYBR Green PCR Master Mix (which includes SYBR Green dye, AmpliTaq Gold DNA Polymerase, dNTPs with dUTP, Passive Reference, and optimized buffer components) an internal control (housekeeping gene) is also needed as a point of comparison for our data.

In each well of a MicroAmp Optical 96-Well Reaction Plate were transferred, 0,5 μ l Forward Primer, 0,5 μ l Reverse Primer from each gene of interest and 10 μ l Master Mix. For each gene of interest the reaction was done twice. After finishing pipetting, the plate was sealed with a MicroAmp Optical Adhesive Film.

Finally, the plate was briefly centrifuged and transferred to the thermal cycler block, where the qPCR was performed in the following program.

Thermal Cycler Profile			
Stage	Repetitions	Temperature	Time
1	1	50.0 °C	2:00
2	1	95.0 °C	10:00
3	40	95.0 °C	0:15
		60.0 °C	1:00
4 (Dissociation)	1	95.0 °C	0:15
		60.0 °C	1:00
		95.0 °C	0:15

The same amount of KGN cells were vitrified according to each vitrification protocol, thawed with sucrose gradient solutions, and separated in two tubes. One tube was left 1 hour at room temperature after the thawing procedure, and then we undergo in RNA extraction and cDNA synthesis, whereas with the second tube we undergo immediately in RNA extraction and cDNA synthesis.

Data from real-time qPCR are Ct, or threshold cycle, values. Ct is the cycle number at which a detectable signal is achieved. A lower Ct means a larger amount of starting template in sample, and higher Ct means a smaller amount of starting template.

The normalization has been done against three reference genes (18sRNA, GAPDH 70bp, GAPDH 101bp) as multiple reference genes can give us a more accurate quantification. A reference gene has a stable expression level in all samples and its expression is not changed by any treatments. Additionally, KGN cells, that were not vitrified were used as calibrator, which was also the experimental control.

Many approaches for normalization exist. We used the $\Delta\Delta Ct$ method, according to which:

- we first have to normalize the Ct of the gene of interest to the Ct of the reference gene:
 $\Delta Ct (\text{control}) = Ct (\text{gene of interest, control}) - Ct (\text{reference gene, control})$
 $\Delta Ct (\text{vitrified sample}) = Ct (\text{gene of interest, vitr.}) - Ct (\text{reference gene, vitr.})$
- we then have to normalize the ΔCt of the vitrified sample to the ΔCt of the calibrator-control
 $\Delta\Delta Ct = \Delta Ct (\text{vitrified sample}) - \Delta Ct (\text{control})$
- finally, we have to calculate the expression ratio
 $2^{-\Delta\Delta Ct} = \text{normalized expression ratio}$

The normalized expression ration give us the fold difference of the vitrified KGN cells in correlation to the control.

3.2.13 Double Staining of KGN cells in slides with -Cell stain- Double Staining Kit

-Cell stain- Double Staining Kit (Fluka Analytical) consists of two staining compounds, Calcein-AM and Propidium Iodide (PI). This kit is utilized for the simultaneous detection of viable and dead cells by using a fluorescent microscope. Calcein-AM is cell membrane permeable, and the Calcein generated by esterase activity in the viable cell emits strong green color fluorescence. Therefore, viable cells can be monitored as green fluorescent-colored cells under the microscope. On the other hand, PI can enter a dead cell through a damaged cell membrane and intercalate DNA of a dead cell. PI emits red color fluorescence in DNA double helix, so dead cells can be monitored as red fluorescent-colored cells. Since both Calcein and PI-DNA can be excited with 490 nm, simultaneous monitoring of viable and dead cells is possible with a fluorescence microscope.

First, the staining solution was prepared and used up in one day because of the poor stability of Calcein-AM. Before opening the vials of the kit, they had to be warmed at RT. Then, 10 μ l EthD-1 were added to 5 ml DPBS, and the solution was vortexed. 2,5 μ l Calcein-AM was added subsequently. The staining solution had as final concentrations 2 μ M Calcein-AM and 4 μ M EthD-1. KGN cells have been already prepared in slides and let growth. The growth medium was discarded and the cells were washed with DPBS 3 times in order to eliminate esterase activity of the media.

In each slide 1 ml of the staining solution was added, and incubation lasted 15 minutes at 37°C. Living cells, stained yellowish-green fluorescent, and dead cells stained red fluorescent were observed using an excitation filter at 490+10 nm under fluorescence microscope. The cells were counted by imagej, a Java-based image processing program.

3.2.14 Flow Cytometry and Fluorescence-Activated Cell Sorting (FACS):

Flow cytometry is a biological method used to measure various parameters of cells. In this study we used it for cell cycle analysis and cell viability analysis of KGN cells.

Flow cytometry obtains when a sample of cells is injected into a fluid of another population of cells, and funneled to give a single line of ordered cells, this single line of the sample cells passes through a laser beam where detectors collect the FSC (Forward Scatter Channel) and SSC (Side Scatter Channel) lights to give information on the sample. More specifically, flow cytometry is based on a population of cells that are hydrodynamically-focused to organize random cells from a sample into a fluid stream with ordered cells in a straight line. This is done by having a tube, in which the inner walls built up of a moving stream of fluid ("sheath flow"). The sample of cells is injected into the middle of this sheath flow. The two liquids will not mix as their density/viscosity is different, thus forming a stable two-layer flowing fluid. The tube narrows down into a funnel, thus constricting the sheath fluid along with the sample that orders the cells into a single line.

The single line of ordered cells pass through a single wavelength laser, which analyses the sample using two detectors. The light that is scattered through the sample and collected forward from the cell (Forward Scatter Channel - FSC) gives information on the cells' size, whether they are alive big round cells, or small dead cell debris. The light that is scattered sideways at a 90° angle from the laser beam due to reflection or fluorescence (Side Scatter Channel - SSC) gives information on the fluorescence of a cell or its granularity thus enables to identify the type of cell. This information is collected and displayed on a SSC by FSC graph the X-axis gives the cell size and the Y-axis gives their fluorescence/granularity (Sabban Sari 2011).

3.2.14.1 KGN VIABILITY ANALYSIS (PROPIDIUM IODIDE STAINING)

Propidium iodide (PI) has been used to analyze the viability of vitrified KGN cells.

After thawing, the cells have been transferred into FACs tubes, washed twice with 2 ml D-PBS, the centrifugation last 4 minutes in 1200 rpm, the supernatant was removed and the pellet of cells was re-suspended in 0,5 ml D-PBS, the samples were kept on ice. A 5 µl ready-to-use Propidium Iodide (PI) solution was added to each tube just prior to analysis of nonviable cells in a FACscan flow cytometer. A minimum of 10000 events was collected and analyzed.

Propidium iodide (PI) flow cytometric assay has been widely used for the evaluation of apoptosis in different experimental models (Riccardi and Nicoletti 2006). These dyes cannot pass through an alive, healthy, intact cell membranes, but may freely enter cells with compromised cell membranes. Upon entering dead cells, Propidium Iodide will intercalate into double-stranded DNA or double-stranded RNA in a stoichiometric manner. Use of PI makes possible a rapid and precise evaluation of cellular DNA content by flow cytometric analysis.

Because we stained only with PI, we collected PI fluorescence in the FL-2 channel. Unstained cells and cells that had not been vitrified were also acquired and the data used as control.

The data were observed in a SSC – FL2 Dot Plot and the results were analyzed by Flow Cytometry Analysis Software, FLOWJO.

3.2.14.2 KGN CELL CYCLE ANALYSIS (PI/RNASE STAINING BUFFER)

The vitrified KGN cell cycle was analyzed by using a fluorescence labeling, PI/RNase Staining Buffer. Propidium Iodide (PI) is a fluorescent vital dye that stains DNA and RNA, and has also been used for the viability analysis.

KGN cells were grown in flasks until 70% of confluent. Then the cells were detached from the flasks (see 1.7), transferred to FACs tubes, and fixed at -20 °C 70% Ethanol for 20 minutes at RT. Fixation is necessary to ensure free access of the PI/RNase Staining Buffer.

After fixation, the cells were washed twice with 2 ml D-PBS. Centrifugation lasted 4 minutes in 1200 rpm. The supernatant was removed and the pellet of cells was resuspended in 500 µl PI/RNase Staining Buffer. The tubes were incubated on ice for 15 minutes, and analyzed in a FACscan flow cytometer. A minimum of 10000 events was collected and analyzed.

Fluorescence labeling of the nuclei of cells in suspension allows the analysis of the fluorescence properties of each cell in the population. Quiescent and G1 cells will have one copy of DNA and will therefore have 1X fluorescence intensity. Cells in G2/M phase will have two copies of DNA and, accordingly, 2X intensity. Since the cells in S phase are synthesizing DNA, they will have fluorescence values between the 1X and 2X populations.

The acquired data were collected in the FL-2 channel as we stained only with PI.

3.2.15 Statistics

The statistical analyses were performed at the VassarStats website (<http://vassarstats.net/>). The differences at $p < 0.05$ were considered as statistically significant. qPCR results have been analyzed using Student's t-test, and FACs results by using ANOVA for independent samples.

4 RESULTS

4.1 INFLUENCE OF VITRIFICATION ON MOUSE OVARIES

To investigate the influence of the vitrification procedure on C57BL/6J mouse ovaries, first, mouse ovaries sections of fresh and vitrified mouse ovaries were stained with hematoxylin and observed by fluorescence microscope. Further, follicles were dissociated from the ovarian tissue by using collagenase, stained with Calcein-AM, and observed by light microscope. Finally, the viability of fresh and vitrified mouse ovaries was checked by their progesterone production ability.

4.1.1 Hematoxylin Staining Of Mouse Ovaries Sections

Fresh mouse ovaries, and vitrified with DMSO were cut, stained with hematoxylin, and observed by fluorescence microscope in order to find morphological differences. The experiment was repeated 3 times. Fig.4 shows cuts of fresh ovaries (A and B) and of vitrified-thawed mouse ovaries (C and D). Arrows indicate a primary follicle, with the oocyte visibly surrounded by granulosa cells. No significant morphological changes were observed between the fresh and the vitrified ovaries.

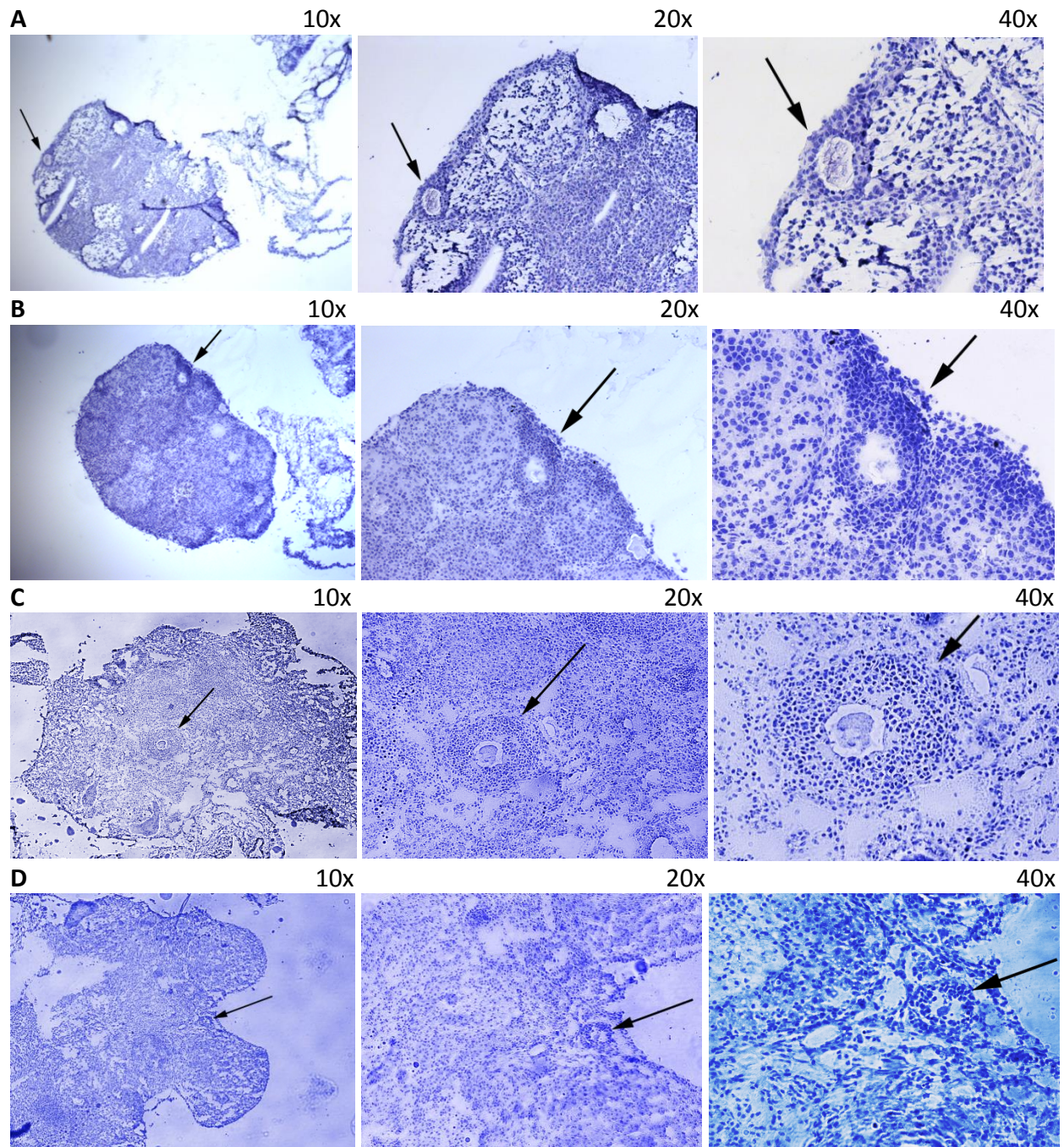


Figure 4. Hematoxylin stained cuts of fresh and vitrified mouse ovaries. 3 fresh and 3 vitrified mouse ovaries were used, all of them were 1 day old. 4 pictures (A, B, C, and D) were taken, each of which represents 3 magnifications (10x, 20x, and 40x) of an ovary. A and B are pictures of a fresh ovary. C and D of a vitrified-/thawed mouse ovary.

4.1.2 Ovarian Tissue Vitality Test (Collagenase)

Hematoxylin staining allowed to compare the morphology of the fresh and vitrified ovaries only, but gave no information about the viability of the follicles. Collagenase was used to dissociate the ovarian tissue, and to observe by means of staining with Calcein-AM alive follicles. The follicles in the sample were found by using a light microscope. Using a fluorescence microscope allowed to see whether the follicles were alive or not. Although the extraction of follicles was possible, in Fig.5 are shown unstained follicles extracted from a mouse ovary by using collagenase, the staining was not successful, and counting of alive follicles was impossible.

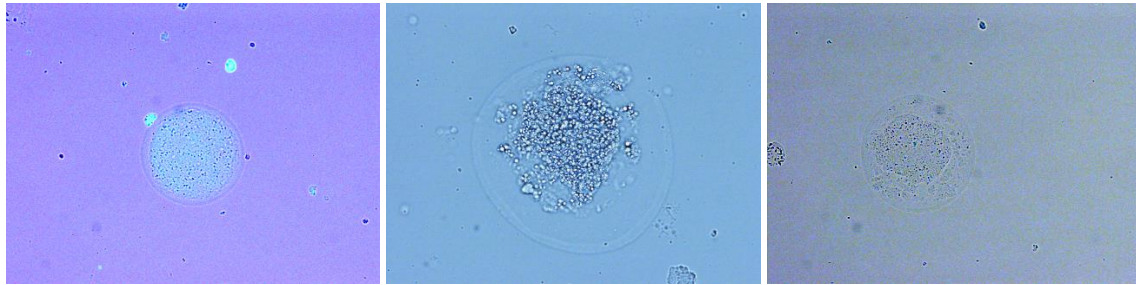


Figure 5. Unstained follicles, extracted from 4 mouse ovaries by using Collagenase.

4.1.3 Progesterone production ability of mouse ovaries

The viability of fresh and vitrified mouse ovaries was checked additionally by their progesterone production ability. Each ovary was cut in two pieces and put in a flask with DMEM/Gentamicin. The media were collected at four time points - 24, 48, 72, and 168 hours - and the amount of progesterone was measured by ELISA. For this experiment, 4 groups of ovaries were used: 1-day old fresh ovaries, 1-day old vitrified ovaries, 5-days old fresh ovaries and 5-days old vitrified ovaries. For each group the experiment was repeated twice. Figs. 6 and 7 show how the progesterone production is reduced by the time of 1-day old fresh and 1-day old vitrified mouse ovaries ($p>0.05$), and 5-days old fresh and 5-days old vitrified mouse ovaries ($p>0.05$), respectively. In both cases, the vitrified ovaries have a lower amount of progesterone than the fresh ovaries in every time point measurement.

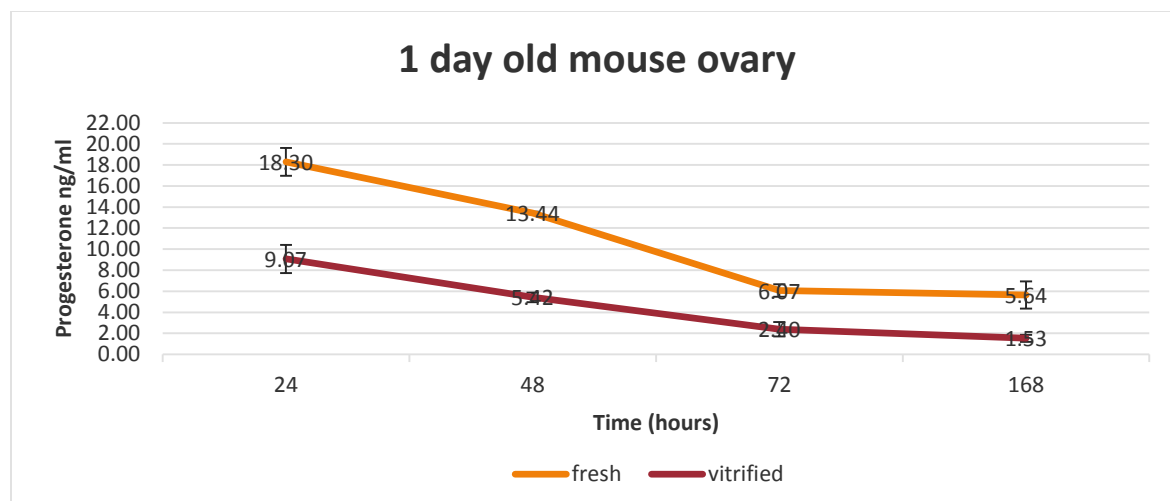


Figure 6. Progesterone production of 1-day old fresh and 1-day old vitrified mouse ovaries. The experiment was performed twice (mean from two independent experiments \pm SD). Progesterone production is indicated in yellow for the fresh ovaries, in red for the vitrified ovaries. Reduction of progesterone is shown by the time for both groups of ovaries ($p > 0.05$).

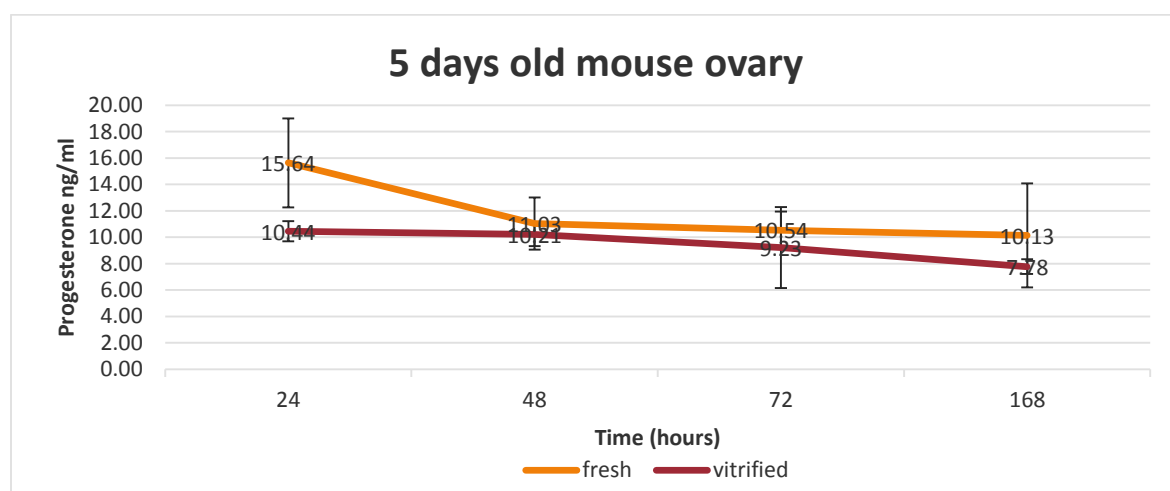


Figure 7. Progesterone production of 5-days old fresh and 5-days old vitrified mouse ovaries. The experiment was performed twice (mean from two independent experiments \pm SD). Progesterone production is indicated in yellow for the fresh ovaries and in red for the vitrified ovaries. Reduction of progesterone is shown by the time for both groups of ovaries ($p > 0.05$).

Figs. 6 and 7 not only show differences between same age fresh and vitrified mouse ovaries, but also between the 2 different groups. Figs. 5 and 6 display the progesterone production difference between 1-day and 5-days old fresh ovaries ($p > 0.05$), and 1-day and 5-days old vitrified ovaries ($p < 0.05$), respectively.

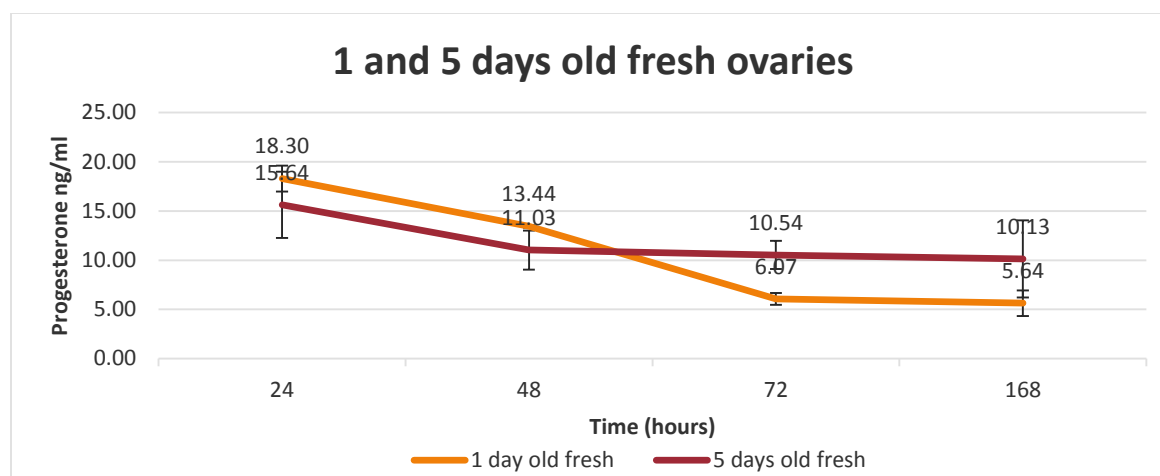


Figure 8. Progesterone production of 1-day and 5-days old fresh mouse ovaries. The experiment was performed twice (mean from two independent experiments \pm SD). Progesterone production is indicated in yellow for the 1-day old fresh ovaries and in red for the 5-days old fresh ovaries ($p > 0.05$).

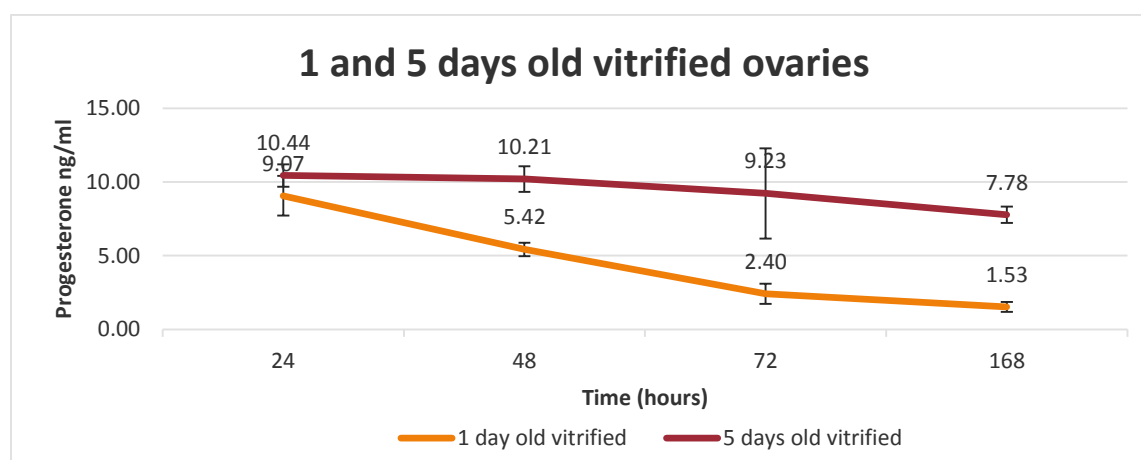


Figure 9. Progesterone production of 1-day and 5-days old vitrified mouse ovaries. The experiment was performed twice (mean from two independent experiments \pm SD). Progesterone production is indicated in yellow for the 1-day old vitrified ovaries, in red for the 5-days old vitrified ovaries ($p < 0.05$).

Fig. 8 shows a reduction of progesterone in time for both groups of ovaries, with the 5-days old fresh ovaries having a reduced rate of decline of progesterone in contrast to the 1-day old fresh ovaries. Fig. 9 also shows a reduction of progesterone by the time for both groups of ovaries, with the 5-days old vitrified ovaries having a reduced rate of decline of progesterone in contrast to the 1-day old vitrified ovaries.

This experiment shows that mouse ovaries progesterone production is reduced after vitrification in contrast to fresh ovaries. Moreover, the 1-day old fresh and vitrified mouse ovaries present a

higher progesterone reduction rate in contrast to the 5-days old fresh and vitrified ovaries, respectively. The results were not statistically significant.

4.2 INFLUENCE OF VITRIFICATION ON KGN CELLS

KGN cell line was used for the comparison of the two vitrification methods, which were compared in terms of cell survival rates, changes in selected-gene expression, and changes of the cell cycle.

4.2.1 KGN characterization experiments

4.2.1.1 *Expression of Progesterone Receptors and LH/hCG in KGN cells*

To characterize the KGN cells, a PCR was run to determine the expression of nuclear and membrane progesterone receptors. Template of KGN cells and primers of the nuclear progesterone receptors PRA/B, and PRB, and of the membrane progesterone receptors alpha, beta, gamma, and delta (mPR α , mPR β , mPR γ , mPR δ), of the progesterone receptor membrane component-1 (PGRMC1) and of luteinizing hormone/choriogonadotropin receptor (LH/hCG) were used. As shown in Fig.10, KGN cells express membrane bound mPR α , mPR β , mPR γ , mPR δ , PGRMC1, as well as the nuclear receptors PRA/B, PRB, and LH receptor. This findings show that KGN cells are a good model for studying human granulosa cells.

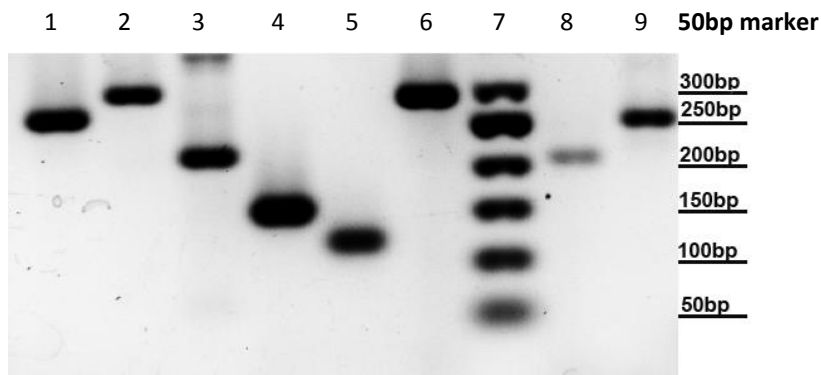


Figure 10. Representative picture of the expression of progesterone receptors and LH/hCG receptor in KGN cells by PCR. 1. PRA/B (progesterone receptor isoform A/B). 2. mPR α (membrane progestin receptor alpha). 3. mPR β (membrane progesterone receptor beta). 4. mPR γ (membrane progesterone receptor gamma). 5. mPR δ (membrane progesterone receptor delta). 6. PGRMC1 (progesterone receptor membrane component 1). 7. 50bp marker. 8. PRB (progesterone receptor isoform B). 9. LH/hCG (luteinizing hormone/choriogonadotropin receptor).

4.2.1.2 Viability test of KGN cells after fixation with 70% Ethanol

In order to further characterize KGN cells, their viability was checked after fixation with ethanol. The cells were stained with propidium iodide, and their viability was measured by means of FACs. Four flasks with KGN cells were trypsinized, and half of them were fixed with 70% ethanol. As ethanol disrupts hydrophobic and hydrogen bonding it can affect the structure of proteins on cell membranes, and propidium iodide can access into the cells and stain them. Fig. 11 displays three representative pictures from FLOWJO Flow Cytometry Analysis Software. Fig. 12 shows the viability rates of unfixed and fixed cells. In total, 8 measurements were made, and the experiment was repeated 3 times.

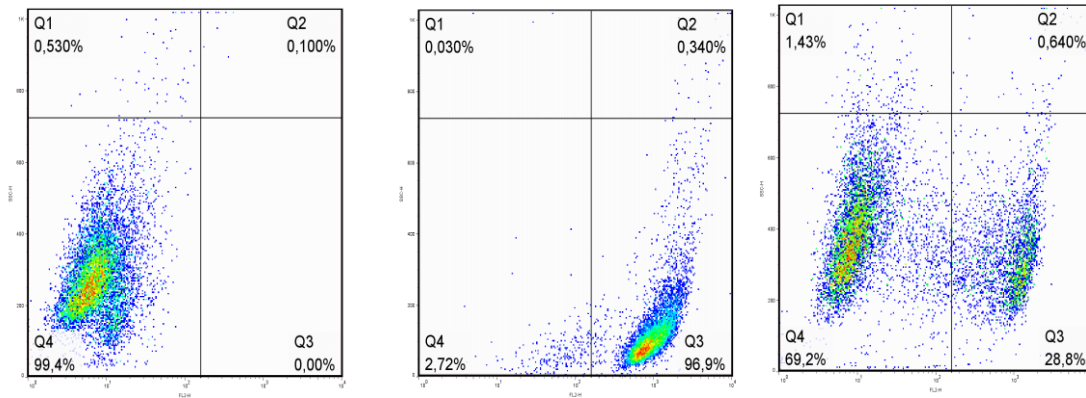


Figure 11. Representative pictures from FLOWJO viability measurement. In quatrate Q4 are the alive cells, in Q3 the dead cells. The first picture shows the unstained cells, the second picture the stained fixed cells treated by triton, and the third picture are 50% fixed and 50% unfixed stained cells.

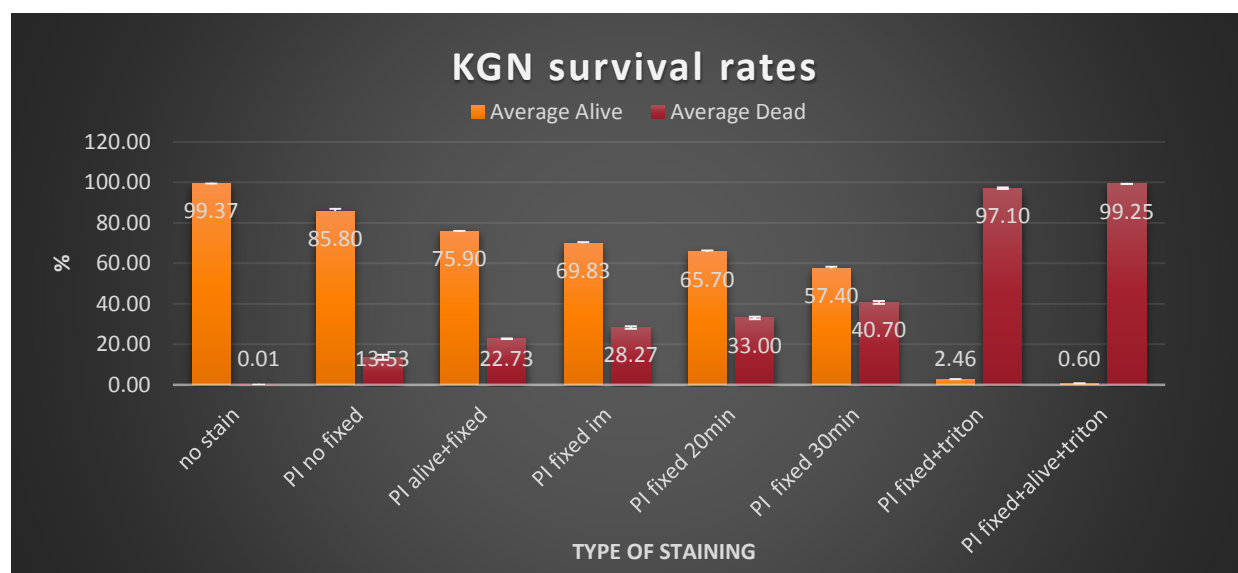


Figure 12. Viability rates of fixed and unfixed KGN cells with 70% ethanol. The following measurements were made: no stained cells; stained unfixed cells; 50% fixed and 50% unfixed stained cells; stained fixed cells with immediate measurement; stained fixed cells with measurement after 20 min; stained fixed cells with measurement 30 min later; stained fixed cells with triton treatment; 50% fixed and 50% unfixed stained cells treated with triton. The experiment has been done 3 times (mean from 3 independent experiments \pm SD).

Fig. 12 shows, a 100% viability for the unstained sample (no staining), which means that the cells have a self-fluorescence. The unfixed stained sample (PI alive) has a small percentage of dead cells. The sample with fixed and unfixed cells (PI alive+fixed) has a percentage of dead cells between the sample with only unfixed and the sample with only fixed cells. The fixed stained samples (PI fixed im, PI 20min, PI 30min) show an increasing percentage of dead cells as longer the staining last. And the samples treated with triton (PI fixed+triton, PI fixed+alive+triton) show almost 100% dead cells. Those results mean that staining with PI is toxic for KGN cells.

4.2.1.3 KGN Cell Cycle Analysis in the presence of Ethanol

The last experiment for the characterization of KGN cells concerned the analysis of the cell cycle in the presence of ethanol. The cells were stained with PI/RNase Staining Buffer, and the rates of G1, G2/M, and S phase were measured by means of FACs. Four concentrations of ethanol were checked (0%, 0.5%, 1%, and 1.5%), and the experiment was repeated four times. When ethanol was added, the incubation lasted for 2 hours. The results are shown in Fig. 13.

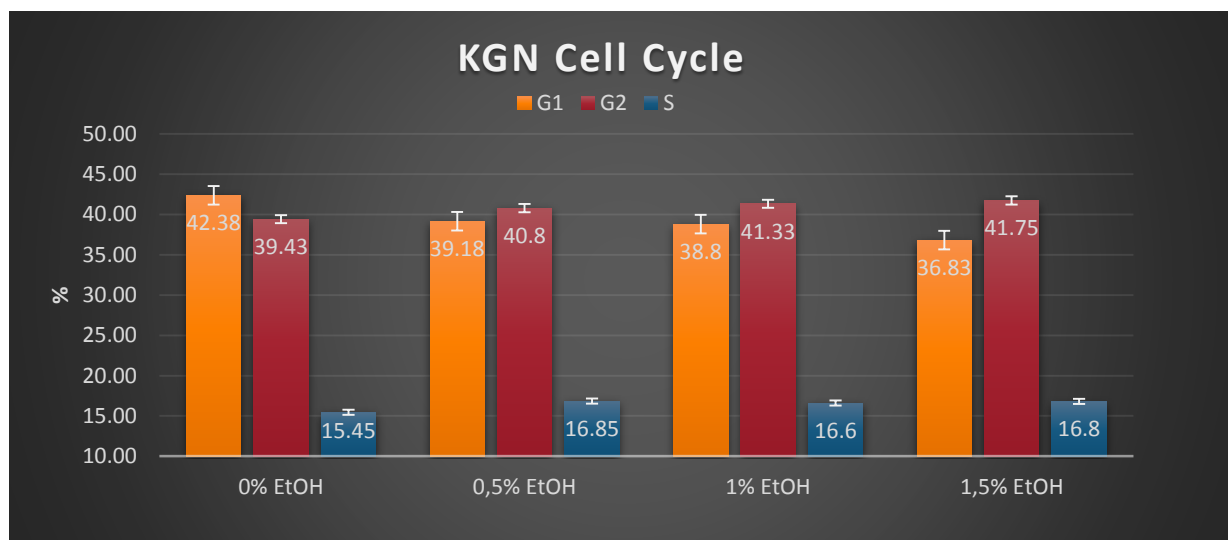


Figure 13. KGN cell cycle analysis in presence of ethanol. Four concentrations of ethanol were checked (0%, 0.5%, 1%, and 1.5%) and the amount of cells in G1, G2, and S phase were measured. The experiment was performed 4 times (mean from four independent experiments \pm SD); G1 $p < 0.05$, G2 $p > 0.05$, S $p < 0.05$.

Fig. 10 shows that if the amount of ethanol increases, the amount of cells in G1 phase decreases, in G2 phase increases, and in S phase has a tendency to increase. This means that in the presence of ethanol, the cells proliferate faster than in its absence. According to the statistical analysis, G1 and S phase results are statistical significant ($p < 0.05$), in contrast G2 results are not statistical significant ($p > 0.05$).

4.3 VIABILITY TEST OF KGN CELLS

The cell survival rates of the two vitrification methods were compared by viability tests of KGN cells with double staining (Double Staining Kit (Fluka Analytical)) and by means of FACS.

4.3.1 Viability test of KGN cells by double staining

5 slides were vitrified according to each vitrification protocol, thawed, and stained by Double Staining Kit. In Fig. 14 are shown pictures of the stained cells using fluorescence microscope, in Fig. 15 are represent the KGN survival rates calculated by imagej. According to this kit, Calcein emits in the viable cell a strong green color fluorescence, and PI emits a red color fluorescence in DNA double helix, so dead cells can be monitored as red fluorescent-colored cells.

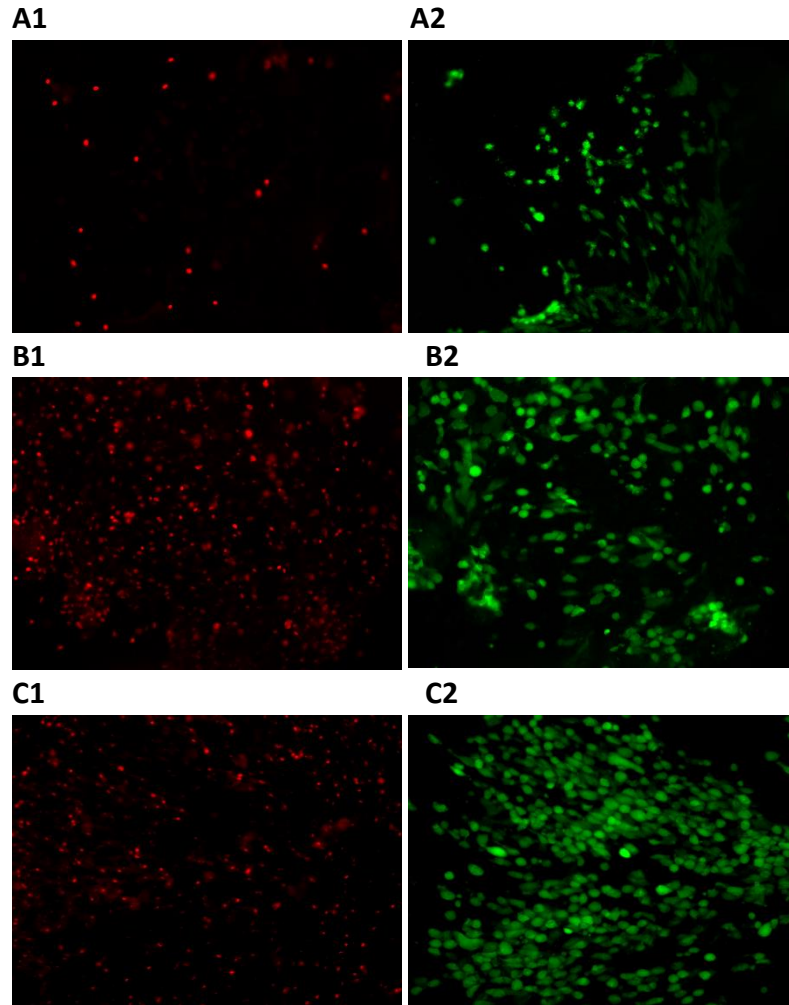


Figure 14. Fluorescence pictures of vitrified KGN cells in slides. The experiment was performed 5 times. Red: dead cells (PI stained cells), Green: alive cells (Calcein stained cells). A1-2: control slide, B1-2: vitrification method 1 and C1-2: vitrification method 2. Between the methods no noticeable difference is shown, as between the methods and the control is shown an appreciable difference.

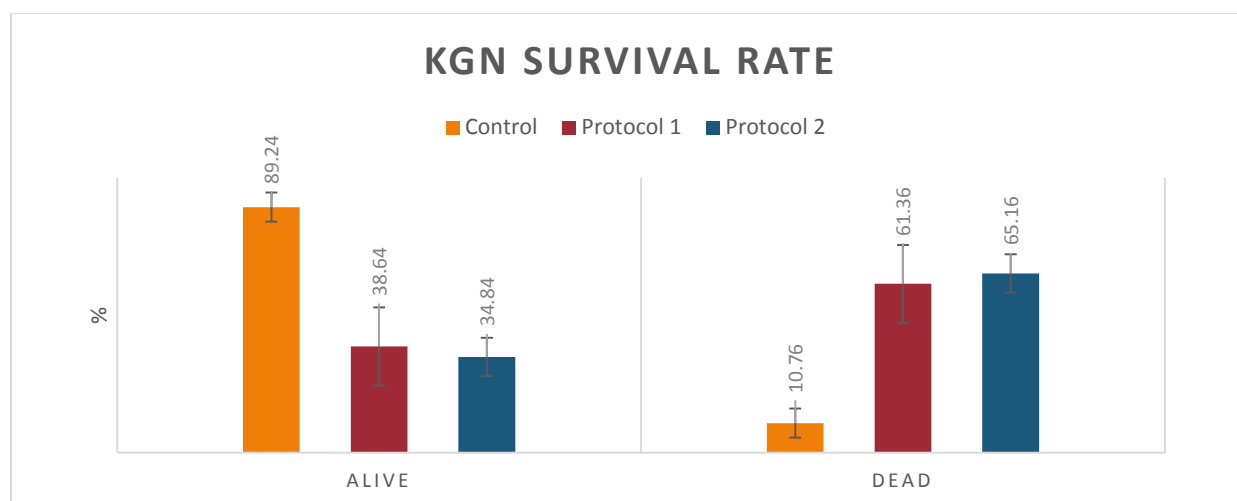


Figure 15. KGN survival rates, of vitrified cells in slides, calculated by imagej. With yellow are indicated the rates of the control, with red the rates of Protocol 1, and with blue the rates of Protocol 2. The experiment was performed 5 times (means from 5 independent experiments \pm SD). Between the methods a small difference is shown, with protocol 1 having better survival rates as protocol 2. Between the methods and the control is shown a great difference. The difference of viability rates between all the samples was not statistically significant ($p > 0.05$). In addition, the mortality rate between the vitrification protocols was non-significant ($p > 0.05$). In contrast, the difference of the mortality rates, between control and the protocols was statistically significant ($p < 0.05$).

In figs. 14 and 15 is shown a substantial percentage difference between control and both vitrification methods, whereas between the two vitrification methods we can see a small difference, with protocol 1 having a smaller mortality rate and greater viability rate than protocol 2. The mortality rates between control and the protocols were statistical significant ($p < 0.05$).

4.3.2 Viability test of KGN cells by Propidium Iodide staining

Viability rates of KGN cells were additionally checked by flow cytometric analysis. KGN cells were vitrified according to each vitrification protocol, thawed, and stained with Propidium Iodide (PI). This experiment was repeated 6 times, and the results are shown in Fig. 16.

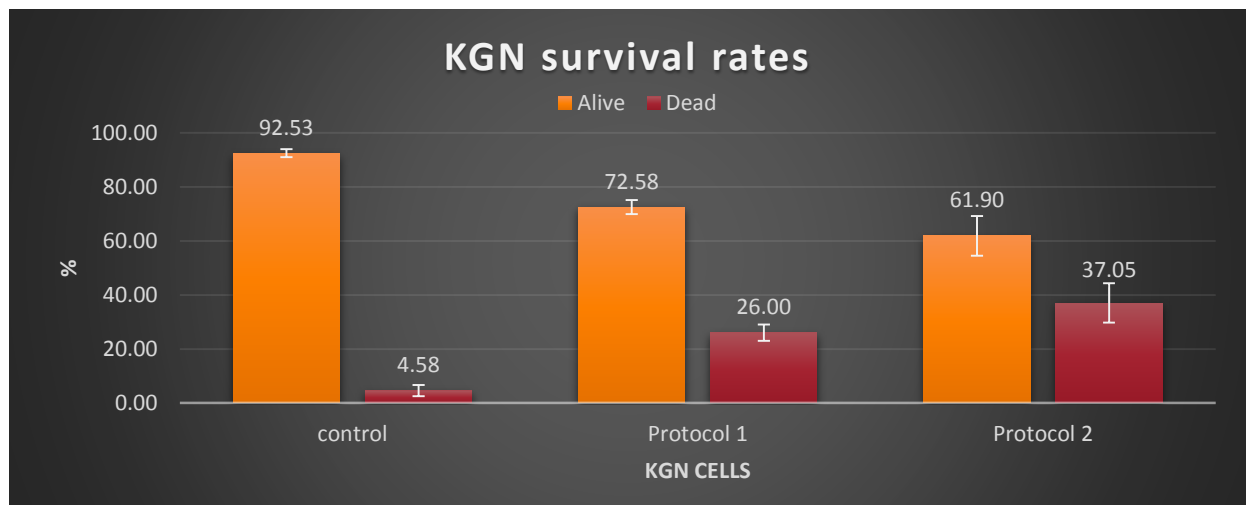


Figure 16. Survival and mortality rates of vitrified KGN cells by means of FACs. With yellow are indicated the percentages of the alive cells, with red the percentages of the dead cells. The experiment was performed 6 times (means from 6 independent experiments \pm SD). Both protocols show a great difference in contrast to the control. Between the protocols, protocol 1 shows better survival rates than protocol 2. Viability results for control vs. protocols are statistically significant ($p < .01$). In contrast viability results between protocol 1 and protocol 2 are nonsignificant ($p > .05$). Mortality results for control vs. protocols and between protocol 1 and protocol 2 are statistically significant ($p < .05$).

In Fig. 16, we can see a notable statistically significant viability percentage difference between control and both vitrification methods ($p < 0.05$), as well between the two vitrification methods, with protocol 1 having greater viability rates than protocol 2 (non-significant). Mortality differences are statistically significant for control vs. protocols and between protocols ($p < 0.05$).

4.4 VITRIFIED KGN CELL CYCLE ANALYSIS

The cell cycle of vitrified KGN cells by the two vitrification protocols was analyzed to observe the vitrification influence on cell division. KGN cells were vitrified according to each vitrification protocol, thawed, stained with PI/RNase Staining Buffer, and analyzed by using flow cytometry. This experiment was repeated 5 times and the results are shown in Fig. 17.

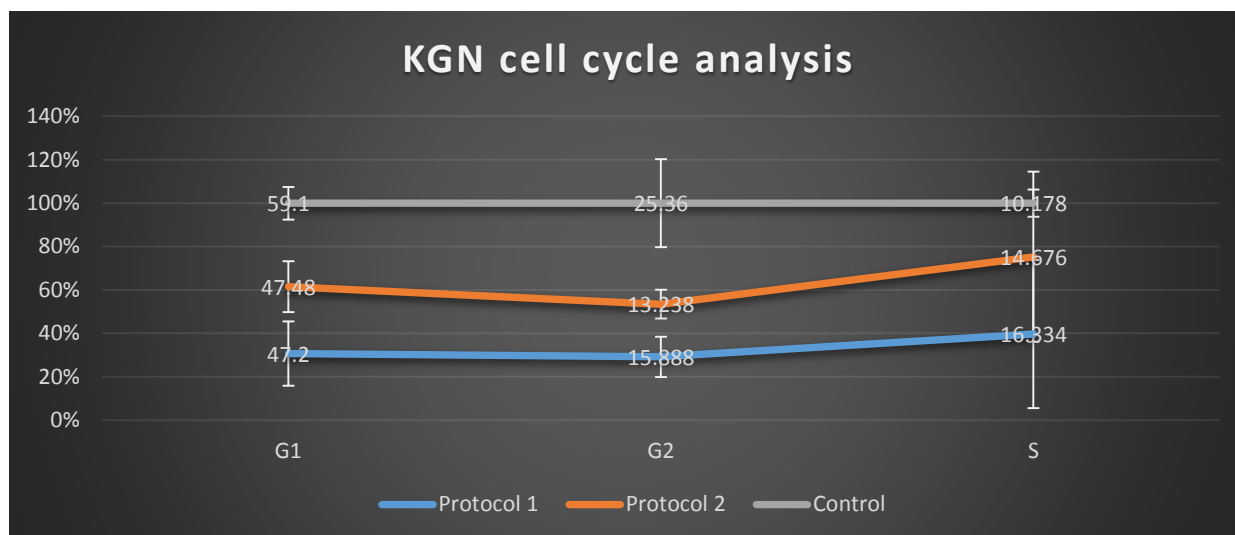


Figure 17. KGN cell cycle analysis by means of FACs. With grey is indicated the control (not vitrified KGN cells), with yellow the KGN cells vitrified by protocol 2, and with blue the KGN cells vitrified by protocol 1. The experiment was performed 5 times (means from 5 independent experiments \pm SD). Both protocols show a decrease in G1 and G2 phase rates in contrast to the control, whereas S phase rate increases, with protocol 1 shown a lightly greater increase in S phase. G1 and G2 results are statistically significantly different between control and the protocols ($p < .01$), and non-significant between the protocols ($p > .05$). S results are not significantly different.

The line chart in Fig. 17 indicates that both vitrification methods, compared to the control, show a decrease in G1 (11,8% for both protocols) and G2 (10,47% and 12,13% for protocol 1 and 2, respectively) phase rates (significant difference), whereas S phase rate increases by 6,93% with protocol 1 and 6% with protocol 2 (non-significant). Protocol 1 yielded a lightly greater increase of S phase rate than protocol 2 (non-significant).

G1, S, and G2 are the phases of interphase. Interphase is the phase of the cell cycle in which the cell prepares for cellular division. Specifically, in G1 phase, a high amount of protein synthesis occurs and the cell grows, in S phase, the cell duplicates its DNA, and in G2 phase, the cell resumes its growth in preparation for division (Cooper 2000. Chapter 14).

4.5 SELECTED-GENE EXPRESSION ANALYSIS OF VITRIFIED KGN CELLS

To determine whether certain genes are influenced by the vitrification/thawing process, and whether their expression is different also between the different vitrification protocols, 17 genes were analyzed by means of quantitative PCR to detect their relative gene expression level. The analysis was conducted additionally, after 1 hour incubation at room temperature, in order to

allow possible damage, caused by vitrification, to be expressed. The experiment was repeated 5 times with 5 different cDNAs:

1. vitrified KGN cells by protocol 1, further treatment immediately (p1i)
2. vitrified KGN by protocol 2, further treatment immediately (p2i)
3. vitrified KGN cells by protocol 1, further treatment one hour after the thawing procedure (p1h)
4. vitrified KGN by protocol 2, further treatment one hour after the thawing procedure (p2h)
5. not vitrified KGN cells, used as control (ctr)

The normalization was done by using the $\Delta\Delta C_t$ method. The normalized expression ratio give us the fold difference of the vitrified KGN cells in correlation to the control. The reference genes used were 18sRNA, GAPDH 70bp, and GAPDH 101bp.

The genes analyzed were separated in 3 groups, genes associated with apoptosis, genes responded by stresses, and genes associated with cell development.

Figs. 18, 19, 20 show the normalized expression ratio of the genes associated with apoptosis, against the reference genes 18sRNA, GAPDH 70bp, and GAPDH 101bp respectively. The normalized expression ration give us the fold difference of the vitrified KGN cells in correlation to the control and to the other vitrification protocols as following:

- p1i versus p2i;
- p1i versus p1h;
- p2i versus p2h;
- p1h versus p2h;
- p1i versus ctr;
- p2i versus ctr;
- p1h versus ctr;
- p2h versus ctr.

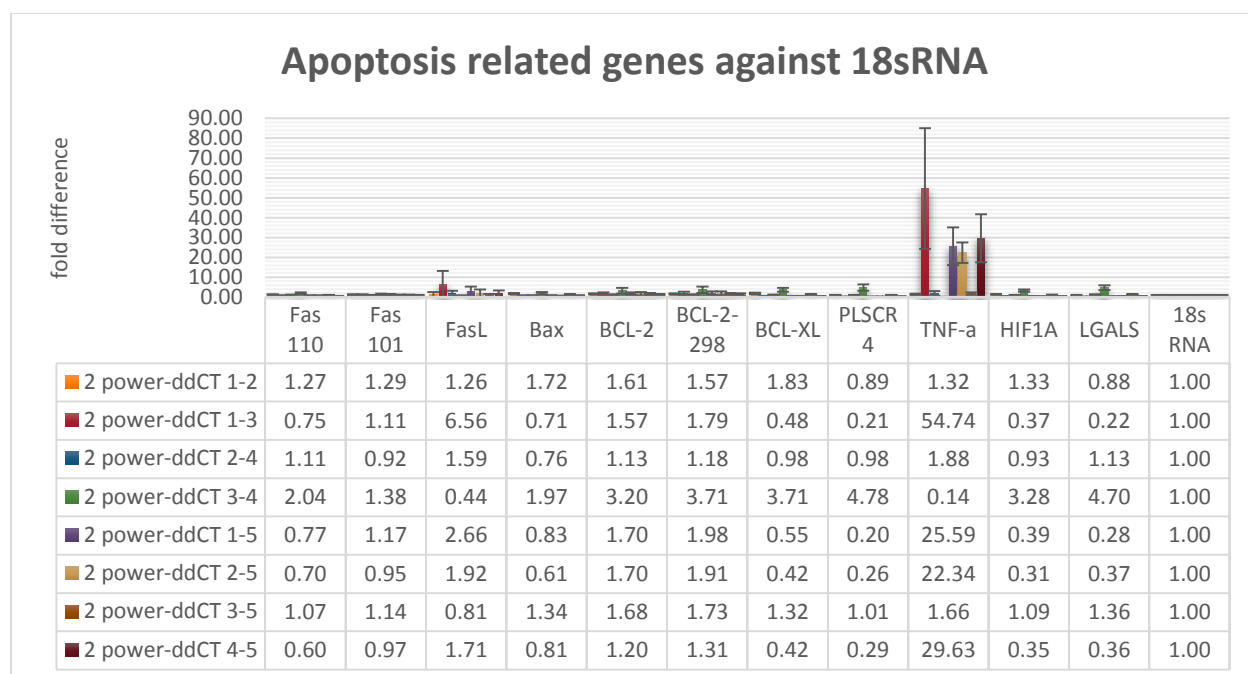


Figure 18. Fold difference between the protocols for the normalized expression ratio of each gene related to apoptosis in correlation to the reference gene 18sRNA. The experiment was performed 5 times. The fold difference was calculated for: p1i (1)-p2i (2) ($2^{-\Delta\Delta CT 1-2}$); p1i (1)-p1h (3) ($2^{-\Delta\Delta CT 1-3}$); p2i (2)-p2h (4) ($2^{-\Delta\Delta CT 2-4}$); p1h (3)-p2h (4) ($2^{-\Delta\Delta CT 3-4}$); p1i (1)-ctr (5) ($2^{-\Delta\Delta CT 1-5}$); p2i (2)-ctr (5) ($2^{-\Delta\Delta CT 2-5}$); p1h (3)-ctr (5) ($2^{-\Delta\Delta CT 3-5}$); p2h (4)-ctr (5) ($2^{-\Delta\Delta CT 4-5}$). Results of Fas110, Fas101, FasL, Bax, Bcl-2, Bcl-2-298 and Bcl-xl are non-significantly different ($p > .05$), HIF1A results are significantly different between P1i, P2i, P1h and control ($p < .05$), and TNF-a, LGALS and PLSCR4 results between all four protocols and the control ($p < .05$), respectively.

Fig. 18 shows, the fold difference when normalization against the reference gene 18sRNA, no fold difference (f.d) for p1h - control for all genes, in contrast, for the protocols p1i, p2i, and p2h and control is shown, a 0.2; 0.26; 0.3 f.d for PLSCR, a 25.6; 22.3; 29.6 f.d for TNF-a, a 0.4; 0.3; 0.35 f.d for HIF1A, and a 0.28; 0.37; 0.36 f.d for LGALS, respectively. Additionally FasL shows a 2.6 f.d for p1i and control, and Bcl-xL a 0.4 between p2i and control. Between the protocols, no f.d is shown for p1i - p2i, and p2i - p2h. For p1i - p1h is shown a f.d 6.56 for FasL, 54.7 for TNF-a, 0.2 for PLSCR, 0.37 for HIF1A, and 0.22 for LGALS, and for p1h - p2h is shown a f.d, 2 for Fas110, 0.44 for FasL, 3.2 for Bcl-2, 3.7 for Bcl-2-298, and Bcl-xL, 4.8 for PLSCR, 0.14 for TNF-a, 3.28 for HIF1A, and 4.7 for LGALS. According to this experiment, vitrification protocol p1h seems not to influence the expression of the selected genes, in contrast to the p1i, p2i, and p2h, with TNF-a expression influenced at most.

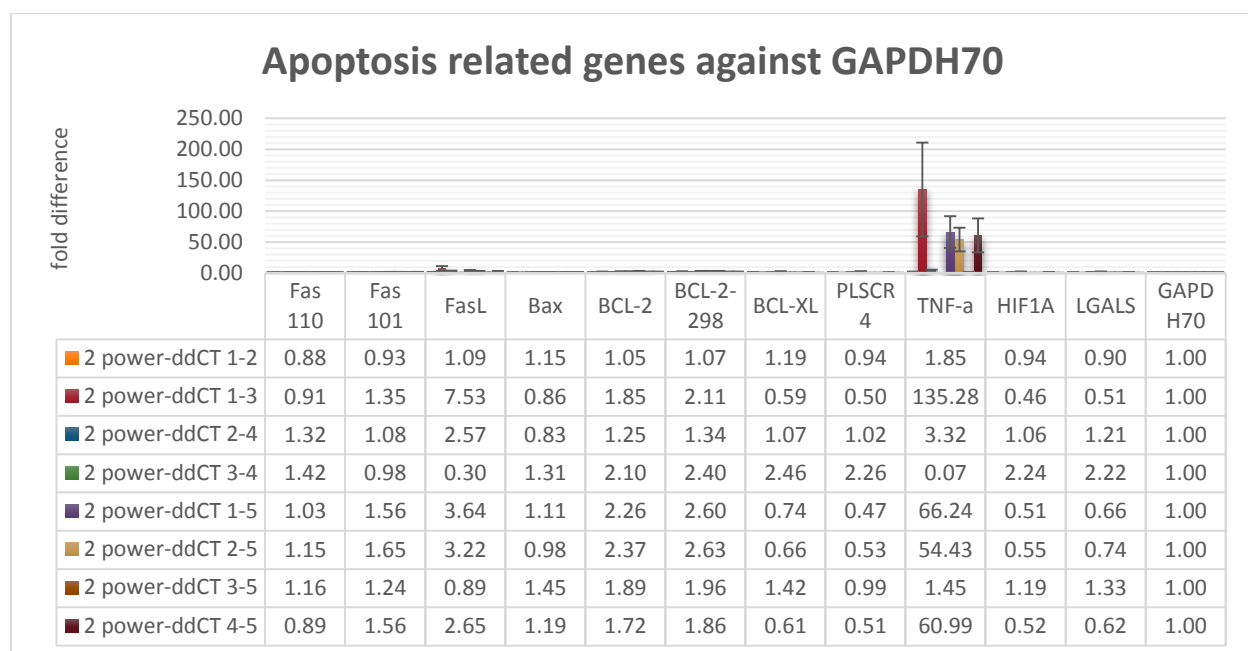


Figure 19. Fold difference between the protocols for the normalized expression ratio of each gene related to apoptosis in correlation to the reference gene GAPDH 70bp. The experiment was performed 5 times. The fold difference was calculated for: p1i-p2i ($2^{-\Delta\Delta CT 1-2}$); p1i-p1h ($2^{-\Delta\Delta CT 1-3}$); p2i-p2h ($2^{-\Delta\Delta CT 2-4}$); p1h-p2h ($2^{-\Delta\Delta CT 3-4}$); p1i-ctr ($2^{-\Delta\Delta CT 1-5}$); p2i-ctr ($2^{-\Delta\Delta CT 2-5}$); p1h-ctr ($2^{-\Delta\Delta CT 3-5}$); p2h-ctr ($2^{-\Delta\Delta CT 4-5}$). Fas101, Bcl-2, and Bcl-xl results are non-significantly different ($p > .05$), Fas110, FasL, Bax, Bcl-2-298, HIF1A results are significantly different between P1i, P2i, P1h and control ($p < .05$), TNF-a results between all four protocols and the control ($p < .05$), LGALS results between P1h and control ($p < .05$), and PLSCR4 results between P1i and control ($p < .05$), respectively.

Fig. 19 shows, the fold difference when normalization against the reference gene GAPDH70, no fold difference (f.d) between p1h and control for all genes, in contrast, for the protocols p1i, p2i, and p2h and control is shown, a 3.6; 3.2; 2.65 f.d for FasL, respectively, and a 66.2; 54.4; 61 f.d for TNF-a. Additionally Bcl-2 and Bcl-2-298 show a 2.3 and 2.6 f.d between p1i and control, and a 2.4 and 2.6 f.d between p2i and control. Between the protocols, no f.d is shown for p1i - p2i. For p1i - p1h FasL has a 7.5 f.d, Bcl-2-298 a 2 f.d, TNF-a a 135.3 f.d, and HIF1a 0.46 f.d. For p2i - p2h, FasL and TNF-a have a 2.6 and 3.3 f.d respectively. And for p1h - p2h FasL has a 0.3; Bcl-2 a 2.1; Bcl-2-298 a 2.4; Bcl-xl a 2.46; PLSCR a 2.3; TNF-a a 0.07; HIF1a a 2.2; and LGALS a 2.2 f.d. According to this experiment, again vitrification protocol p1h seems not to influence the expression of the selected genes, in contrast to the p1i, p2i, and p2h, with TNF-a expression influenced at most.

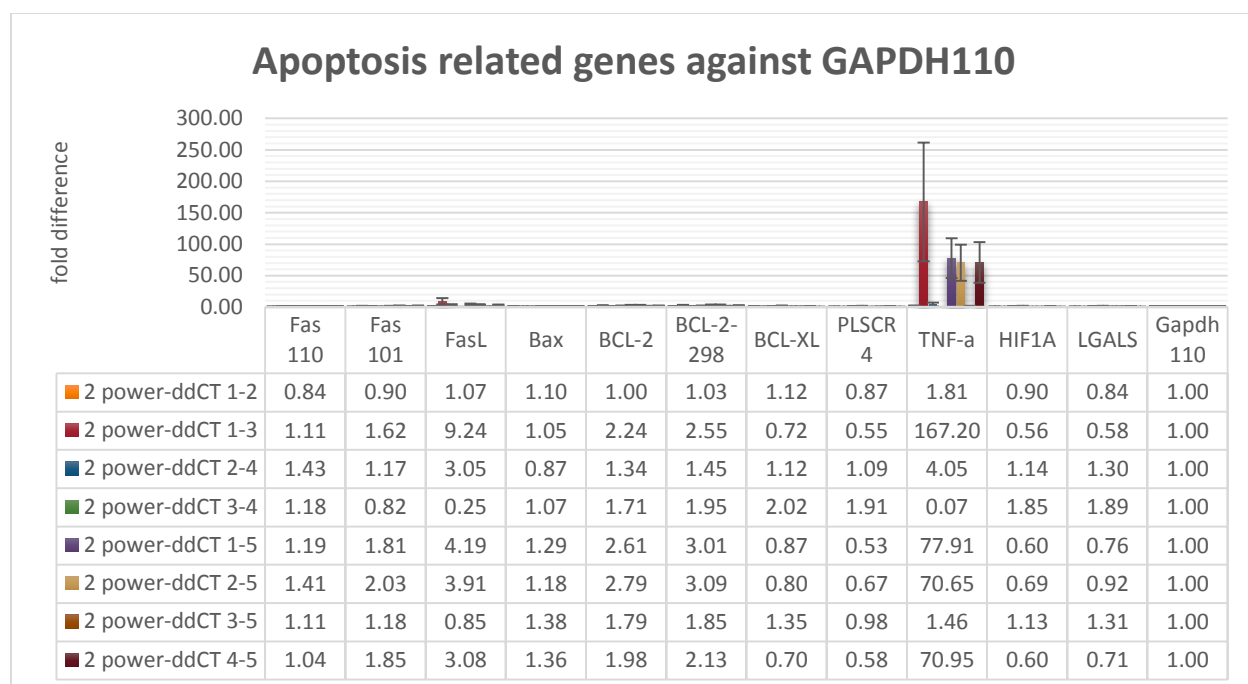


Figure 20. Fold difference between the protocols for the normalized expression ratio of each gene related to apoptosis in correlation to the reference gene GAPDH 101bp. The experiment was performed 5 times. The fold difference was calculated for: p1i-p2i ($2^{-\Delta\Delta CT 1-2}$); p1i-p1h ($2^{-\Delta\Delta CT 1-3}$); p2i-p2h ($2^{-\Delta\Delta CT 2-4}$); p1h-p2h ($2^{-\Delta\Delta CT 3-4}$); p1i-ctr ($2^{-\Delta\Delta CT 1-5}$); p2i-ctr ($2^{-\Delta\Delta CT 2-5}$); p1h-ctr ($2^{-\Delta\Delta CT 3-5}$); p2h-ctr ($2^{-\Delta\Delta CT 4-5}$). Fas110, Fas101, FasL, Bax, Bcl-2, Bcl-2-298, Bcl-xl, and HIF1A results are significantly different between P1i, P2i, P1h and the control ($p < .05$), TNF-a, LGALS, and PLSCR4 results between all protocols and control ($p < .05$), respectively.

Fig. 20 shows, the fold difference when normalization against the reference gene GAPDH110, no fold difference (f.d) between p1h and control for all genes, in contrast, for the protocols p1i, p2i, and p2h and control is shown, a 4.2; 3.9; 3 f.d for FasL, respectively, a 2.6; 2.8; 2 f.d for Bcl-2, a 3; 3.1; 2.1 f.d for Bcl-2-298, and a 78; 70.6; 71 f.d for TNF-a. Additionally Fas101 shows a 2 f.d between p2i and control. Between the protocols, no f.d is shown for p1i - p2i. For p1i – p1h FasL has a 9.2 f.d; Bcl-2 a 2.2; Bcl-2-298 a 2.55; and TNF-a a 167.2 f.d. For p2i – p2h, FasL and TNF-a have a 3. and 4. f.d respectively. And for p1h – p2h FasL has a 0.25; Bcl-xl a 2; and TNF-a a 0.07 f.d. According to this experiment, again vitrification protocol p1h seems not to influence the expression of the selected genes, in contrast to the p1i, p2i, and p2h, with TNF-a expression influenced at most.

According to the Figs. 18, 19, and 20, p1i and p2i seems to similarly influence gene expression; p1h does not influence gene expression, as it shows no fold difference to the control. Furthermore, from all selected genes, TNF-a seems to be the most sensitive gene to the vitrification/ thawing procedure, less influenced are FasL, Bcl-2, PLSCR, HIF1a, and LGALS, and Fas, and Bax seems to have a stable expression.

Figs. 21, 22, and 23 show the fold difference of the stress responded genes against the reference genes 18sRNA, GAPDH 70bp, and GAPDH 101bp, respectively.



Figure 21. Fold difference between the protocols for the normalized expression ratio of genes influenced by temperature, against the reference gene 18sRNA. The experiment was performed 5 times. The fold difference is calculated for: $p1i-p2i$ ($2^{-\Delta\Delta CT 1-2}$); $p1i-p1h$ ($2^{-\Delta\Delta CT 1-3}$); $p2i-p2h$ ($2^{-\Delta\Delta CT 2-4}$); $p1h-p2h$ ($2^{-\Delta\Delta CT 3-4}$); $p1i-ctr$ ($2^{-\Delta\Delta CT 1-5}$); $p2i-ctr$ ($2^{-\Delta\Delta CT 2-5}$); $p1h-ctr$ ($2^{-\Delta\Delta CT 3-5}$); $p2h-ctr$ ($2^{-\Delta\Delta CT 4-5}$). CIRBP1, RBM3, Hsp47, HspH1 results are significantly different between all four protocols and the control ($p < .05$), Hsp27 results are significantly different between P2i, P1h, P2h and control ($p < .05$), and Hsp70 results are non-significantly different ($p > .05$).

Fig. 21 shows, the fold difference when normalization against the reference gene 18sRNA, no fold difference (f.d) between p1h and control for all genes, in contrast, for the protocols p1i, p2i, and p2h and control is shown, a 0.27; 0.31; 0.4 f.d for CIRBP, a 0.21; 0.28; 0.26 f.d for RBM3, a 0.22; 0.3; 0.3 f.d for HSP47, and a 0.27; 0.4; 0.38 f.d for HSPH1. Additionally HSP70 shows a 0.47 f.d between p2h and control, and HSP27 a 0.3 and 0.43 f.d for p2i – control and p2h – control, respectively. Between the protocols, no f.d is shown for p1i - p2i, and p2i – p2h. For p1i – p1h CIRBP has a 0.24 f.d; RBM3 a 0.23; HSP47 and HSPH1 a 0.2; and HSP27 a 0.46 f.d. And for p1h – p2h CIRBP has a 4.1 f.d; RBM3 a 4.8; HSP47 a 5.7; HSPH1 a 5.; HSP70 a 2.6; and HSP27 a 2.5 f.d. According to this experiment, vitrification protocol p1h seems not to influence the expression of the selected genes, in contrast to the p1i, p2i, and p2h, which seems to similarly influence gene expression.

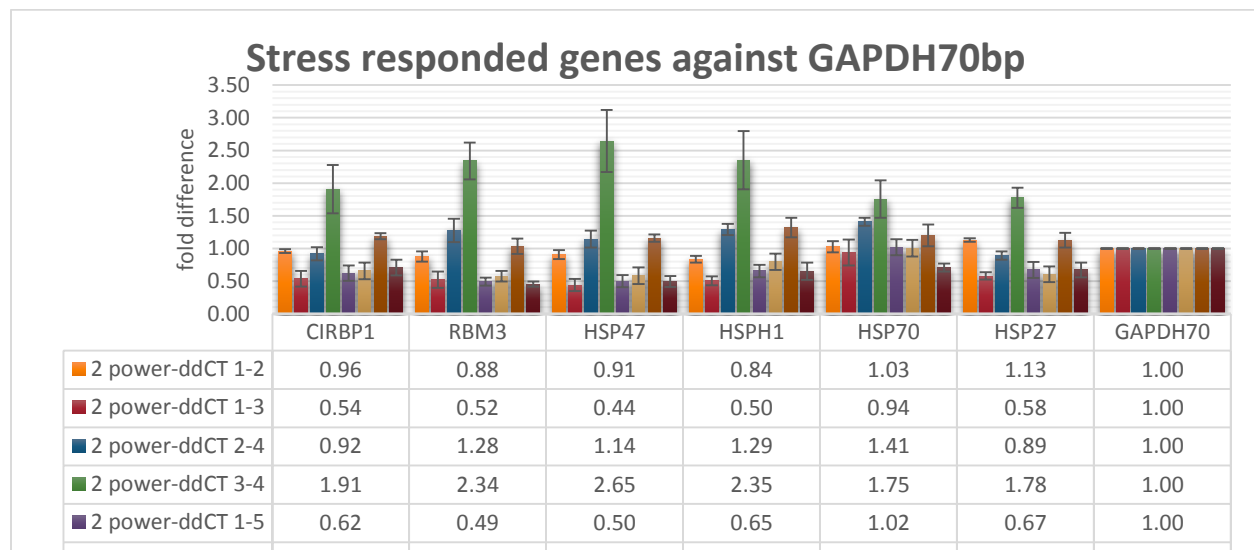


Figure 22. Fold difference between the protocols for the normalized expression ratio of genes influenced by temperature, against the reference gene GAPDH70bp. The experiment was performed 5 times. The fold difference is calculated for p1i-p2i ($2^{-\Delta\Delta CT 1-2}$); p1i-p1h ($2^{-\Delta\Delta CT 1-3}$); p2i-p2h ($2^{-\Delta\Delta CT 2-4}$); p1h-p2h ($2^{-\Delta\Delta CT 3-4}$); p1i-ctr ($2^{-\Delta\Delta CT 1-5}$); p2i-ctr ($2^{-\Delta\Delta CT 2-5}$); p1h-ctr ($2^{-\Delta\Delta CT 3-5}$); p2h-ctr ($2^{-\Delta\Delta CT 4-5}$). CIRBP1, RBM3 results are significantly different between all four protocols and control ($p < .05$), HSP47, HspH1, Hsp70, and Hsp27 results are non-significantly different ($p > .05$).

Fig. 22 shows, the fold difference when normalization against the reference gene GAPDH70, no fold difference (f.d) between p1h-control, and p2i – control, for all genes, in contrast, for the protocols p1i and p2h and control is shown, a 0.49; 0.45 f.d for RBM3, and a 0.5; 0.5 f.d for HSP47. Between the protocols, no f.d is shown for p1i - p2i, and p2i – p2h. For p1i – p1h CIRBP has a 0.54 f.d; RBM3 a 0.52; HSP47 a 0.44; and HSPH1 a 0.5 f.d. And for p1h – p2h CIRBP has a 1.9 f.d; RBM3 a 2.34; HSP47 a 2.65; and HSPH1 a 2.35 f.d. According to this experiment, vitrification protocol p1h and p2i seems not to influence the expression of the selected genes, in contrast to the p1i and p2h, which seems to similarly influence gene expression.

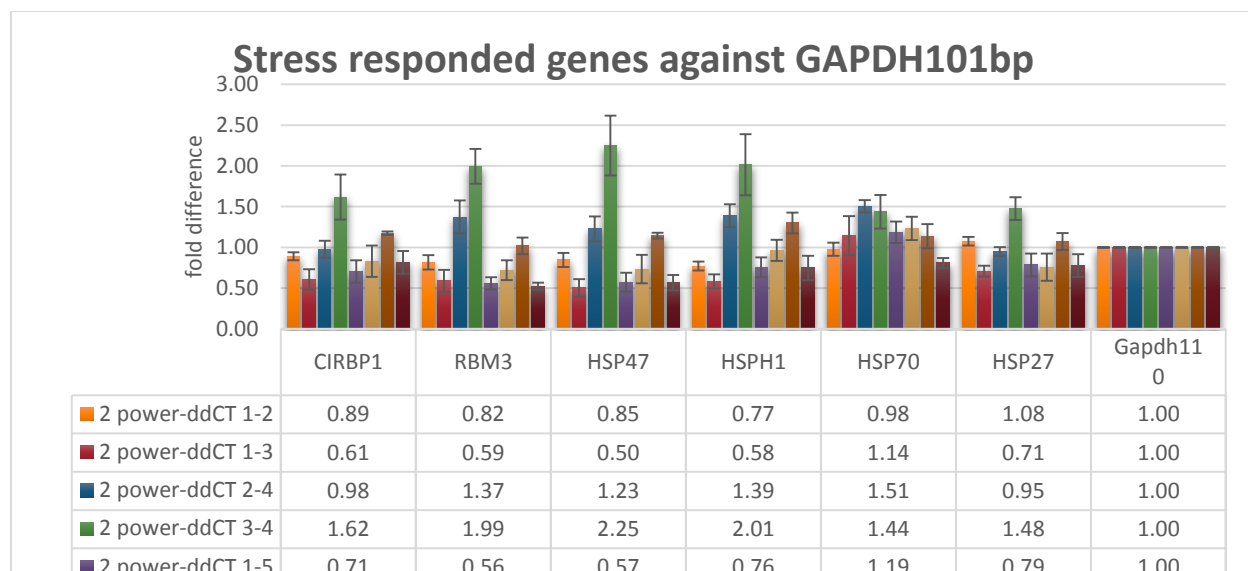


Figure 23. Fold difference between the protocols for the normalized expression ratio of genes influenced by temperature, against the reference gene GAPDH101bp. The experiment was performed 5 times. The fold difference is calculated for: p1i-p2i ($2^{-\Delta\Delta CT 1-2}$); p1i-p1h ($2^{-\Delta\Delta CT 1-3}$); p2i-p2h ($2^{-\Delta\Delta CT 2-4}$); p1h-p2h ($2^{-\Delta\Delta CT 3-4}$); p1i-ctr ($2^{-\Delta\Delta CT 1-5}$); p2i-ctr ($2^{-\Delta\Delta CT 2-5}$); p1h-ctr ($2^{-\Delta\Delta CT 3-5}$); p2h-ctr ($2^{-\Delta\Delta CT 4-5}$). CIRBP1 results are significantly different between P1i and the control ($p < .05$), RBM3, Hsp47, HspH1 results between P1i, P1h, P2h and the control ($p < .05$), and Hsp70, Hsp27 results between P1i, P2i, P1h and control ($p < .05$), respectively.

Fig. 23 shows, the fold difference when normalization against the reference gene GAPDH110, no fold difference (f.d) between p1h-control, and p2i – control, for all genes, in contrast, for the protocols p1i and p2h and control is shown, a 0.56; 0.52 f.d for RBM3, and a 0.57; 0.57 f.d for HSP47. Between the protocols, no f.d is shown for p1i - p2i, and p2i – p2h. For p1i – p1h CIRBP and RBM3 have a 0.6 f.d; HSP47 a 0.5; and HSPH1 a 0.58 f.d. And for p1h – p2h RBM3 has a 2.; HSP47 a 2.25; and HSPH1 a 2. f.d. According to this experiment, vitrification protocol p1h and p2i seems not to influence the expression of the selected genes, in contrast to the p1i and p2h, which seems to similarly influence gene expression.

According to Figs. 21, 22, and 23, p1h and p2i seems not to influence the expression of the selected genes. Additionally, p1i and p2h seems to similarly influence gene expression. RBM3 and HSP47 are the most sensitive genes to the vitrification/ thawing procedure, and less influenced are the CIRBP, HSPH1, HSP70, and HSP27. Protocols p1h and p2h, seems to differ the most, and protocols p1i – p2i seems to be similar.

Finally, in Figs. 24, 25, and 26 is shown the fold difference of genes, which have a role in cell development, against the reference genes 18sRNA, GAPDH 70bp, and GAPDH 101bp, respectively.

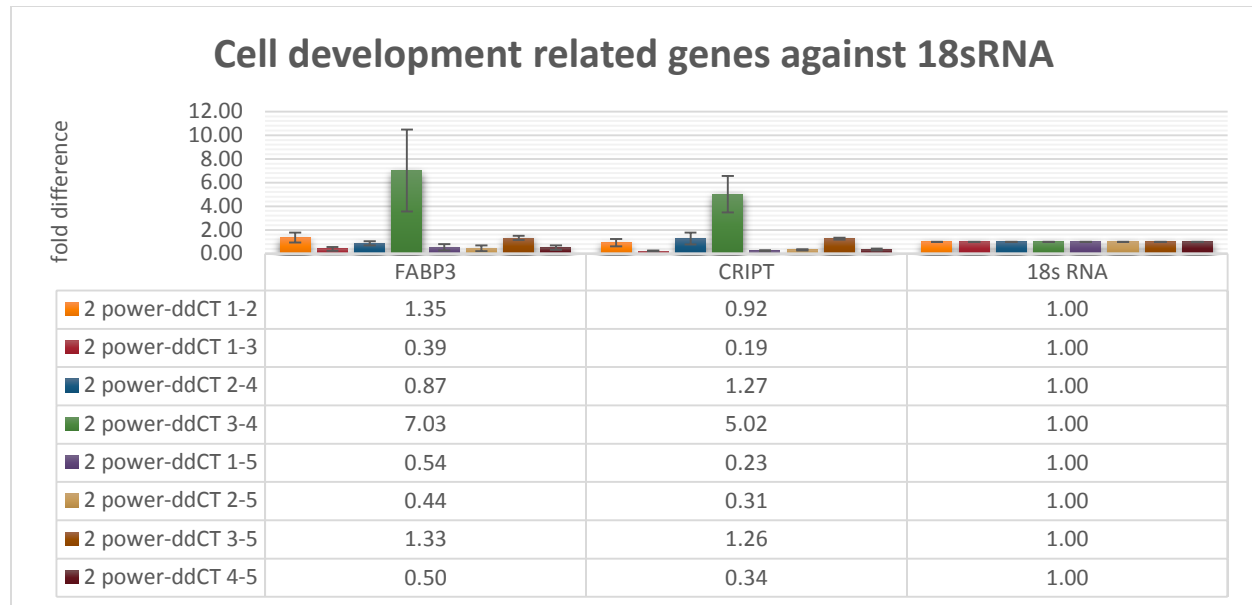


Figure 24. Fold difference between the protocols for the normalized expression ratio of genes having a role in cell development, against the reference gene 18sRNA. The experiment was performed 5 times. The fold difference is calculated for $p1i-p2i$ ($2^{-\Delta\Delta CT 1-2}$); $p1i-p1h$ ($2^{-\Delta\Delta CT 1-3}$); $p2i-p2h$ ($2^{-\Delta\Delta CT 2-4}$); $p1h-p2h$ ($2^{-\Delta\Delta CT 3-4}$); $p1i-ctr$ ($2^{-\Delta\Delta CT 1-5}$); $p2i-ctr$ ($2^{-\Delta\Delta CT 2-5}$); $p1h-ctr$ ($2^{-\Delta\Delta CT 3-5}$); $p2h-ctr$ ($2^{-\Delta\Delta CT 4-5}$). FABP3 and CRIPT results are significantly different between P1i, P2i, P1h and the control ($p < .05$).

Fig. 24 shows, the fold difference when normalization against the reference gene 18sRNA, no fold difference (f.d) between p1h-control, in contrast, for the protocols p1i, p2i and p2h and control is shown, a 0.54; 0.44; 0.5 f.d, for FABP3 respectively, and a 0.23; 0.31; 0.34 f.d for CRIPT. Between the protocols, no f.d is shown for p1i - p2i, and p2i - p2h. For p1i - p1h FABP3 and CRIPT have a 0.4 f.d respectively.. And for p1h - p2h FABP3 has a 7.; and CRIPT a 5. f.d. According to this experiment, vitrification protocol p1h seems not to influence the expression of the selected genes, in contrast to the p1i, p2i and p2h, which seems to similarly influence gene expression.

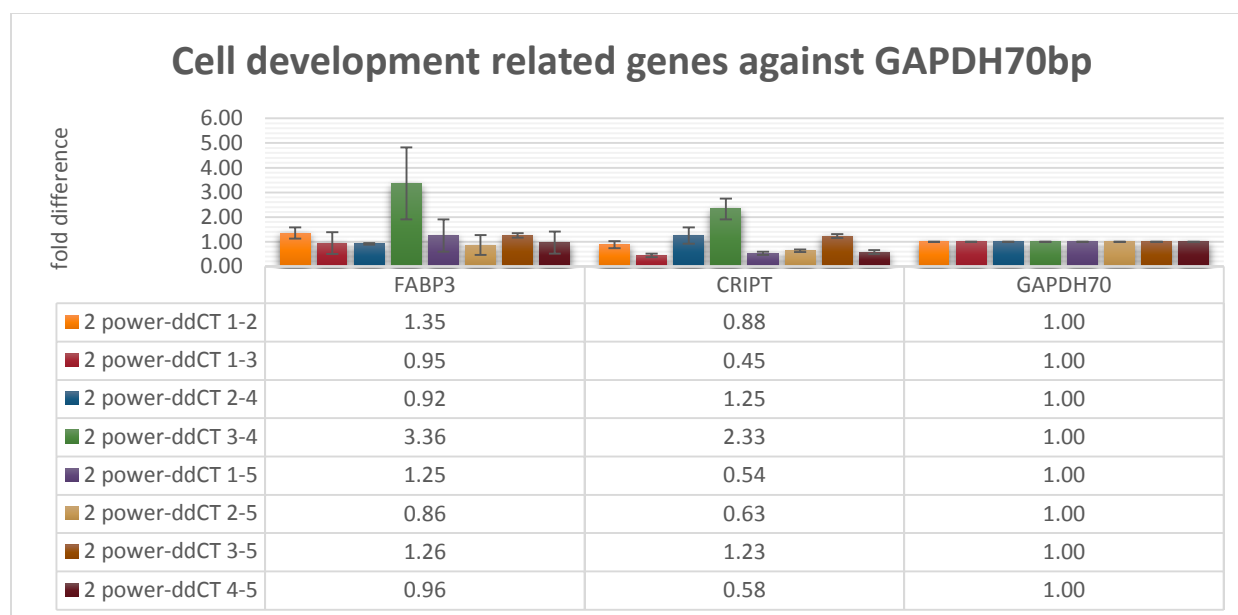


Figure 25. Fold difference between the protocols for the normalized expression ratio of genes having a role in cell development, against the reference gene GAPDH70bp. The experiment was performed 5 times. The fold difference is calculated for: p1i-p2i ($2^{-\Delta\Delta CT 1-2}$); p1i-p1h ($2^{-\Delta\Delta CT 1-3}$); p2i-p2h ($2^{-\Delta\Delta CT 2-4}$); p1h-p2h ($2^{-\Delta\Delta CT 3-4}$); p1i-ctr ($2^{-\Delta\Delta CT 1-5}$); p2i-ctr ($2^{-\Delta\Delta CT 2-5}$); p1h-ctr ($2^{-\Delta\Delta CT 3-5}$); p2h-ctr ($2^{-\Delta\Delta CT 4-5}$). FABP3 results are significantly different between all four protocols, and the control ($p < .05$) and CRIPT results between P1i, P1h and the control ($p < .05$), respectively.

Fig. 25 shows, the fold difference when normalization against the reference gene GAPDH70, no fold difference (f.d) between p1h-control, and p2i – control, in contrast, for the protocols p1i and p2h and control is shown, a 0.54; 0.58 f.d for CRIPT. Between the protocols, no f.d is shown for p1i - p2i, and p2i – p2h. For p1i – p1h CRIPT has a 0.45 f.d. Last, for p1h – p2h FABP3 has a 3.36; and CRIPT a 2.3 f.d. According to this experiment, vitrification protocol p1h and p2i seems not to influence the expression of the selected genes, in contrast to the p1i and p2h, which seem to influence similar the expression of CRIPT.

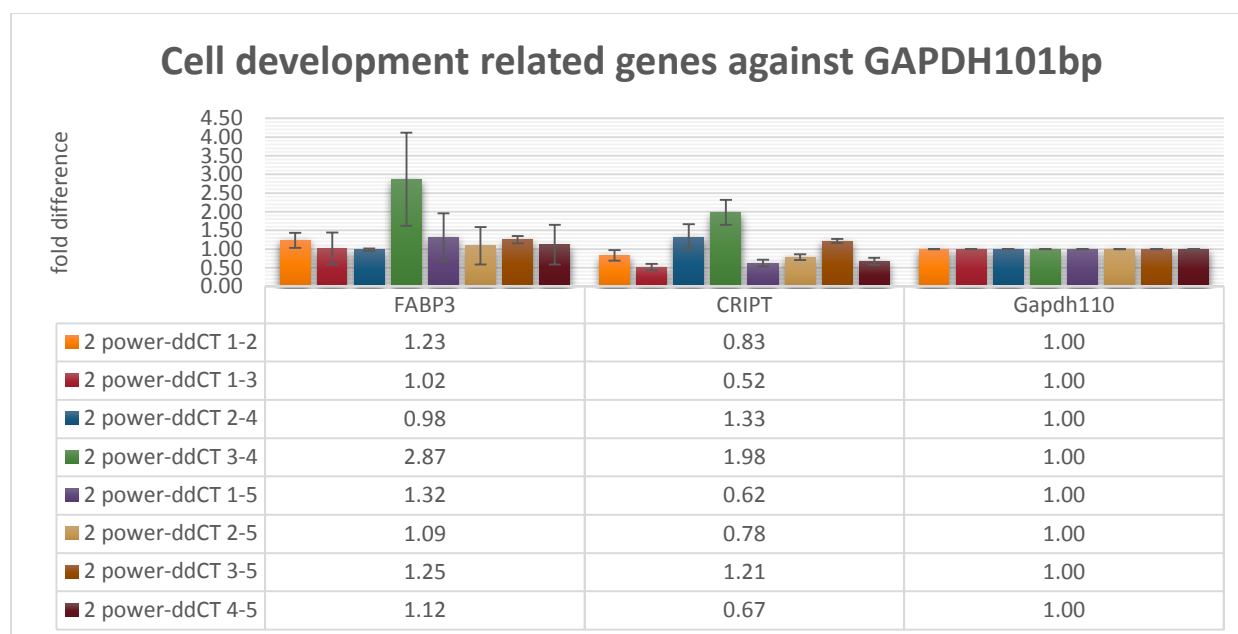


Figure 26. Fold difference between the protocols for the normalized expression ratio of genes having a role in cell development, against the reference gene GAPDH101bp. The experiment was performed 5 times. The fold difference is calculated for: p1i-p2i ($2^{-\Delta\Delta CT 1-2}$); p1i-p1h ($2^{-\Delta\Delta CT 1-3}$); p2i-p2h ($2^{-\Delta\Delta CT 2-4}$); p1h-p2h ($2^{-\Delta\Delta CT 3-4}$); p1i-ctr ($2^{-\Delta\Delta CT 1-5}$); p2i-ctr ($2^{-\Delta\Delta CT 2-5}$); p1h-ctr ($2^{-\Delta\Delta CT 3-5}$); p2h-ctr ($2^{-\Delta\Delta CT 4-5}$). FABP3 results are significantly different between P1i and the control ($p < .05$), and CRIPT results between all four protocols and control ($p < .05$), respectively.

Fig. 26 shows, the fold difference when normalization against the reference gene GAPDH110, no fold difference (f.d) between all four protocols and the control. Between the protocols, no f.d is shown for p1i - p2i, and p2i - p2h. For p1i - p1h CRIPT has a 0.52 f.d. Finally, for p1h - p2h FABP3 has a 2.87; and CRIPT a 2. f.d. According to this experiment, none of the vitrification protocols seem to influence the expression of the selected genes.

According to Figs. 24, 25, and 26, the expression of the selected genes, FABP3 and CRIPT, is not influenced by the p1h vitrification-/thawing process. Moreover, the protocols p1i, p2i, and p2h do not affect significantly their expression. CRIPT is more sensitive than FABP3. Protocols p1h and p2h seem to differ the most, and protocols p1i, p2i, and p2h seem to be similar.

5 DISCUSSION

Tissue cryopreservation maintains the cellular metabolism in a quiescence state and makes the conservation possible for an indefinite period of time. The choice of an appropriate cryopreservation protocol is essential for maintenance of cryopreserved tissue banks. This study investigated, in the human granulosa cell line KGN, two vitrification solutions, a self-manufactured and a commercial, and the relative protocols to them, Protocol 1 (P1) and Protocol 2 (P2) respectively, to observe if freezing-thawing procedure influences cell viability, cell proliferation, and the expression of selected genes having a role in apoptosis, cell development, or a response to stresses.

The experiments carried out showed that cell viability is significantly dependent on vitrification ($p < 0.05$), with the self-manufactured protocol (P1) having greater viability rates than the commercial one (P2) (no significant difference). Further, cell proliferation is promoted after vitrification-thawing procedure in contrast to the control (non-significant difference). These results are consistent to those of gene expression analysis, where TNF- α expression increase significant in both protocols, especially for P2, the commercial vitrification solution.

The viability of KGN cells was estimated by two distinct experiments and presented similar results. In the first experiment - Cell stain - Double Staining Kit (Fluka Analytical) has been used and the cells were counted by imagej. In the second experiment was used Propidium Iodide and KGN viability was analyzed by FACs. A substantial significant viability difference was shown between the non-vitrified KGN cells (control) and the vitrified. A 51,6 % greater viability rate was shown contrast to P1 ($p < 0.05$) and a 54,4% contrast to P2 ($p < 0.05$), by double staining experiments. Similarly, a 19,95 % greater viability rate was shown for the control against P1 ($p < 0.05$), and a 30,63% against P2 ($p < 0.05$), by propidium iodide staining experiments. Between the two vitrification protocols a smaller non-significant difference was shown, with the self-manufactured protocol having greater viability rates than the commercial one, 3,8% for the double staining experiments and 11,68% for the iodide staining experiments.

Cell cycle experiments showed that both vitrification methods, compared to the control, had a significant decrease of G1 and G2 phase ($p < 0.05$), whereas S phase rate increased (non-significant). As S phase is the phase where the cell duplicates its DNA, cell cycle analysis indicates that more KGN cells tend to double their DNA after the vitrification-thawing procedure, in contrast to the control cells. This tendency was more pronounced for the self-manufactured protocol than the commercial one ($p < 0.05$).

The results mentioned above leads to the conclusion that vitrification-thawing process influences strongly cell viability, and according to which cryoprotectant is used this outcome can vary. Further, cell cycle analysis is shown that cells survived the vitrification process, tend to double their DNA faster than the control cells. In both experiments self-manufactured protocol (P1)

seems to have better outcomes than the commercial one. Da-Croce et al. enhance the viability results of this study as they show similarly, a significant decrease of cell viability when compared vitrified small fragments of umbilical cord to fresh ones. However, they show that cell proliferation in vitro was preserved, may be because of the different study model used (Da-Croce et al. 2013).

The majority of changes in cryopreservation protocols have been due to empirical measurements. Investigating the effects of cryopreservation on cellular biology, such as gene expression, is fundamental to improving techniques and protocols. Larman et al. (2011) have shown that vitrification can influence gene expression. In this study an expression analysis of the genes Fas, FasL, Bax, Bcl2, Bcl-xL, PLSCR4, TNF- α , HIF1A, LGALS, CIRBP1, RBM3, HSP47, HSPH1, HSP70, HSP27, FABP3, CRIPT was conducted, by using Real Time PCR, as soon as the KGN cells were warmed and after one hour incubation at room temperature, resulting in four protocols: (p1i) vitrification by P1 and further treatment, as soon as the sample was thawed; (p1h) vitrification by P1 and further treatment one hour after the thawing procedure; (p2i) vitrification by P2 and further treatment, as soon as the sample was thawed; (p2h) vitrification by P2 and further treatment one hour after the thawing procedure. Hovatta et al. (1996) and Keros et al. (2009) also proposed to have an incubation period after thawing procedure to allow possible damage caused by vitrification to be expressed. Indeed, differences in genes expression were observed.

Real Time PCR results were analyzed by $\Delta\Delta CT$ method, where the ΔCT s were normalized to three reference genes 18sRNA, GAPDH70bp, and GAPDH110bp and the fold difference was estimated between all four protocols and between the protocols and the control (non-vitrified KGN cells). P1h was the only process that did not influence the expression of any investigated gene, and differ the most to p2h. Vitrification by p2i, p2h, and p1i, influenced the genes expression in a similar way.

After vitrification-thawing procedure by p2i, p2h, and p1i: TNF- α ; FasL; Bcl2 expression was up-regulated, Fas; Bax; Bcl-xL; HSP70 expression was not influenced, and PLSCR4; HIF1A; LGALS; CIRBP1; RBM3; HSP47; HSPH1; HSP27; FABP3; CRIPT expression was down-regulated. Just TNF- α results were statistically significant ($p < 0.05$) for all four protocols, and all three reference genes. For the rest genes the significance was varying according the reference gene and is shown in Figs. 18 – 26, this may be rely on the different conditions the experiments were conducted.

Many studies have been performed using various model systems to investigate gene expression after cryopreservation. Although, to my best knowledge not all genes expression investigated in this study, were investigated in vitrified samples by other studies. Abdollahi et al. (2013) and Mazoochi et al. (2009) resulted that in vitrified human ovarian tissue and mouse ovaries, respectively, by a vitrification protocol consisting ethylene glycol (EG) as cryoprotectant, FasL, Bax and Bcl-2 expression was not influenced, and Fas expression was up-regulated. Further, Jo et

al. (2012) showed also that Bax was not influenced by vitrification, in contrast Bcl-2 was down-regulated. To my best knowledge TNF- α expression is not investigated on vitrified samples, but its expression is responding to stresses, like cold stress. Zao et al. (2013) investigated the effect of cold stress, among others, on Hsp70, Hsp27 and TNF- α expression in hearts of chickens. All three genes expression was increased in cold stress groups relative to control groups. Further many studies showed that HSPs expression is increased after vitrification (Zhao et al. 2014; Liu et al. 2000; Shin et al. 2011). Furthermore, Al-Fageeh & Smales, and Shin et al. supported the up-regulation of CIRBT and RBM3 (Al-Fageeh & Smales 2009; Shin et al. 2011).

All these studies mentioned above, other times agree and other times disagree to this study results, which can lead to the conclusion that the model system used, the cryoprotectants or generally the conditions that the experiments were conducted, have a great influence on gene expression.

Considering the pro-apoptotic vs. the anti-apoptotic genes expression ratio, and the remarkable 22-78 fold over-expression of TNF- α , correlated to the control, the results of KGN cell viability experiments are consistent, as TNF- α high expression can induce apoptosis in many cells. It can be concluded that TNF- α expression is increased by the vitrification process and thereby cell viability decreases.

At the level of the ovary, TNF- α has been proposed as an intraovarian modulator of granulosa cell function; granulosa cells are a source of ovarian TNF- α . Additionally, TNF- α has been shown to alter ovarian steroidogenesis, by effecting dose-dependent alterations in the elaboration of progesterone and androstenedione, but not estrogen. TNF- α may play also a role in the processes of atresia or luteolysis. It is also possible that locally produced TNF- α plays an important role as an autocrine and/or paracrine mediator in the corpus luteum during pregnancy. Luteal TNF- α may contribute to maintaining the pregnancy by stimulating the production of PGF2 α and PGE2 by the corpus luteum, indirectly resulting in an increase in progesterone output. TNF- α also stimulates thecal progestin production in adult rat preovulatory follicles (Terranova et al. 1991; Kol et al. 2008; Lanuza et al. 2002).

Having all these functions and additionally being its expression highly influenced by the vitrification conditions makes TNF- α an excellent gene marker for vitrification influence on cells and tissues.

In response to low temperature, mammalian cells change various physiological functions. Cold stress changes the lipid composition of cellular membranes, and suppresses the rate of protein synthesis and cell growth. Cold stress induces the synthesis of several cold-shock proteins like RBM3 and CIRBT, in these study both are down-regulated. Under conditions of RBM3 down-regulation, is shown that cells undergo mitotic catastrophe, because RBM3 increases mRNA stability and translation of otherwise rapidly degraded transcripts, further CIRBT is shown to suppress cell proliferation (Nishiyama et al. 1997; Sureban et al. 2008). Additionally to CIRBT, FABP3 also suppress cell proliferation and LGALS which have been shown to regulate cell growth

and cell cycle, by arresting G₁ or G₂/M phase, were down-regulated (Zhu et al. 2011; Liu et al. 2002; Hsu et al. 2015).

Considering RBM3 down-regulation and the lower suppression of cell proliferation because of CIRBT and FABP3 down-regulation, the results of KGN cell cycle analysis, where G₁ and G₂ phase rates decrease ($p < 0.05$) and S phase rate increase (non-significant), are consistent.

Concurrently, to the KGN experiments were done also progesterone production ability tests on C57BL/6J mouse ovaries to evaluate their viability after vitrification.

This experiment showed that mouse ovaries progesterone production is reduced after vitrification in contrast to fresh ovaries. Moreover, progesterone production rate declined slower over time for mouse ovaries which were kept 5 days at 4°C and then vitrified, than when vitrified the first day. The results were not statistically significant, therefore more repeats would be necessary, nevertheless is shown that an incubation time at 4°C, prior vitrification has an important influence on progesterone production. Zhao et al. (2013) showed by histopathological analysis that chickens heart tissues were seriously injured after cold stress, this result agrees to the viability rate decrease and the progesterone reduction outcomes of this study.

Considering all previous mentioned experiments, the results lead to the conclusion that incubation time after thawing procedure but also the cryoprotectants used for vitrification, play a significant role on genes expression.

This study recommends vitrification with increasing concentrations of dimethyl sulphoxide (DMSO) (P1), and treatment of the sample one hour after thawing, relying to the cell viability, cell cycle and gene expression analysis results. DMSO was proposed since 1960 as cryoprotectant, and was used by Donnez et al. for their study that led to the live birth after orthotopic transplantation of cryopreserved ovarian tissue (Mazur 1970; Donnez et al. 2004).

Nonetheless, this protocol was investigated just in KGN cells, therefore the best approach would probably be to focus on this protocol and after obtaining consistent results, in future studies, for example on cow or sheep ovaries as they are very similar to those of humans (Newton et al. 1999), the protocol could be improved step by step, changing one parameter at a time, if necessary, adapting it according to tissue requirements and progressing toward a specific protocol for ovarian tissue vitrification.

6 TABLE OF FIGURES

Figure 1. Representative picture of a primary follicle -----	12
Figure 2. The main steps of folliculogenesis -----	14
Figure 3. The sequence of events that make ovulation occur -----	16
Figure 4. Hematoxylin stained cuts of fresh and vitrified mouse ovaries -----	58
Figure 5. Unstained follicles -----	59
Figure 6. Progesterone production of 1-day old fresh and 1-day old vitrified mouse ovaries ---	60
Figure 7. Progesterone production of 5-days old fresh and 5-days old vitrified mouse ovaries-	60
Figure 8. Progesterone production of 1-day and 5-days old fresh mouse ovaries-----	61
Figure 9. Progesterone production of 1-day and 5-days old vitrified mouse ovaries -----	61
Figure 10. Representative picture of the expression of progesterone receptors and LH/hCG receptor in KGN cells by PCR -----	62
Figure 11. Representative pictures from FLOWJO viability measurement -----	63
Figure 12. Viability rates of fixed and unfixed KGN cells with 70% ethanol -----	64
Figure 13. KGN cell cycle analysis in presence of ethanol -----	65
Figure 14. Fluorescence pictures of vitrified KGN cells in slides -----	66
Figure 15. KGN survival rates, of vitrified cells in slides, calculated by imagej -----	67
Figure 16. Survival and mortality rates of vitrified KGN cells by means of FACs -----	68
Figure 17. KGN cell cycle analysis by means of FACs -----	69
Figure 18. Fold difference between the protocols for the normalized expression ratio of each gene related to apoptosis in correlation to the reference gene 18sRNA -----	71
Figure 19. Fold difference between the protocols for the normalized expression ratio of each gene related to apoptosis in correlation to the reference gene GAPDH 70bp -----	72
Figure 20. Fold difference between the protocols for the normalized expression ratio of each gene related to apoptosis in correlation to the reference gene GAPDH 101bp -----	73
Figure 21. Fold difference between the protocols for the normalized expression ratio of genes influenced by temperature, against the reference gene 18sRNA -----	74
Figure 22. Fold difference between the protocols for the normalized expression ratio of genes influenced by temperature, against the reference gene GAPDH70bp -----	75
Figure 23. Fold difference between the protocols for the normalized expression ratio of genes influenced by temperature, against the reference gene GAPDH101bp-----	76
Figure 24. Fold difference between the protocols for the normalized expression ratio of genes having a role in cell development, against the reference gene 18sRNA -----	77
Figure 25. Fold difference between the protocols for the normalized expression ratio of genes having a role in cell development, against the reference gene GAPDH70bp -----	78
Figure 26. Fold difference between the protocols for the normalized expression ratio of genes having a role in cell development, against the reference gene GAPDH101bp-----	79

7 ACKNOWLEDGEMENTS

Frank Herbert wrote: “There is no real ending. It’s just the place where you stop the story.”

Exactly at the moment when I stop my story about “Vitrification impact on Ovarian Tissue and Cells” I would like to express my thanks to all of those who helped me during this story.

First of all, Dr. Detlef Pietrowski, who was near me all the time during the practical and theoretical part of this story. Thank you for editing my manuscripts, for your honest comments, excellent guidance, scientific discussions, and friendly attitude!

Univ.Prof. Dr. Christian Schneeberger, for accepting me as your student and for being there every time I needed you.

Prof. Werner Callebaut for being my friend, for supporting me in any field, and for never getting tired of editing my manuscripts.

Dr. Mario Mairhofer and Nadja Leditznig for taking the time to answer all my questions and help me during my work in laboratory.

My friend Vaso Papastergiou for being near me and helping with her knowledge.

Finally, I would like to thank my family for their physical and psychological support, and for being with me in all difficult moments, also if some of them are far away.

8 REFERENCES

Books

1. Donnez Jacques and S. Samuel Kim (2011), *Principles and Practice of Fertility Preservation*. Ed. Cambridge University Press.
 - Domingo Javier, Cobo Ana, S´anchez Maria and Pellicer Antonio (2011), *Fertility preservation in non-cancer patients* (p.23-34).
 - Wallace W. H. B., Anderson R. A. and Meirow D. (2011). *The effect of chemotherapy and radiotherapy on the human reproductive system* (p.11-22)
2. Hoffman B., Schorge J., Schaffer J., Halvorson L., Bradshaw K., Cunningham F. (2012) *Williams Gynecology*, Sec. Ed. The McGraw-Hill Companies, Inc.
3. Rogers Kara (2011), *The reproductive system*. Ed. Britannica Educational Publishing.
4. Schorge J., Schaffer J., Halvorson L., Hoffman B., Bradshaw K., Cunningham F. (2008) *Williams Gynecology*. The McGraw-Hill Companies, Inc.
5. Sciarra John J., *Gynecology and Obstetrics CD-ROM*, 2004 Edition. (Vol 5, Chap 12), Lippincott Williams & Wilkins.
6. Silber Sherman J., M.D. (2007), *How to get pregnant*. Ed. Little, Brown and Company.
7. Wallace Hayes A., Kruger Claire L. (2014), *Hayes' Principles and Methods of Toxicology*, Sixth Edition. CRC Press.
8. Sherwood Lauralee (2010), *Human Physiology: From Cells to Systems*, 7th edition. Brooks/Cole, Cengage Learning.
9. Gracia C. and Woodruff T.K. (eds.), (2012), *Oncofertility Medical Practice: Clinical Issues and Implementation*, DOI 10.1007/978-1-4419-9425-7_1. Springer Science+Business Media New York.
10. Tekoa L. King, Mary C. Brucker, (2010), *Pharmacology for Women's Health*. Jones & Bartlett Publishers,
11. Cooper GM (2000). *The cell: a molecular approach*. "Chapter 14: The Eukaryotic Cell Cycle". (2nd ed.). Washington, D.C: ASM Press

Papers and reviews

1. Abdollahi M, Salehnia M, Salehpour S, Ghorbanmehr N. *Human ovarian tissue vitrification/warming has minor effect on the expression of apoptosis-related genes*. Iran Biomed J. 2013;17(4):179-86.
2. Adhikari D and Liu K, *Molecular mechanisms underlying the activation of mammalian primordial follicles*. 30:438-464, Endocr Rev 2009.
3. Al-Fageeh MB, Smales CM. *Cold-inducible RNA binding protein (CIRP) expression is modulated by alternative mRNAs*. RNA. 2009 Jun; 15(6):1164-76. doi: 10.1261/rna.1179109. Epub 2009 Apr 27.
4. Amorim CA., Curaba M., Van Langendonck A., Dolmans, MM, Donnez J, *Vitrification as an alternative means of cryopreserving ovarian tissue*. Reproductive BioMedicine Online; (160), Aug 2011, Vol. 23 Issue 2.
5. Anderson RA and Wallace WH, *Fertility preservation in girls and young women*. Clin Endocrinol 75:409-419 (Oxf) 2011.
6. Aparna Vidyasagar, Nancy A Wilson and Arjang Djamali. *Heat shock protein 27 (HSP27): biomarker of disease and therapeutic target*. Vidyasagar et al. Fibrogenesis & Tissue Repair 2012, 5:7
7. Atan Gross, James M. McDonnell and Stanley J. Korsmeyer, *BCL-2 family members and the mitochondria in apoptosis*. Genes Dev. 1999 13: 1899-1911
8. Barondes SH, Cooper DN, Gitt MA, Leffler H. *Galectins. Structure and function of a large family of animal lectins*. J Biol Chem. 1994 Aug 19;269 (33):20807-10.
9. Baud V, Karin M, *Signal transduction by tumor necrosis factor and its relatives*. Trends Cell Biol. 2001 Sep;11 (9):372-7.
10. Beck-Peccoz P, Persani L (2006), *Premature ovarian failure*. Orphanet J Rare Dis 1: 9. doi:10.1186/1750-1172-1-9. PMC 1502130. PMID 16722528.
11. Biotium Inc., retrieved December 04, 2012, *GelRed and GelGreen: Environmentally safe and ultra-sensitive nucleic acid gel stains for replacing EtBr*.
12. Boiso I, Marti M, Santalo J, Ponsa M, Barri PN and Veiga A (2002) *A confocal microscopy analysis of the spindle and chromosome configurations of human oocytes cryopreserved at the germinal vesicle and metaphase II stage*. Hum Reprod 17,1885–1891.

13. Brougham Mark F. H. and Wallace W. H. B. *Subfertility in children and young people treated for solid and haematological malignancies*, 2005, (131, 143–155), Blackwell Publishing Ltd, British Journal of Haematology,.
14. Burston SG, Clarke AR. *Molecular chaperones: physical and mechanistic properties*. Essays Biochem. 1995;29:125-36.
15. Cai L, Ma X, Liu S, Liu J, Wang W, Cui Y, Ding W, Mao Y, Chen H, Huang J, Zhou Z, Liu J. *Effects of upregulation of Hsp27 expression on oocyte development and maturation derived from polycystic ovary syndrome*. PLoS One. 2013 Dec 31;8(12):e83402. doi: 10.1371/journal.pone.0083402. eCollection 2013.
16. Cao Y, Xing Q, Zhang ZG, Wei ZL, Zhou P and Cong L, *Cryopreservation of immature and in-vitro matured human oocytes by vitrification*. Reprod Biomed Online 2009; 19:369-373.
17. Charles A. Sklar , Ann C. Mertens , Pauline Mitby , John Whitton , Marilyn Stovall , Catherine Kasper , Jean Mulder , Daniel Green , H. Stacy Nicholson , Yutaka Yasui , Leslie L. Robison. *Premature menopause in survivors of childhood cancer: a report from the childhood cancer survivor study*. J Natl Cancer Inst, 2006; 98: 890–6.
18. Chen C, *Pregnancy after human oocyte cryopreservation*. Lancet 1986; 1:884-886.
19. Chen CH, Zhang X, Barnes R, Confino E, Milad M, Puscheck E and Kazer RR, *Relationship between peak serum estradiol levels and treatment outcome in in vitro fertilization cycles after embryo transfer on day 3 or day 5*. Fertil Steril 2003; 80:75-79.
20. Chian RC, Wang Y, Li YR. *Oocyte vitrification: advances, progress and future goals*. J Assist Reprod Genet. 2014 Apr;31(4):411-20. doi: 10.1007/s10815-014-0180-9. Epub 2014 Jan 30.
21. Chmurzyńska A, *The multigene family of fatty acid-binding proteins (FABPs): function, structure and polymorphism*. J Appl Genet. 2006;47(1):39-48.
22. Cobo A, Domingo J, Perez S, Crespo J, Remohi J and Pellicer A. *Vitrification: an effective new approach to oocyte banking and preserving fertility in cancer patients*, Clin Transl Oncol 2008; 10:268-273.
23. Da-Croce L, Gambarini-Paiva GH, Angelo PC, Bambirra EA, Cabral AC, Godard AL. *Comparison of vitrification and slow cooling for umbilical tissues*. Cell Tissue Bank. 2013 Mar;14(1):65-76.
24. Dafforn TR, Della M, Miller AD (2001), *The molecular interactions of heat shock protein 47 (Hsp47) and their implications for collagen biosynthesis*. J. Biol. Chem. 276 (52): 49310–9. doi:10.1074/jbc.M108896200. PMID 11592970).

25. Danno S, Itoh K, Matsuda T, Fujita J, *Decreased expression of mouse Rbm3, a cold-shock protein, in Sertoli cells of cryptorchid testis*. Am J Pathol. 2000 May;156(5):1685-92.
26. Danno S, Nishiyama H, Higashitsuji H, Yokoi H, Xue JH, Itoh K, Matsuda T, Fujita J, *Increased transcript level of RBM3, a member of the glycine-rich RNA-binding protein family, in human cells in response to cold stress*. Biochem Biophys Res Commun, 1997, 236(3):804-7 Jul 30.
27. De Maio A, *Extracellular Hsp70: export and function*. Curr Protein Pept Sci., 2014, May;15(3):225-31.
28. De Maio A, *Heat shock proteins: facts, thoughts, and dreams*. Shock, 1999 Jan;11(1):1-12.
29. DeSantis CE, Lin CC, Mariotto AB, Siegel RL, Stein KD, Kramer JL, Alteri R, Robbins AS, Jemal A. *Cancer treatment and survivorship statistics, 2014*. CA Cancer J Clin. 2014 Jul-Aug;64(4):252-71. doi: 10.3322/caac.21235.
30. Deura I, Harada T, Taniguchi F, Iwabe T, Izawa M, Terakawa N. *Reduction of estrogen production by interleukin-6 in a human granulosa tumor cell line may have implications for endometriosis-associated infertility*. Fertil Steril. 2005 Apr;83 Suppl 1:1086-92.
31. Dolmans Marie-Madeleine, corresponding author Pascale Jadoul, Sébastien Gilliaux, Christiani A. Amorim, Valérie Luyckx, Jean Squifflet, Jacques Donnez, and Anne Van Langendonck, *A review of 15 years of ovarian tissue bank activities*. J Assist Reprod Genet. Mar 2013; 30(3): 305–314.
32. Dolmans MM, Demylle D, Martinez-Madrid B and Donnez J, *Efficacy of in vitro fertilization after chemotherapy*. Fertil Steril, 2005; 83:897-901.
33. Donnez J, Dolmans MM, Demylle D, Jadoul P, Pirard C, Squifflet J, Martinez-Madrid B and van Langendonck A, *Livebirth after orthotopic transplantation of cryopreserved ovarian tissue*. Lancet, 2004; 364:1405-1410.
34. Donnez J, Dolmans MM, Pellicer A, Diaz-Garcia C, Sanchez Serrano M, Schmidt KT, Ernst E, Luyckx V, Andersen CY (2013), *Restoration of ovarian activity and pregnancy after transplantation of cryopreserved ovarian tissue: a review of 60 cases of reimplantation*. Fertil Steril 99(6):1503-13
35. Donnez J, Dolmans MM. *Fertility preservation in women*. Nat Rev Endocrinol, 2013, Dec;9(12):735-49. doi: 10.1038/nrendo.2013.205. Epub 2013 Oct 29.
36. Donnez J, Martinez-Madrid B, Jadoul P, Van Langendonck A, Demylle D, Dolmans MM. *Ovarian tissue cryopreservation and transplantation: a review*, Hum Reprod Update, 2006, Sep-Oct;12(5):519-35. Epub 2006 Jul 18.

37. Douglas N.W. Cooper and Samuel H. Barondes. *God must love galectins; He made so many of them*. Glycobiology vol. 9 no. 10, 1999,(979–984).
38. Duncan R. Smith, *Agarose Gel Electrophoresis” Methods in Molecular Biology* Volume 58, 1996, (17-21).
39. Ehlén A, Brennan DJ, Nodin B, O'Connor DP, Eberhard J, Alvarado-Kristensson M, Jeffrey IB, Manjer J, Brändstedt J, Uhlén M, Pontén F, Jirstrom K. *Expression of the RNA-binding protein RBM3 is associated with a favourable prognosis and cisplatin sensitivity in epithelial ovarian cancer*. J Transl Med, 2010, Aug 20;8:78. doi: 10.1186/1479-5876-8-78.
40. Ehlén Å, Nodin B, Rexhepaj E, Brändstedt J, Uhlén M, Alvarado-Kristensson M, Pontén F, Brennan DJ, Jirstrom K. *RBM3-regulated genes promote DNA integrity and affect clinical outcome in epithelial ovarian cancer*. Transl Oncol, 2011, Aug;4(4):212-21. Epub 2011 Aug 1.
41. Emori C, Sugiura K, *Role of oocyte-derived paracrine factors in follicular development*. Anim Sci J. 2014.
42. Eppig JJ, *Intercommunication between mammalian oocytes and companion somatic cells* Bioessays., 1991, (569-574).
43. Eppig JJ, *Growth and development of mammalian oocytes in vitro*. Arch Pathol Lab Med, 1992, (379-382).
44. Erickson GF, Case E: *Epidermal growth factor antagonizes ovarian theca-interstitial cyto-differentiation*. Mol Cell Endocrinol ,1983, (31: 71).
45. Erickson, G, Glob. libr. women's med., (ISSN: 1756-2228) 2008; DOI 10.3843/GLOWM.10289.
46. Faddy MJ. *Follicle dynamics during ovarian ageing*. Mol Cell Endocrinol, 2000, (43- 48).
47. Farrant J. *Water transport and cell survival in cryobiological procedures*. Philos Trans R Soc Lond B Biol Sci, 1977, Mar 29;278(959):(191-205).
48. Field SL, Dasgupta T, Cummings M, Orsi NM. *Cytokines in ovarian folliculogenesis, oocyte maturation and luteinisation*. Mol Reprod Dev, 2014, Apr;81(4)(284-314).
49. Foghi A, Teerds KJ, van der Donk H, Dorrington J: *Induction of apoptosis in rat thecal/interstitial cells by transforming growth factor alpha plus transforming growth factor beta in vitro*. J Endocrinol 153, 1997, (169).
50. Fu-Tong Liu & Gabriel A, Rabinovich. *Galectins as modulators of tumour progression*. Nature Reviews Cancer 5, 29-41 (2005) | doi:10.1038/nrc1527.

51. Georges A, Auguste A, Bessière L, Vanet A, Todeschini AL, Veitia RA. *FOXL2: a central transcription factor of the ovary*. J Mol Endocrinol, 2013, Dec 19;52(1):R17-33. doi: 10.1530/JME-13-0159. Print 2014 Feb.
52. Gilchrist R.B, Ritter L.J, Armstrong D.T. *Oocyte–somatic cell interactions during follicle development in mammals*, Animal Reproduction Science Volume 82, Complete , 2004, (431-446).
53. Gleeson H K and Shalet S M, *The impact of cancer therapy on the endocrine system in survivors of childhood brain tumours*. Endocrine-Related Cancer, 2004, (11: 589–602).
54. Goswami D, Conway GS: *Premature ovarian failure*. Hum Reprod Update, 2005, (11:391-410).
55. Gougeon A, *Human ovarian follicular development: from activation of resting follicles to preovulatory maturation*. Ann Endocrinol (Paris), 2010; (71:132-143).
56. Gougeon A: *Regulation of ovarian follicular development in primates: facts and hypotheses*. Endocr Rev, 1996, (17:121-55).
57. Guicciardi ME1, Gores GJ. *Life and death by death receptors*. FASEB J. 2009 Jun; 23(6):1625-37. doi: 10.1096/fj.08-111005. Epub, 2009, Jan 13.
58. Hamid AA, Mandai M, Fujita J, Nanbu K, Kariya M, Kusakari T, Fukuhara K, Fujii S. *Expression of cold-inducible RNA-binding protein in the normal endometrium, endometrial hyperplasia, and endometrial carcinoma*. Int J Gynecol Pathol, 2003, Jul; 22(3):240-7.
59. Harald Wajant, *The Fas signaling pathway: more than a paradigm*. Science (Impact Factor: 31.2). 06/2002; 296(5573):1635-6. DOI: 10.1126/science.1071553.
60. Hashimoto T, Kusakabe T, Sugino T, Fukuda T, Watanabe K, Sato Y, Nashimoto A, Honma K, Kimura H, Fujii H, Suzuki T. *Expression of heart-type fatty acid-binding protein in human gastric carcinoma and its association with tumor aggressiveness, metastasis and poor prognosis*. Pathobiology. 2004; 71(5):267-73.
61. Havelock JC, Rainey WE, Carr BR. *Ovarian granulosa cell lines*. Mol Cell Endocrinol, 2004, Dec 30; 228(1-2):67-78.
62. Horling K, Santos AN, Fischer B. *The AhR is constitutively activated and affects granulosa cell features in the human cell line KGN*. Mol Hum Reprod. 2011 Feb;17(2):104-14. doi: 10.1093/molehr/gaq074. Epub 2010 Sep 7.
63. Houzelstein D, Gonçalves IR, Fadden AJ, Sidhu SS, Cooper DN, Drickamer K, Leffler H, Poirier F. *Phylogenetic analysis of the vertebrate galectin family*. Mol Biol Evol. 2004 Jul;21(7):1177-87. Epub 2004 Feb 12.

64. Hovatta O, 2005, *Methods for cryopreservation of human ovarian tissue*. Reproductive BioMedicine Online 10(6):729–34.
65. Hovatta O, *Cryopreservation and culture of human ovarian cortical tissue containing early follicles*. Eur J Obstet Gynecol Reprod Biol.,2004, Apr 5;113 Suppl 1:S50-4.
66. Hovatta O, Silye R, Krausz T, Abir R, Margara R, Trew G, Lass A and Winston RM. *Cryopreservation of human ovarian tissue using dimethylsulphoxide propanediolsucrose as cryoprotectants*. Hum Reprod, 1996; (11:1268-1272).
67. Howell S, Shalet S, *Gonadal damage from chemotherapy and radiotherapy*. Endocrinol Metab Clin North Am,1998, Dec;27(4):927-43.
68. Hsu DK, Yang RY, Saegusa J, Liu FT. *Analysis of the intracellular role of galectins in cell growth and apoptosis*. Methods Mol Biol. 2015;1207:451-63. doi: 10.1007/978-1-4939-1396-1_29.
69. Huang DC, Hahne M, Schroeter M, Frei K, Fontana A, Villunger A, Newton K, Tschopp J, Strasser A. *Activation of Fas by FasL induces apoptosis by a mechanism that cannot be blocked by Bcl-2 or Bcl-x(L)*. Proc Natl Acad Sci U S A. 1999 Dec 21;96(26):14871-6.
70. Isachenko E, Isachenko V, Rahimi G, Nawroth F. *Cryopreservation of human ovarian tissue by direct plunging into liquid nitrogen*, Eur J Obstet Gynecol Reprod Biol. 2003 Jun 10;108(2):186-93.
71. Isachenko V, Isachenko E, Weiss JM. *Human ovarian tissue: vitrification versus conventional freezing*. Hum Reprod,2009, Jul;24(7):1767-8; author reply 1768-9. doi: 10.1093/humrep/dep094. Epub 2009 Apr 22.
72. Jo JW, Jee BC, Suh CS, Kim SH. *The beneficial effects of antifreeze proteins in the vitrification of immature mouse oocytes*. PLoS One. 2012;7(5):e37043. doi: 10.1371/journal.pone.0037043. Epub 2012 May 23.
73. Kalantaridou SN, Davis SR and Nelson LM, (1998), *Premature ovarian failure*. Endocrinol Metab Clin North Am 27, 989–1006.
74. Keros V, Xella S, Hultenby K, Pettersson K, Sheikhi M, Volpe A, Hreinsson J, Hovatta O. *Vitrification versus controlled-rate freezing in cryopreservation of human ovarian tissue*. Hum Reprod. 2009 Jul;24(7):1670-83. doi: 10.1093/humrep/dep079. Epub 2009 Apr 9.
75. Kevin C. Kregel, Invited Review: *Heat shock proteins: modifying factors in physiological stress responses and acquired thermotolerance*. Journal of Applied Physiology, 2002, Vol. 92, 2001,no 2177-2186 DOI: 10.1152/jappphysiol.01267.
76. Knight PG, Glister C, *TGF-beta superfamily members and ovarian follicle development*. Reproduction. 2006 Aug; 132(2):191-206.

77. Kol S, Rohan R, et al, Glob. libr. women's med., (ISSN: 1756-2228), 2008; DOI 10.3843/GLOWM.10288.
78. Konc J, Kanyó K, Kriston R, Somoskő B, Cseh S. *Cryopreservation of Embryos and Oocytes in Human Assisted Reproduction*. Biomed Res Int, 2014;:307268. Epub, 2014, Mar 23.
79. Kort JD, Eisenberg ML, Millheiser LS, Westphal LM. *Fertility issues in cancer survivorship*. CA Cancer J Clin. 2014 Mar-Apr;64(2):118-34. doi: 10.3322/caac.21205.
80. Kumar TR, Wang Y, Lu N, Matzuk MM: *Follicle stimulating hormone is required for ovarian follicle maturation but not male fertility*. Nat Genet, 1997, (15:201-4).
81. Kuwayama M, *Highly efficient vitrification for cryopreservation of human oocytes and embryos: the Cryotop method*. Theriogenology, 2007, Jan 1;67(1):73-80
82. Lanuza GM, Saragüeta PE, Bussmann UA, Barañao JL. *Paradoxical effects of tumour necrosis factor-alpha on rat granulosa cell DNA synthesis*, Reprod Fertil Dev, 2002;14(3-4):133-9.
83. Larman MG, Katz-Jaffe MG, McCallie B, Filipovits JA, Gardner DK, (2011), *Analysis of global gene expression following mouse blastocyst cryopreservation*. Hum Reprod 26(10):2672-80.
84. Levine J. *Fertility preservation in children and adolescents with cancer*. Minerva Pediatr. 2011 Feb;63(1):49-59.
85. Liu FT, Patterson RJ, Wang JL. *Intracellular functions of galectins*. Biochim Biophys Acta. 2002 Sep 19;1572(2-3):263-73.
86. Liu K, Yang Y, Mansbridge J. *Comparison of the stress response to cryopreservation in monolayer and three-dimensional human fibroblast cultures: stress proteins, MAP kinases, and growth factor gene expression*. Tissue Eng. 2000 Oct;6(5):539-54.
87. Lopez-Hernandez FJ, Ortiz MA, Piedrafita FJ. *The extrinsic and intrinsic apoptotic pathways are differentially affected by temperature upstream of mitochondrial damage*, 2006, Apoptosis.
88. Lüschen S, Falk M, Scherer G, Ussat S, Paulsen M, Adam-Klages S. *The Fas-associated death domain protein/caspase-8/c-FLIP signaling pathway is involved in TNF-induced activation of ERK*. Exp Cell Res, 2005, Oct 15;310(1):33-42.
89. Malyshev Igor (2013). *Immunity, Tumors and Aging: The Role of HSP70*.
90. Mayer M. P. and Bukau B., *Hsp70 chaperones: Cellular functions and molecular mechanism*. Cell Mol Life Sci. Mar 2005; 62(6): 670–684. doi: [10.1007/s00018-004-4464-6](https://doi.org/10.1007/s00018-004-4464-6).

91. Mazoochi T, Salehnia M, Pourbeiranvand S, Forouzandeh M, Mowla SJ, Hajizadeh E. *Analysis of apoptosis and expression of genes related to apoptosis in cultures of follicles derived from vitrified and non-vitrified ovaries*. Mol Hum Reprod. 2009 Mar;15(3):155-64. doi: 10.1093/molehr/gap002. Epub 2009 Jan 19
92. Mazur P. *Cryobiology: The Freezing of Biological Systems*. 1970 SCIENCE, VOL. 168.
93. Mazur P. *Kinetics of Water Loss from Cells at Subzero Temperatures and the Likelihood of Intracellular Freezing*. J Gen Physiol, 1963; 47:347-369.
94. McDonald Evens Emily, MPH, (2004), *A Global Perspective on Infertility: An Under Recognized Public Health Issue* Carolina Papers International Health.
95. Meirow D and Nugent D, *The effects of radiotherapy and chemotherapy on female reproduction*. Hum Reprod Update, 2001; 7: 535–43.
96. Meirow D, Dor J, Kaufman B, Shrim A, Rabinovici J, Schiff E, Raanani H, Levron J, Fridman E. *Cortical fibrosis and blood-vessels damage in human ovaries exposed to chemotherapy. Potential mechanisms of ovarian injury*. Hum Reprod, 2007, Jun;22(6):1626-33. Epub, 2007, Feb 26.
97. Meirow D, EpsteinM, Lewis H et al. *Administration of cyclophosphamide at different stages of follicular maturation in mice: effects on reproductive performance and fetal malformations*. Hum Reprod, 2001; 16: 632–7.
98. Michelmann H. W., Nayudu P., *Cryopreservation of Human Embryos*, 2006, Volume 7, Issue 2, (135-141).
99. Michels J, Kepp O, Senovilla L, Lissa D, Castedo M, Kroemer G, Galluzzi L. *Functions of BCL-X L at the Interface between Cell Death and Metabolism*. Int J Cell Biol. 2013; 2013:705294. doi: 10.1155/2013/705294. Epub 2013 Feb 28.
100. Morgan S, Anderson RA, Gourley C, Wallace WH, Spears N. *How do chemotherapeutic agents damage the ovary?* Hum Reprod Update. 2012 Sep-Oct;18(5):525-35. doi: 10.1093/humupd/dms022. Epub 2012 May 30.
101. Nakayama K, Kanzaki A, Hata K, Katabuchi H, Okamura H, Miyazaki K, Fukumoto M, Takebayashi Y. *Hypoxia-inducible factor 1 alpha (HIF-1 alpha) gene expression in human ovarian carcinoma*. Cancer Lett. 2002 Feb 25;176(2):215-23.
102. Newton H, Fisher J, Arnold JR, Pegg DE, Faddy MJ, Gosden RG. *Permeation of human ovarian tissue with cryoprotective agents in preparation for cryopreservation*. Hum Reprod,1998, Feb;13(2):376-80.

103. Newton H, Picton H, Gosden RG. *In vitro growth of oocyte-granulosa cell complexes isolated from cryopreserved ovine tissue*. J Reprod Fertil. 1999 Jan;115(1):141-50.
104. Niethammer M, Valtschanoff JG, Kapoor TM, Allison DW, Weinberg RJ, Craig AM, Sheng M. *CRIP1, a novel postsynaptic protein that binds to the third PDZ domain of PSD-95/SAP90*. Neuron, 1998, Apr;20(4):693-707.
105. Nishi Y, Yanase T, Mu Y, Oba K, Ichino I, Saito M, Nomura M, Mukasa C, Okabe T, Goto K, Takayanagi R, Kashimura Y, Haji M, Nawata H. *Establishment and characterization of a steroidogenic human granulosa-like tumor cell line, KGN, that expresses functional follicle-stimulating hormone receptor*. Endocrinology, 2001;142(1):437-45.
106. Nishiyama H, Higashitsuji H, Yokoi H, Itoh K, Danno S, Matsuda T, Fujita J. *Cloning and characterization of human CIRP (cold-inducible RNA-binding protein) cDNA and chromosomal assignment of the gene*. Gene. 1997 Dec 19;204(1-2):115-20.
107. Nishiyama H, Itoh K, Kaneko Y, Kishishita M, Yoshida O, Fujita J. *A glycine-rich RNA-binding protein mediating cold-inducible suppression of mammalian cell growth*. J Cell Biol. 1997 May 19;137(4):899-908.
108. Onuki R, Suyama E, Taira K. *Retraction: Identification of genes that function in the TNF-alpha-mediated apoptotic pathway using randomized hybrid ribozyme libraries*. Nat Biotechnol. 2006 Sep;24(9):1170.
109. Orisaka M, Tajima K, Tsang BK, Kotsuji F. *Oocyte-granulosa-theca cell interactions during preantral follicular development*. J Ovarian Res. 2009 Jul 9;2(1):9. doi: 10.1186/1757-2215-2-9.
110. Passafaro M, Sala C, Niethammer M, Sheng M. *Microtubule binding by CRIP1 and its potential role in the synaptic clustering of PSD-95*. Nat Neurosci, 1999, Dec;2(12):1063-9
111. Pegg DE. *Principles of cryopreservation*. Methods Mol Biol, 2007,(368:39-57).
112. Pena JE, Chang PL, Chan LK, Zeitoun K, Thornton MH, 2nd and Sauer MV, *Supraphysiological estradiol levels do not affect oocyte and embryo quality in oocyte donation cycles*. Hum Reprod, 2002; (17:83-87).
113. Peters H. *The development of the mouse ovary from birth to maturity*. ACTA Endocrinol., 62 (1969),(98–116).
114. Phillippe M, Bradley DF, Ji H, Oppenheimer KH, Chien EK. *Phospholipid scramblase isoform expression in pregnant rat uterus*. J Soc Gynecol Investig. 2006 Oct;13(7):497-501. Epub 2006 Sep 15

115. Picton HM, Kim SS and Gosden RG. *Cryopreservation of gonadal tissue and cells*. Br Med Bull,2000; (56:603-615).
116. Pietrowski D, Gong Y, Mairhofer M, Gessele R, Sator M. *Effects of progesterone and its metabolites on human granulosa cells*. Horm Metab Res, 2014, Feb; 46(2):133-7
117. Piserchio A, Spaller M, Mierke DF. *Targeting the PDZ domains of molecular scaffolds of transmembrane ion channels*. AAPS J.,2006, Jun 2;8(2):E396-401.
118. Qian Q, Kuo L, Yu YT, Rottman JN. *A concise promoter region of the heart fatty acid-binding protein gene dictates tissue-appropriate expression*. Circ Res, 1999, Feb 19;84(3):276-89.
119. Razzaque MS, Taguchi T, *The possible role of colligin/HSP47, a collagen-binding protein, in the pathogenesis of human and experimental fibrotic diseases*. Histol Histopathol,1999 Oct;14(4):(1199-212).
120. Reddy P, Zheng W and Liu K, *Mechanisms maintaining the dormancy and survival of mammalian primordial follicles*. Trends Endocrinol Metab, 2010; (21:96-103).
121. Reeka N, Berg FD, and Brucker C: *Presence of transforming growth factor alpha and epidermal factor in human ovarian tissue and follicular fluid*. Hum Reprod 13:1998, (2199).
122. Reverchon M, Cornuau M, Cloix L, Ramé C, Guerif F, Royère D, Dupont J. *Visfatin is expressed in human granulosa cells: regulation by metformin through AMPK/SIRT1 pathways and its role in steroidogenesis*. Mol Hum Reprod. 2013 May;19(5):313-26. doi: 10.1093/molehr/gat002. Epub 2013 Jan 11.
123. Reverchon M, Cornuau M, Ramé C, Guerif F, Royère D, Dupont J. *Chemerin inhibits IGF-1-induced progesterone and estradiol secretion in human granulosa cells*. Hum Reprod. 2012 Jun;27(6):1790-800. doi: 10.1093/humrep/des089. Epub 2012 Mar 23.
124. Riccardi C, Nicoletti I. *Analysis of apoptosis by propidium iodide staining and flow cytometry*. Nat Protoc. 2006;1(3):1458-61.
125. Ricci MS, Zong WX, *Chemotherapeutic approaches for targeting cell death pathways*. Oncologist.,2006, Apr;11(4):342-57.
126. Richards JS, Pangas SA. *The ovary: basic biology and clinical implications*. J Clin Invest. 2010 Apr;120(4):963-72. doi: 10.1172/JCI41350. Epub 2010 Apr 1.
127. Robitaille H, Simard-Bisson C, Larouche D, Tanguay RM, Blouin R, Germain L, *The small heat-shock protein Hsp27 undergoes ERK-dependent phosphorylation and redistribution to the cytoskeleton in response to dual leucine zipper-bearing kinase expression*. J Invest Dermatol. 2010 Jan;130(1):74-85. doi: 10.1038/jid.2009.185.

128. Rodriguez-Wallberg KA, Hovatta O. (2010) *Cryopreservation of human ovarian tissue*. J Reprod Stem Cell Biotechnol 1(2):141-49
129. Sabban, Sari, (2011), *Development of an in vitro model system for studying the interaction of Equus caballus IgE with its high- affinity FcεRI receptor*. (PhD thesis), The University of Sheffield.
130. Sahu SK, Gummadi SN, Manoj N, Aradhyam GK (2007). *Phospholipid scramblases: an overview*. Arch. Biochem. Biophys. 462 (1): 103–14. doi:10.1016/j.abb.2007.04.002. PMID 17481571.
131. Sánchez F, Smitz J. *Molecular control of oogenesis*. Biochim Biophys Acta, 2012 Dec;1822(12):1896-912. doi: 10.1016/j.bbadis.2012.05.013. Epub 2012 May 24.
132. Santoro N: *Mechanisms of premature ovarian failure*. Ann Endocrinol, 2003, 64:87-92
133. Saxena A, Banasavadi-Siddegowda YK, Fan Y, Bhattacharya S, Roy G, Giovannucci DR, Frizzell RA, Wang X. *Human heat shock protein 105/110 kDa (Hsp105/110) regulates biogenesis and quality control of misfolded cystic fibrosis transmembrane conductance regulator at multiple levels*. J Biol Chem. 2012 Jun 1;287(23):19158-70. doi: 10.1074/jbc.M111.297580. Epub, 2012, Apr 13.
134. Schipper I, Hop WC, Fauser BC. *The follicle-stimulating hormone (FSH) threshold/window concept examined by different interventions with exogenous FSH during the follicular phase of the normal menstrual cycle: duration, rather than magnitude, of FSH increase affects follicle development*. J Clin Endocrinol Metab, 1998, Apr;83(4):1292-8.
135. Semenza GL, Rue EA, Iyer NV, Pang MG, Kearns WG (June 1996). *Assignment of the hypoxia-inducible factor 1alpha gene to a region of conserved synteny on mouse chromosome 12 and human chromosome 14q*. Genomics 34 (3): 437–9. doi:10.1006/geno.1996.0311. PMID 8786149.
136. Sheikhi M, Hultenby K, Niklasson B, Lundqvist M, Hovatta O. *Preservation of human ovarian follicles within tissue frozen by vitrification in a xeno-free closed system using only ethylene glycol as a permeating cryoprotectant*. Fertil Steril. 2013 Jul;100(1):170–7.
137. Shen Y, Song G, Liu Y, Zhou L, Liu H, Kong X, Sheng Y, Cao K, Qian L. *Silencing of FABP3 inhibits proliferation and promotes apoptosis in embryonic carcinoma cells*. Cell Biochem Biophys. 2013 May;66(1):139-46. doi: 10.1007/s12013-012-9462-y.

138. Shin HD, Kim LH, Park BL, Jung HS, Cho YM, Moon MK, Lee HK, Park KS. *Polymorphisms in fatty acid-binding protein-3 (FABP3) - putative association with type 2 diabetes mellitus*. Hum Mutat, 2003, Aug;22(2):180.
139. Shin MR, Choi HW, Kim MK, Lee SH, Lee HS, Lim CK. *In vitro development and gene expression of frozen-thawed 8-cell stage mouse embryos following slow freezing or vitrification*. Clin Exp Reprod Med. 2011 Dec;38(4):203-9. doi: 10.5653/cerm.2011.38.4.203. Epub 2011 Dec 31.
140. Sonmezer M, Oktay K. *Fertility preservation in female patients*. Hum Reprod Update. 2004 May-Jun;10(3):251-66.
141. Spener F, Unterberg C, Borchers T, Grosse R. *Characteristics of fatty acid-binding proteins and their relation to mammary-derived growth inhibitor*. Mol Cell Biochem, 1990, Oct 15-Nov 8;98(1-2):57-68.
142. Sureban SM, Ramalingam S, Natarajan G, May R, Subramaniam D, Bishnupuri KS, Morrison AR, Dieckgraefe BK, Brackett DJ, Postier RG, Houchen CW, Anant S. *Translation regulatory factor RBM3 is a proto-oncogene that prevents mitotic catastrophe*. Oncogene. 2008 Jul 31;27(33):4544-56. doi: 10.1038/onc.2008.97. Epub 2008 Apr 21.
143. Terranova P. F., Roby K. F., Sancho-Tello M., Weed J., Lyles R.. *TNF α : Altering Thecal and Granulosa Cell Steroidogenesis. Signaling Mechanisms and Gene Expression in the Ovary*. Sero Symposia USA, 1991, (178-189).
144. Timmreck LS, Reindollar RH: *Contemporary issues in primary amenorrhea*. Obstet Gynecol Clin North Am, 2003, 30:287-302.
145. Trounson A, Mohr L. *Human pregnancy following cryopreservation, thawing and transfer of an eight-cell embryo*. Nature, 1983, Oct 20-26;305(5936):707-9.
146. Vicente JS, García-Ximénez F. *Osmotic and cryoprotective effects of a mixture of DMSO and ethylene glycol on rabbit morulae*. Theriogenology,1994;42(7):1205-15.
147. Wajant H, Pfizenmaier K and Scheurich P. *Tumor necrosis factor signaling. Cell Death and Differentiation* (2003) 10, 45–65. doi:10.1038/sj.cdd.4401189.
148. Wallace W.H.B., Thomson A.B.and.Kelsey T.W. *The radiosensitivity of the human oocyte*. Human Reproduction, 2003; 18: (117–21).
149. Wallace WHB, Anderson RA and Irvine DS. *Fertility preservation for young patients with cancer: who is at risk and what can be offered?* Lancet Oncol, 2005; 6: 209–18
150. Wang GL, Jiang BH, Rue EA, Semenza GL. *Hypoxia-inducible factor 1 is a basic-helix-loop-helix-PAS heterodimer regulated by cellular O₂ tension*. Proc Natl Acad Sci U S A, 1995, Jun 6;92(12):5510-4.

151. Wang Y, Xiao Z, Li L, Fan W, Li SW. Novel needle immersed vitrification: a practical and convenient method with potential advantages in mouse and human ovarian tissue cryopreservation. *Hum Reprod.* 2008 Oct;23(10):2256–65.
152. Wellmann S, Bühner C, Moderegger E, Zelmer A, Kirschner R, Koehne P, Fujita J, Seeger K. *Oxygen-regulated expression of the RNA-binding proteins RBM3 and CIRP by a HIF-1-independent mechanism.* *J Cell Sci*, 2004, Apr 1;117(Pt 9):1785-94. Epub, 2004, Mar 16
153. Wellmann S, Truss M, Bruder E, Tornillo L, Zelmer A, Seeger K, Bühner C. *The RNA-binding protein RBM3 is required for cell proliferation and protects against serum deprivation-induced cell death.* *Pediatr Res.* 2010 Jan;67(1):35-41. doi: 10.1203/PDR.0b013e3181c13326.
154. Wikland M, Hardarson T, Hillensjö T, Westin C, Westlander G, Wood M and Wennerholm UB. *Obstetric outcomes after transfer of vitrified blastocysts.* *Hum Reprod*, 2010; 25:1699-1707.
155. Woodruff TK, Shea LD, *The role of the extracellular matrix in ovarian follicle development.* *Reprod Sci*, 2007, Dec;14(8 Suppl):6-10. doi: 10.1177/1933719107309818.
156. Xiang H, Kinoshita Y, Knudson CM, Korsmeyer SJ, Schwartzkroin PA, Morrison RS. *Bax involvement in p53-mediated neuronal cell death.* *J Neurosci.* 1998 Feb 15;18(4):1363-73.
157. Yamagishi N, Ishihara K, Saito Y, Hatayama T, *Hsp105 but not Hsp70 family proteins suppress the aggregation of heat-denatured protein in the presence of ADP.* *FEBS Lett*, 2003, Dec 4;555(2):390-6.
158. Yang Y, Spitzer E, Kenney N, Zschiesche W, Li M, Kromminga A, Müller T, Spener F, Lezius A, Veerkamp JH, et al, *Members of the fatty acid binding protein family are differentiation factors for the mammary gland.* *J Cell Biol*, 1994, Nov;127(4):1097-109.
159. Yi C.H., Vakifahmetoglu-Norberg H. and Yuan J., *Integration of Apoptosis and Metabolism.* *Cold Spring Harb Symp Quant Biol* 2011. 76: 375-387. doi: 10.1101/sqb.2011.76.010777
160. Yip KW, Reed JC. *Bcl-2 family proteins and cancer.* *Oncogene.* 2008 Oct 27;27(50):6398-406. doi: 10.1038/onc.2008.307.
161. Zeilmaker GH, Alberda AT, van Gent I, Rijkman CM and Drogendijk AC, *Two pregnancies following transfer of intact frozen-thawed embryos.* *Fertil Steril* 1984; 42:293-296.

162. Zhao FQ, Zhang ZW, Qu JP, Yao HD, Li M, Li S, Xu SW. *Cold stress induces antioxidants and Hsps in chicken immune organs*. Cell Stress Chaperones. 2014 Sep;19(5):635-48. doi: 10.1007/s12192-013-0489-9. Epub 2014 Jan 4.
163. Zhao FQ, Zhang ZW, Wang C, Zhang B, Yao HD, Li S, Xu SW. *The role of heat shock proteins in inflammatory injury induced by cold stress in chicken hearts*. Cell Stress Chaperones. 2013 Nov;18(6):773-83. doi: 10.1007/s12192-013-0429-8. Epub 2013 May 2.
164. Zhu C, Hu DL, Liu YQ, Zhang QJ, Chen FK, Kong XQ, Cao KJ, Zhang JS, Qian LM. *Fabp3 inhibits proliferation and promotes apoptosis of embryonic myocardial cells*. Cell Biochem Biophys, 2011, Jul;60(3):259-66. doi: 10.1007/s12013-010-9148-2.

Sources of internet

1. www.ncbi.nlm.nih.gov/gene/10808
2. www.ncbi.nlm.nih.gov/gene/871
3. <http://stainsfile.info/StainsFile/stain/hematoxylin/hxintro.htm>
4. www.genecards.org/cgi-bin/carddisp.pl?gene=PLSCR4
5. Hill, M.A. (2014) Embryology Main Page. Retrieved September 6, 2014, from https://php.med.unsw.edu.au/embryology/index.php?title=Main_Page
6. www.ncbi.nlm.nih.gov/gene/581

9 APPENDIX

Fig. 3. Original data

	<i>1-DAY OLD FRESH OVARIES</i>		<i>1-DAY OLD VITRIFIED OVARIES</i>	
	1st measurement	2d measurement	1st measurement	2d measurement
24H	19.239	17.364	9.60	8.53
48H	13.350	13.537	5.22	5.63
72H	6.493	5.651	1.82	2.99
168H	6.559	4.722	1.24	1.82

Fig.3 data. Progesterone production of 1-day old fresh and 1-day old vitrified mouse ovaries.

<i>HOURS</i>	<i>FRESH±SD</i>	<i>VITRIFIED±SD</i>
24	18.30±1.33	9.07±1.34
48	13.44±0.13	5.42±0.46
72	6.07±0.60	2.40±0.68
168	5.64±1.30	1.53±0.34

Fig. 4. Original data

	<i>5-DAYS OLD FRESH OVARIES</i>		<i>5-DAYS OLD VITRIFIED OVARIES</i>	
	1st measurement	2d measurement	1st measurement	2d measurement
24H	13.814	17.460	9.857	11.033
48H	9.316	12.740	9.603	10.811
72H	9.358	11.718	6.583	11.874
168H	6.734	13.530	7.399	8.153

Fig. 4 data. Progesterone production of 5-days old fresh and 5-days old vitrified mouse ovaries.

<i>HOURS</i>	<i>FRESH±SD</i>	<i>VITRIFIED±SD</i>
24	15.64±3.37	10.44±0.76
48	11.03±1.98	10.21±0.87
72	10.54±1.42	9.23±3.07
168	10.13±3.93	7.78±0.55

Fig. 5. Original data

	<i>1-DAY OLD FRESH OVARIES</i>		<i>5-DAYS OLD FRESH OVARIES</i>	
	1st measurement	2d measurement	1st measurement	2d measurement
24H	19.239	17.364	13.814	17.460
48H	13.350	13.537	9.316	12.740
72H	6.493	5.651	9.358	11.718
168H	6.559	4.722	6.734	13.530

Fig. 5 data. Progesterone production of 1-day and 5-days old fresh mouse ovaries.

<i>HOURS</i>	<i>1 DAY OLD FRESH±SD</i>	<i>5 DAYS OLD FRESH±SD</i>
24	18.30±1.33	15.64±3.37
48	13.44±0.13	11.03±1.98
72	6.07±0.60	10.54±1.42
168	5.64±1.30	10.13±3.93

Fig. 6. Original data

	1-DAY OLD VITRIFIED OVARIES		5-DAYS OLD VITRIFIED OVARIES	
	1st measurement	2d measurement	1st measurement	2d measurement
24H	9.60	8.53	9.857	11.033
48H	5.22	5.63	9.603	10.811
72H	1.82	2.99	6.583	11.874
168H	1.24	1.82	7.399	8.153

Fig. 6 data. Progesterone production of 1-day and 5-days old vitrified mouse ovaries

HOURS	1 DAY OLD VITRIFIED±SD	5 DAYS OLD VITRIFIED±SD
24	9.07±1.34	10.44±0.76
48	5.42±0.46	10.21±0.87
72	2.40±0.68	9.23±3.07
168	1.53±0.34	7.78±0.55

Fig. 9. Original data

%	NO STAIN	PI NO FIXED	PI ALIVE + FIXED	PI FIXED IM	PI FIXED 20MIN	PI FIXED 30MIN	PI FIXED + TRITON	PI FIXED +ALIVE +TRITON
1ST MEASUREMENT	99.4	87	76	70.6	65.70	57.40	2.67	0.66
2D MEASUREMENT	99.3	85.6	75.8	69.7			2.72	0.53
3D MEASUREMENT	99.4	84.8	75.9	69.2			2	

Fig. 9 Data: Viability rates of fixed and unfixed KGN cells with 70% ethanol.

STAIN TYPE	AVERAGE ALIVE±SD	AVERAGE DEAD±SD
NO STAIN	99.37±0.06	0.01±0.01
PI NO FIXED	85.80±1.11	13.53±1.26
PI ALIVE+FIXED	75.90±0.10	22.73±0.15
PI FIXED IM	69.83±0.71	28.27±0.61
PI FIXED 20MIN	65.70±0.73	33.00±0.68
PI FIXED 30MIN	57.40±0.83	40.70±0.75
PI FIXED+TRITON	2.46±0.40	97.10±0.44
PI FIXED+ALIVE+TRITON	0.60±0.09	99.25±0.07

Fig. 10. Original data

	G1				G2				S			
	0% EtO H	0,5 % EtO H	1% EtO H	1,5 % EtO H	0% EtO H	0,5 % EtO H	1% EtO H	1,5 % EtO H	0% EtO H	0,5 % EtO H	1% EtO H	1,5 % EtO H
1ST MEASUREMEN T	45.4	35.9	42	39	35.5	43.6	39.3	39.7	16.4	16.9	15.7	17.9
2D MEASUREMEN T	41	39.3	39.8	34.5	40.3	40.4	40.1	44.7	15.4	16.8	16.4	16.6
3D MEASUREMEN T	40.6	38.1	37.6	36	41.3	42.6	42.6	42.2	15.7	16.9	16.8	16.5
4TH MEASUREMEN T	42.5	43.4	35.8	37.8	40.6	36.6	43.3	40.4	14.3	16.8	17.5	16.2

Fig.10 data. KGN cell cycle analysis in presence of ethanol.

	0% ETOH±	0,5% ETOH±	1% ETOH±	1,5% ETOH±
G1	42.38±2.18	39.18±3.15	38.8±2.69	36.83±2.47
G2	39.43±2.65	40.8±3.10	41.33±1.93	41.75±2.74
S	15.45±0.87	16.85±0.06	16.6±0.75	16.8±0.68

Fig. 12. Original data

CELLS COUNTED BY IMAGEJ (IMAGE PROCESSING AND ANALYSIS IN JAVA)				
		Control	Protocol 1	Protocol 2
1ST MEASUREMENT	alive	1434	995	138
	dead	166	758	342
2D MEASUREMENT	alive	1248	281	402
	dead	206	669	837
3D MEASUREMENT	alive	223	291	601
	dead	5	697	696
4TH MEASUREMENT	alive	428	76	413
	dead	25	229	935
5TH MEASUREMENT	alive		310	537
	dead		749	1101
6TH MEASUREMENT	alive		117	
	dead		724	

Fig.12 data. KGN survival rates, of vitrified cells in slides, calculated by imagej.

%	CONTROL±SD	PROTOCOL 1±SD	PROTOCOL 2±SD
ALIVE	89.24±5.28	38.64±14.14	34.84±6.98
DEAD	10.76±5.28	61.36±14.14	65.16±6.98

Fig. 13. Original data

	CONTROL		PROTOCOL 1		PROTOCOL 2	
	<i>alive (cells)</i>	<i>dead (cells)</i>	<i>alive (cells)</i>	<i>dead (cells)</i>	<i>alive (cells)</i>	<i>dead (cells)</i>
1ST MEASUREMENT	13583	1086	7109	2785	9047	5826
2D MEASUREMENT	13816	520	11031	3781	10359	4462
3D MEASUREMENT	14024	776	11354	3484	10588	4324
4TH MEASUREMENT	14085	367	10717	4104	9333	5600
5TH MEASUREMENT			10337	4533	7567	7288
6TH MEASUREMENT			11242	3331	8814	5870

Fig. 13 data. Survival and mortality rates of vitrified KGN cells by means of FACs.

%	ALIVE±SD	DEAD±SD
CONTROL	92.53±1.50	4.58±2.10
PROTOCOL 1	72.58±2.57	26.00±3.03
PROTOCOL 2	61.90±7.38	37.05±7.25

Fig. 14. Original data

(CELLS)	CONTROL			PROTOCOL 1			PROTOCOL 2		
	G1	G2	S	G1	G2	S	G1	G2	S
1ST MEASUREMENT	4685	3707	676	2816	846	276	2493	656	259
2D MEASUREMENT	4752	3281	1327	3172	863	1191	1130	314	364
3D MEASUREMENT	5556	1934	1062	2369	542	1177	3456	782	613
4TH MEASUREMENT	6038	2216	1066	688	949	1633	1694	773	2873
5TH MEASUREMENT	7306	1051	767	2313	572	48	4419	1179	260

Fig.14 data. KGN cell cycle analysis by means of FACs.

%	G1±SD	G2±SD	S±SD
PROTOCOL 1	47.2±22.87	15.888±5.06	16.334±14.06
PROTOCOL 2	47.48±18.03	13.238±3.61	15.448±15.60
CONTROL	59.1±11.59	25.36±11.05	9.406±3.71

Tables 1-10. Original data (the measurements have been done in doublicates) of Figs. 15-23.

Table 1.

1ST EXPERIMENT						
GENES	P1i (Ct)	P2i (Ct)	P1h (Ct)	P2h (Ct)	ctr1 (Ct)	ctr2 (Ct)
FAS110	25.42	25	25.13	24.48	24.8	25.39
	25.27	24.96	24.97	24.46	24.68	25.37
BCL-2-298	27.57	27.19	27.4	27.06	28.83	28.2
	27.37	26.98	27.42	26.77	29.08	28.27
BCL-2	26.12	25.75	26.18	25.33	27.44	26.77
	26.05	25.79	25.94	25.38	27.18	27.14
18SRNA	14.11	14.06	14.14	13.88	13.89	14.03
	14.1	14.07	14.14	13.88	13.89	14.01
GAPDH70BP	17.58	17.3	17.37	17.05	17.02	17.52
	17.7	17.31	17.39	17.06	17.01	17.53
GAPDH110BP	17.45	17.15	17.25	16.81	16.61	17.12
	17.45	17.09	17.25	16.82	16.61	17.18
HSP70	23.29	23.14	23.8	22.73	23.06	23.13
	23.38	23.27	23.89	22.86	23.13	23.12
FASL	32.58	34.11	34.54	35.44	34.44	39.74
	32.22	32.42	32.2	32.45	Undetermined	34.61
BAX	24.42	24.26	24.31	23.99	24.19	25.03
	24.38	24.26	24.33	24.09	24.22	25.04
BCL-XL	22.58	22.49	23.05	22.7	22.1	22.63
	22.57	22.53	22.97	22.71	22.04	22.65
FAS101	25.23	25.23	25.09	25.11	25.52	25.89
	25.11	25.22	25.01	25.09	25.56	25.86
HSP27	22.13	22.03	22.11	22.06	20.57	20.68
	22.1	22.01	22.12	22.05	20.56	20.73
HIF1A	20.51	20.4	20.3	20.35	19.19	19.52
	20.66	20.38	20.43	20.43	19.3	19.62

Table 2.

1ST EXPERIMENT						
GENES	P1i (Ct)	P2i (Ct)	P1h (Ct)	P2h (Ct)	ctr1 (Ct)	ctr2 (Ct)
FABP3	28.02	27.84	28.17	28.37	27.04	28.45
	27.98	27.81	28.26	28.24	27.01	27.83
CIRBPI	22.25	21.39	22.06	21.77	19.31	19.83
	22.26	21.39	22.04	21.75	19.43	19.87
RBM3	22.33	21.04	22.63	21.93	19.3	19.32
	22.34	21.08	22.5	21.94	19.23	19.3
HSP47	21.69	20.45	21.56	21.25	18.16	18.5
	21.66	20.39	21.61	21.27	18.21	18.44
HSPH1	24.18	23.11	24.26	23.71	20.24	20.15
	24.22	23.12	24.25	23.77	20.28	20.19
18S RNA	14.14	13.87	14.04	14.08	13.36	13.42
	14.15	13.82	14.04	14.11	13.37	13.42
TNFA	28.43	28.3	28.25	27.67	29.17	31.59
	28.19	28.08	28.41	27.62	29.17	31.49
CRIP1	25.33	23.17	25.14	24.4	21.03	21.49
	25.21	23.23	25.05	24.4	21.18	21.39
LGALS	26.85	25.52	26.92	26.42	23.26	23.41
	26.79	25.78	26.6	26.44	23.25	23.45
PLSCR4	28.24	27.6	28.42	28.37	25.9	26.13
	28.71	27.61	28.25	28.18	26.09	25.96
GAPDH70BP	18.08	17.13	17.71	17.53	15.67	16.19
	17.89	17.19	17.69	17.56	15.64	16.17
GAPDH110BP	17.63	17.06	17.62	17.24	15.33	15.83
	17.59	17.18	17.58	17.21	15.28	15.79

Table 3.

2D EXPERIMENT						
	P1i (Ct)	P2i (Ct)	P1h (Ct)	P2h (Ct)	ctr1 (Ct)	ctr2 (Ct)
FAS110	25.26	25.9	25.09	24.63	23.75	24.11
	25.02	25.67	25	24.4	23.56	23.8
BCL-2-298	29.73	30.29	29.39	29.08	27.49	26.71
	29.66	31.49	29.41	29.1	27.49	26.45
BCL-2	27.93	29.08	27.68	27.21	26.01	25.17
	28.28	29.22	27.59	27.2	25.81	25.21
18SRNA	13.83	14.21	13.74	13.7	13.53	13.67
	13.85	14.26	13.73	13.71	13.54	13.66

GAPDH70BP	17.04	18.08	16.82	16.63	16.2	16.62
	17.05	18.09	16.84	16.62	16.2	16.62
GAPDH110BP	16.97	17.97	16.57	16.3	15.83	16.26
	17.01	17.94	16.58	16.34	15.85	16.28
HSP70	23.38	24.19	23.22	22.57	21.8	21.61
	23.33	24.21	23.26	22.58	21.85	21.53
FASL	33.13	33.62	34.41	34.39	34.93	32.56
	34.45	34.23	34.08	33.79	Undetermined	31.56
BAX	24.31	25.51	23.75	23.79	22.54	23.8
	24.38	25.93	23.76	24.73	22.67	23.6
BCL-XL	22.64	23.89	22.38	22.03	20.34	21.51
	22.67	24.02	22.27	21.94	20.24	21.47
FAS101	25.16	25.8	24.7	24.22	23.74	24.78
	25.08	25.69	24.79	24.31	23.85	24.74
HSP27	20.75	21.92	20.4	20.35	19.17	19.7
	20.77	21.95	20.4	20.32	19.19	19.68
HIF1A	19.4	20.27	18.87	18.29	17.4	18.26
	19.58	20.23	18.93	18.41	17.44	18.38

Table 4.

2D EXPERIMENT						
	P1i (Ct)	P2i (Ct)	P1h (Ct)	P2h (Ct)	ctr1 (Ct)	ctr2 (Ct)
FABP3	28.47	30.01	28.68	30.37	27.76	28.33
	28.36	29.77	28.48	30.07	27.53	28.32
CIRBPI	21.14	21.81	20.6	21.84	19.91	20.78
	21.09	21.9	20.53	21.77	19.94	20.73
RBM3	21.03	21.8	21.09	21.94	19.99	19.76
	21.05	21.78	21.02	21.93	19.95	19.72
HSP47	20.15	20.86	20.02	21.07	18.66	19.35
	20.16	20.85	20.01	21.1	18.72	19.36
HSPH1	22.88	23.49	22.94	23.92	20.83	22.06
	22.92	23.54	22.98	23.88	20.83	22.11
18S RNA	13.7	13.66	13.59	13.79	13.47	13.7
	13.7	13.66	13.59	13.79	13.47	13.71
TNFA	28.02	25.47	28.36	24.64	29.79	28.37
	27.63	25.45	27.82	24.58	31.5	28.21
CRIP1	23.14	24.14	22.79	24.02	21.5	22.43
	23.1	24.18	22.73	23.91	21.64	22.34
LGALS	25.28	25.99	25.34	26.38	23.75	25.05
	25.36	26.15	25.35	26.23	23.9	25.11

PLSCR4	28.08	28.48	27.48	28.48	26.35	26.32
	27.82	28.42	27.34	28.51	26.26	26.29
GAPDH70BP	17.01	17.8	16.73	17.99	15.99	16.1
	17.03	17.87	16.75	17.75	15.97	16.08
GAPDH110BP	16.95	18.06	16.6	17.83	15.55	15.81
	16.97	18.01	16.6	17.89	15.92	15.86

Table 5.

3D EXPERIMENT						
	P1i (Ct)	P2i (Ct)	P1h (Ct)	P2h (Ct)	ctr1 (Ct)	ctr2 (Ct)
FAS110	26.22	26.96	26.38	27.34	24.28	24.64
	26.03	27.26	26.6	27.41	24.19	24.41
BCL-2-298	30.3	31.2	30.8	31.7	26.93	30.34
	30.03	31.07	30.46	31.4	27.1	30.18
BCL-2	27.9	29.96	29.18	29.71	25.62	28.97
	28.56	29.7	28.87	29.44	25.52	28.62
18SRNA	14.09	14.23	14.1	14.28	13.62	14.03
	14.1	14.23	14.09	14.28	13.63	14.02
GAPDH70BP	17.8	19.2	18.01	19.17	17	16.56
	17.83	19.23	18.02	19.16	16.99	16.55
GAPDH110BP	17.64	19.45	17.83	19.11	16.5	16.27
	17.78	19.36	17.86	19.14	16.49	16.29
HSP70	23.75	25	24.27	25.52	22.04	22.96
	23.92	25.11	24.26	25.28	22.08	23.09
FASL	35.83	36.07	35.48	33.08	Undetermined	34.71
	Undetermined	34.51	38.51	33.24	Undetermined	36.09
BAX	25.52	27.14	25.16	26.62	23.15	24.38
	25.36	26.86	25	26.97	23.19	24.36
BCL-XL	23.35	25.25	23.76	25.04	21.03	21.97
	23.32	25.31	23.73	25.06	20.91	22.01
FAS101	26.49	27.18	26.3	27.15	24.28	24.61
	26.05	27.1	26.1	27.35	24.3	24.46
HSP27	21.4	23.04	21.53	23.16	19.8	20.17
	21.46	23.12	21.61	23.21	19.86	20.17
HIF1A	20.23	21.57	20.37	21.29	17.78	17.86
	21.25	21.52	20.48	21.55	17.86	18.08

Table 6.

3D EXPERIMENT						
	<i>P1i (Ct)</i>	<i>P2i (Ct)</i>	<i>P1h (Ct)</i>	<i>P2h (Ct)</i>	<i>ctr1 (Ct)</i>	<i>ctr2 (Ct)</i>
FABP3	32.66	31.71	30.68	31.13	26.81	28.17
	32.48	32.28	30.4	30.78	26.94	28.12
CIRBPI	23.55	23.34	21.24	22.5	19.26	19.75
	23.49	23.23	21.13	22.42	19.32	19.71
RBM3	22.9	22.44	21.32	22.19	19.14	19.26
	22.88	22.44	21.15	22.14	19.07	19.27
HSP47	22.36	22.13	20.59	21.88	18.07	18.47
	22.45	22.2	20.58	21.99	18.1	18.52
HSPH1	22.9	22.38	21.21	22.48	20.21	20.09
	23	22.41	21.23	22.45	20.19	20.11
18S RNA	14.07	13.96	13.49	14.03	13.33	13.4
	14.07	13.94	13.49	14.04	13.33	13.4
TNFA	26.64	26.52	26.22	26.72	28.52	33.46
	27.06	26.31	26.12	26.33	28.14	31.44
CRIP1	24.33	23.86	22.66	23.74	20.8	21.18
	24.19	23.83	22.63	23.66	20.95	21.15
LGALS	26.32	26.07	25.13	25.95	23.19	23.4
	26.53	26.16	24.76	25.79	23.11	23.36
PLSCR4	30.06	29.74	27.66	28.75	25.79	25.84
	29.8	29.66	28.04	28.97	26.12	25.87
GAPDH70BP	17.81	17.49	16.27	17.27	15.51	16.09
	17.81	17.53	16.29	17.27	15.5	16.07
GAPDH110BP	17.71	17.43	16.12	17.1	15.2	15.66
	17.7	17.4	16.11	17.13	15.19	15.75

Table 7.

4TH EXPERIMENT						
	<i>P1i (Ct)</i>	<i>P2i (Ct)</i>	<i>P1h (Ct)</i>	<i>P2h (Ct)</i>	<i>ctr1 (Ct)</i>	<i>ctr2 (Ct)</i>
FAS110	24.22	24.03	25.03	23.44	24.54	24.51
	24.1	24.04	25.1	23.47	24.57	24.39
BCL-2-298	26.17	26.11	27.16	25.59	28.47	30.03
	26.13	26.05	27.34	25.58	28.41	30.72
BCL-2	24.99	24.79	26.04	24.29	27.18	28.58
	24.96	24.71	25.96	24.13	26.97	28.71
18SRNA	13.72	13.74	13.93	13.67	13.79	13.79

	13.72	13.76	13.92	13.68	13.79	13.78
GAPDH70BP	16.94	17.03	17.45	16.51	16.95	16.34
	16.94	17.06	17.47	16.55	16.92	16.34
GAPDH110BP	16.77	16.91	17.24	16.28	16.49	16.06
	16.85	16.84	17.22	16.31	16.48	16.07
HSP70	22.24	22.21	23.38	21.91	22.85	22.7
	22.23	22.23	23.23	22.03	22.81	22.74
FASL	32.53	33.46	33.32	31.95	36.32	32.76
	31.61	31.85	33.03	31.21	Undetermined	33.06
BAX	23.66	23.65	23.77	22.83	23.91	23.95
	23.55	23.68	23.77	22.68	23.99	23.95
BCL-XL	21.81	21.71	22.35	21.27	21.44	21.48
	21.87	21.7	22.34	21.19	21.36	21.55
FAS101	24.13	24.12	24.65	23.31	24.5	24.55
	24.15	23.93	24.77	23.38	24.55	24.56
HSP27	21.58	21.84	21.76	21.15	20.3	19.95
	21.58	21.85	21.91	21.18	20.35	19.93
HIF1A	19.18	19.04	19.86	18.44	18.19	17.9
	19.27	19.04	19.92	18.52	18.23	18.02

Table 8.

4TH EXPERIMENT						
	P1i (Ct)	P2i (Ct)	P1h (Ct)	P2h (Ct)	ctr1 (Ct)	ctr2 (Ct)
FABP3	30.73	29.09	28.89	30.04	28.09	28.78
	30.37	29.17	29.42	30.36	28.07	28.53
CIRBPI	22.48	21.11	21.35	21.75	19.8	20.92
	22.41	21.11	21.31	21.7	19.98	20.87
RBM3	22.58	20.9	21.32	21.6	19.24	20.15
	22.55	20.85	21.21	21.54	19.19	20.17
HSP47	21.12	19.54	20.04	20.2	18.54	19.52
	21.13	19.62	20.01	20.22	18.52	19.52
HSPH1	23.07	21.35	21.76	22.09	20.23	22.32
	23.11	21.35	21.75	22.14	20.19	22.35
18S RNA	14	13.55	13.62	13.73	13.45	13.72
	14	13.53	13.61	13.73	13.46	13.72
TNFA	25.37	26.39	24.67	26.07	32.05	31.56
	25.06	26.13	24.54	25.65	31.52	30.16
CRIP1	24.36	22.67	23.01	23.13	21.26	22.92
	24.15	22.69	22.84	23.13	21.37	22.79
LGALS	25.89	24.42	25.01	25.27	23.38	25.37

	25.78	24.43	24.74	25.16	23.28	25.28
PLSCR4	29.3	27.46	28.38	28.28	26.04	26.6
	29.06	27.52	27.85	28.14	26.12	26.74
GAPDH70BP	17.74	16.64	16.76	17.18	16.17	16.17
	17.86	16.68	16.84	17.21	16.17	16.18
GAPDH110BP	17.77	16.58	16.69	17.08	15.82	15.89
	17.77	16.56	16.68	17.12	15.82	15.98

Table 9.

5TH EXPERIMENT						
	P1i (Ct)	P2i (Ct)	P1h (Ct)	P2h (Ct)	ctr1 (Ct)	ctr2 (Ct)
FAS110	24.51	25.43	26.03	25.05	24.33	25.03
	24.27	25.66	25.86	25	24.24	24.81
BCL-2-298	27.7	29.54	29.93	28.84	27.01	30.66
	27.61	29.35	30.25	28.75	26.97	30.98
BCL-2	26.31	27.58	28.18	27.41	25.56	28.82
	26.4	28.03	28.31	27.26	25.49	28.94
18SRNA	13.71	14.13	14.26	13.84	13.69	14.07
	13.7	14.12	14.26	13.85	13.68	14.05
GAPDH70BP	17.1	18.16	18.37	17.71	16.88	16.7
	17.11	18.17	18.42	17.69	16.85	16.68
GAPDH110BP	16.88	18.18	18.4	17.68	16.41	16.44
	16.95	18.11	18.37	17.73	16.45	16.54
HSP70	22.62	24.06	24.86	23.75	21.98	23.16
	22.74	24.18	24.83	23.82	22	23.08
FASL	35.87	37.44	34.22	36.41	34.44	32.82
	33.68	34.1	34.14	33.96	33.76	32.94
BAX	23.71	25.02	25.43	24.53	23.07	24.43
	23.66	25.14	25.51	24.52	23.13	24.46
BCL-XL	22.15	23.54	24.11	23.24	20.8	22.1
	22.2	23.53	24.07	23.28	20.75	22.08
FAS101	23.32	24.5	24.68	23.52	24.23	24.86
	23.36	24.45	24.65	23.48	24.32	24.95
HSP27	20.26	21.38	21.75	21.08	19.67	20.29
	20.32	21.46	21.76	21.07	19.66	20.04
HIF1A	18.92	20.21	20.56	19.53	17.71	18.01
	18.94	20.54	20.66	19.6	17.8	18.12

Table 10.

5TH EXPERIMENT						
	<i>P1i (Ct)</i>	<i>P2i (Ct)</i>	<i>P1h (Ct)</i>	<i>P2h (Ct)</i>	<i>ctr1 (Ct)</i>	<i>ctr2 (Ct)</i>
<i>FABP3</i>	32.07	33.16	32.95	32.79	27.79	28.36
	31.91	31.97	Undetermined	32.56	27.42	28.34
<i>CIRBPI</i>	24.03	23.45	23.92	23.7	19.45	20.4
	23.84	23.51	23.77	23.58	19.58	20.43
<i>RBM3</i>	23.29	23.07	23.41	22.84	19.15	19.54
	23.31	23.06	23.23	22.82	19.14	19.57
<i>HSP47</i>	23.01	22.71	23.02	22.76	18.24	19.19
	23.01	22.71	22.93	22.77	18.31	19.2
<i>HSPH1</i>	23.59	23.23	23.92	23.38	20.05	21.74
	23.74	23.24	23.84	23.14	20.04	21.7
<i>18S RNA</i>	14.53	14.56	14.46	14.47	13.34	13.58
	14.55	14.38	14.47	14.48	13.35	13.59
<i>TNFA</i>	26.71	27.3	26.08	27.67	31.54	30.44
	26.33	27.04	25.99	26.91	32.9	30.26
<i>CRIPT</i>	25.2	24.99	24.99	25.06	20.99	22.15
	25.18	25.06	25.03	25	21.06	22.08
<i>LGALS</i>	27.62	27.03	27.48	27.58	23.18	24.62
	27.43	27.01	27.14	27.17	23.19	24.7
<i>PLSCR4</i>	30.66	30.34	30.56	30.47	25.92	26.12
	30.29	30.31	30.37	31	25.66	26.18
<i>GAPDH70BP</i>	18.63	18.24	18.57	18.49	15.93	15.95
	18.69	18.3	18.64	18.47	15.93	15.94
<i>GAPDH110BP</i>	18.49	18.17	18.48	18.28	15.47	15.57
	18.54	18.12	18.53	18.32	15.48	15.61

10 CURRICULUM VITAE

Persönliche Daten

Vorname: Chrysanthi-Maria
Nachname: Kokotsaki
Geburtstag: 14.09.1986
Geburtsort: Chania - Griechenland
Kontakt: E-Mail: mkokotsaki@hotmail.gr
Nationalität: Österreich - Griechenland

Schulbildung und Studium

2004 **Schulabschluss:** Einheitliches Lyzeum Soudas
Beurteilung: 18,6 von 20 möglichen Punkten

2004-2010 **Diplomstudium in Molekularbiologie und Biotechnologie** an der Medizinischen Fakultät der UNI Heraklion/Kreta, am 16. Juli 2010 mit „sehr gut“ abgeschlossen
Abschlussarbeit (01/2009 bis 01/2010) im Labor für Krebsbiologie an der Medizinischen Fakultät der Universität von Heraklion/Kreta
Titel: Untersuchung der Expression des insulinähnlichen Wachstumsfaktors I (IGF-IR) bei mikrometastatischen Patienten mit metastasiertem Brustkrebs vorkommenden Zellen
(Bewertung: 9.5 von 10 möglichen Punkten)
Betreuerin: Dr. Sophia Angelakis (MD, PhD)

2011-2014 **Masterstudium in Genetik und Entwicklungsbiologie** an der UNI Wien, seit 3.10.2011 bis November 2014
Abschlussarbeit (09/2013 bis 11/2014) an der Medizinischen UNI Wien im AKH, Abteilung für Gynäkologische Endokrinologie u. Reproduktionsmedizin
Titel: Impact of Vitrification on Ovarian Tissue and Cells
Betreuer 1: Prof. Dr. Christian Schneeberger
Betreuer 2: Prof. Dr. Ernst Müllner

Forschungstätigkeit

2008-2009	Mitwirkung am Lehrplan des akademischen Jahres 2008-2009 der Klinik für Frauenheilkunde und Geburtshilfe der Universität von Kreta Klinikdirektor: John Matalliotakis, Privatdozent für Geburtshilfe und Gynäkologie
2010	Freiwillige Teilnahme (5 Monate, 02/2010 bis 06/2010) an einem Forschungsprojekt des Labors für Krebsbiologie an der Medizinischen Fakultät der Universität von Kreta Titel: Genomische DNA Bestimmung aus Blutproben von Patienten und SNP-Genotopisierung mit Sequenzierung nach Sanger Betreuer: Dr. Dimitris Mavroudis MD, PhD Die Arbeit wurde zur Veröffentlichung vorgeschlagen.
2010-2011	Freiwillige Tätigkeit (11/2010 bis 8/2011) im Labor für Biochemie sowie Blut- und Hormonuntersuchung, als auch Pathologische Anatomie im Allgemeinen Krankenhaus der Stadt Chania "St. George", Kreta

Teilnahme an Seminaren und Kongressen

- 3. Panhellenischer Kongress der Endometriose und 3. Symposium der Endoskopie, 17. bis 19.10.2008 in Heraklion/Kreta
- 17. Postgraduierten-Konferenz: Klinische Onkologie, 04. bis 08.11.2010 in Heraklion,/Kreta
- 3. Pankretisches Postgraduierten-Seminar für Geburtshilfe - Gynäkologie mit dem Titel "Beckenboden-Pathologie – Entzündung der Harn-und Geschlechts-organe", 24. bis 25.04.2010 in Heraklion/Kreta
- 2. Athener Forum für Geburtshilfe zum Thema "Konflikte in der Embryomytrikalen/Pränatalen Medizin", 12. bis 13.06.2010 in Athen
- MSRM Internationales Treffen „Wiederholte Fehlgeburten – Wissenschaftliche und Klinische Aspekte", 24. bis 26.09.2010, in Chania/Kreta
- 18. Postgraduierten Kongress der Klinischen Onkologie, 04. bis 06.11.2010, in Heraklion/Kreta

- Gemeinsame Jahrestagung Österreichische Gesellschaft für Reproduktionsmedizin und Endokrinologie Und Österreichische IVF-Gesellschaft Und Österreichische Gesellschaft für Sterilität, Fertilität und Endokrinologie Salzburg, 2.– 4. Oktober 2014 in Paracelsus Medizinische Privatuniversität

Sonstige Qualifikationen

Sprachkenntnisse:

1. Griechisch
2. Deutsch
 - Meine Mutter ist Wienerin
 - ÖSD-Sprachdiplom Deutsch B2 Mittelstufe, 2011
3. Englisch
 - Certificate of Competency in English, 2008
 - Michigan Proficiency in English als Fremdsprache, 2010